THE ASTROPHYSICAL JOURNAL, Vol. 157, September 1969

SCANNER ABUNDANCE STUDIES. I. AN INVESTIGATION OF SUPERMETALLICITY IN LATE-TYPE EVOLVED STARS

HYRON SPINRAD AND BENJAMIN J. TAYLOR
Astronomy Department, University of California, Berkeley
Received November 18, 1968; revised February 13, 1969

ABSTRACT

In this paper we describe a new technique for obtaining differential abundances This technique utilizes the following information: (1) Accurate measures of line and molecular-band strengths, obtained by using a photoelectric spectrum scanner in a manner analogous to that of the Cambridge observers; (2) a self-consistent relative temperature scale based on measures of the star's continuum in the yellow, red, and infrared regions of the spectrum, also obtained with a scanner. With these data, stars may be ordered in terms of their molecular abundances; moreover, quantitative relative abundances may be derived from the measures of atomic-line strengths by using the additional information described below; (3) a simple theoretical treatment for the interpretation of the measured line strengths; (4) at least one comparison star with standard abundances in the temperature range considered.

We also describe results we have obtained to date from an application of this technique to K giants and subgiants These results include the following:

1. Evolved K stars with metal abundances greater than those of the Hyades exist in substantial numbers This conclusion is derived from the individual strong-feature data, and is confirmed by blanketing measures and by spot checks with slit spectrograms. Conclusive evidence exists that this interpretation of the data is not confused by variations in microturbulence or surface gravity, and that the abundances found are primordial, not the result of self-enrichment; moreover, there is good indication that high metallicities, not low hydrogen contents, are involved. The abundances found range as high as 4 times the solar values for Ca, Mg, and Na. The cool evolved stars in M67 and NGC 188 have generally 3 times the solar abundances of the above elements; independent data on the hotter stars in M67 indicate that this is probably true of them, also

2 The tendency for the range of abundances in K giants to cause systematic errors in MK spectral classification of these stars makes supplementary red photometry necessary.

3 At least one significant source of error exists in standard differential curve-of-growth and model-atmosphere techniques for giants cooler than about K0.

4 A tight correlation exists between N, Na, and Fe abundances for the stars studied, and is presumably of general validity. This correlation does not, however, extend in full strength to Ca and Mg

5 K giants and subgiants exist which have solar or higher abundances and orbital eccentricities up to 0 5 or maximum heights above the galactic plane of 1.5 kpc. The velocity-abundance correlations found previously by others for G dwarfs are not completely valid for evolved K stars and are probably not strictly valid generally

6. A relatively abrupt cutoff in the production of stars with abundances similar to or higher than those in M67 took place shortly after the epoch of formation of M67 itself. From this result and the results of other investigations, it is concluded that uniform enrichment was probably important during the formation of the halo but has played no significant role in the history of the disk.

I. INTRODUCTION

There are currently two basic techniques available to astrophysicists for studies of differential abundances. One of these requires equivalent widths and/or line profiles measured on high-dispersion spectrograms, and yields a temperature, a surface gravity, a microturbulent velocity, and metal-to-hydrogen ratios for each of several different elements (relative to the comparison star used). The other requires "blanketed" and "blanketing-free" photoelectrically measured colors, and yields a "blanketing index" with which stars may be ordered by overall metallicity (and, in addition, a crude numerical value for the metallicity itself, if a calibration based on the first technique is available). Each technique has at least one major drawback; the first is time-consuming and is restricted to bright stars, while the second yields relatively crude information.

In this paper we describe a new technique which yields detailed abundance information at the efficiency characteristic of photoelectric work. This technique utilizes the following information:

1. Accurate measures of atomic-line and molecular-band strengths, obtained with a photoelectric spectrum scanner.
2. A self-consistent relative temperature scale based on measures of the star's continuum in the yellow, red, and infrared regions of the spectrum, also obtained with a scanner.

With these data, stars may be ordered in terms of their molecular abundances; moreover, quantitative relative abundances may be derived from the measures of line strengths by using the following additional information:

3. A simple theoretical treatment for the interpretation of the measured line strengths.
4. At least one comparison star with standard abundances in the temperature range considered.

We also present and discuss data we have obtained to date by using this method. The thrust of this investigation is directed toward cool stars of very high metallicity; we present evidence for the existence of such stars, discuss their properties, and examine their implications for our knowledge of galactic structure and history.

II. THE OBSERVATIONAL ABUNDANCE PARAMETERS

The method used for obtaining abundance parameters from scanner observations of a given star proceeds through the following four steps.

First, intensities are obtained in specified passbands. These bands contain either strong absorption features or regions as free as possible of absorption; those of the latter kind were selected by inspection of the solar spectrum as depicted in the Utrecht *Atlas* (Minnaert, Mulders, and Houtgast 1940) and the tables of integrated equivalent widths as functions of wavelength given by Wildey *et al.* (1962). The intensities so obtained are corrected for atmospheric extinction by using mean extinction coefficients supplied by Dr. L. V. Kuhi and are transformed to a standard system (to be described in § V) by using observations of standard stars. If necessary, they are also corrected for interstellar reddening by using published or estimated values of $E(B - V)$ and the Whitford reddening law (Whitford 1958).

Second, colors are derived. In order to cover the desired wavelength range, it is necessary to use several combinations of photomultiplier, filter, and grating order. A set of passbands observed by using a given combination of this sort is referred to as a *program*. In order to link observations made in programs covering adjacent wavelength intervals, an overlap passband (which is also a program passband) is observed in each program; the intensities in one of the programs are subsequently scaled so as to match the two values obtained at the overlap passband. The entire set of intensities is also multiplied by the normalization factor $1000/J(5360)$, where $J(5360)$ is the intensity at $\lambda 5360$. The result is a set of colors $I(\lambda)$ related to the intensities $J(\lambda)$ as follows:

$$I(\lambda) = J(\lambda) \frac{1000}{J(5360)} K(\lambda) , \tag{1}$$

where λ is wavelength and $K(\lambda)$ is the scaling factor (or product of scaling factors) derived from the overlap passband(s). (For one of the programs, of course, $K(\lambda) = 1$.) We emphasize that the $I(\lambda)$'s are modified intensity ratios and are not on a magnitude scale.

Third, temperature indices are derived. A red temperature index called T is calculated as follows:

$$T = I(7000) + I(7400) , \tag{2}$$

where $I(\lambda)$ is the color at wavelength λ, derived as described above. A correction must subsequently be made to this index because of the small blanketing effects of the red CN system on the λλ7000 and 7400 passbands; this will be discussed in § VIII. If infrared observations of the star have been made, an infrared temperature index is also computed:

$$T_{\mathrm{IR}} = I(8800) + I(10300) + I(10700)\ . \tag{3}$$

Fourth, measurements of feature strengths are obtained for each absorption feature. This is done in two steps. First, Cambridge-type indices (cf. Griffin and Redman 1960; Deeming 1960) are derived:

$$r = (I_a + I_b)/2I_f\ , \tag{4a}$$

or

$$r = I_a/I_f\ , \tag{4b}$$

where r is the index, I_f is the coloı at the passband containing the feature being measured, and I_a and I_b are colors at continuum points flanking the feature (which were chosen with an eye to just this purpose). The passbands used to measure a given feature are always part of the same program. Second, quantities called w's are computed from the following definition:

$$w = 1 - r_0/r\ , \tag{5}$$

where r_0 is the no-feature, no-background-blanketing value of the index, obtained either from observations of the very metal-poor stars HD 122563 and HD 165195 (Wallerstein *et al.* 1963) or, in the case of Ca II λ8662, from the assumption that the continuum in the neighborhood of the line is flat. The values of w for each feature and of T are the star's primary abundance parameters, and are compared with those of other stars in order to assess relative abundances.

A list of the central wavelengths of the passbands used, the features (if any) contained in these bands, and the photomultiplier-filter-grating combination used for each, is given in Table 1. Table 2 lists the indices, their features and side bands, and the numbers used to identify them in the data tables (see § VI).

The physical significance of w may be assessed as follows. Consider two stars, one with and one without absorption features. For the former star, let I_a, I_b, and I_f be *blanketing-free* colors in two side bands a and b and a feature band f, respectively; let W_a, W_b, and W_f be the total equivalent widths of the background absorption in these same bands; let W be the equivalent width of a feature in the band f being measured; and let $\Delta\lambda$ be the bandwidth used throughout. In this star, the fractions of light lost to blanketing in the side bands will be $W_a/\Delta\lambda$ and $W_b/\Delta\lambda$; if the simplifying assumption is made that there is no interaction between the feature being measured and the background blanketing, the fraction of light lost in the feature band will be $(W_f + W)/\Delta\lambda$. From equation (4a), therefore,

$$r = \frac{I_a(\Delta\lambda - W_a) + I_b(\Delta\lambda - W_b)}{2I_f(\Delta\lambda - W_f - W)}\ . \tag{6}$$

In the case of the unblanketed star, we have, from equation (4a) and the definition of r_0,

$$r = r_0 = (I'_a + I'_b)/2I'_f\ , \tag{7}$$

where I_a', I_b', and I_f' are analogous to I_a, I_b, and I_f, respectively. Because the temperatures of the two stars may be different, the analogous primed and unprimed I's are not necessarily equal. If, however, the temperature range considered is small enough and the side bands are sufficiently close together, r_0 will be essentially independent of temperature. In this case, we may without loss of generality choose an unblanketed star having the same temperature as the blanketed star, and

$$r_0 = (I_a + I_b)/2I_f\ . \tag{8}$$

TABLE 1

WAVELENGTH LIST

Central Wavelength (Å)	Feature	Cell	Filter	Order
3880	CN λ3883	FW 130	Blue	2
4040	Continuum	FW 130	Blue	2
4100	Hδ	FW 130	Blue	2
4200	CN λ4215	FW 130	Blue	2
4227	Ca I	FW 130	Blue	2
4300	CH λ4313	FW 130	Blue	2
4340	Hγ	FW 130	Blue	2
4500	Continuum	FW 130	Blue	2
4715	Continuum	FW 130	Blue	2
4900	Continuum	FW 130	Blue	2
		FW 130	Yellow	2
5000	Continuum	FW 130	Yellow	2
5175	Mg I+MgH	FW 130	Yellow	2
5300	Continuum	FW 130	Yellow	2
5360 . . .	Continuum	FW 130	Yellow	2
		FW 130	Yellow	1
5864	Continuum	FW 130	Yellow	1
5892	Na I (D)	FW 130	Yellow	1
6110	Continuum	FW 130	Yellow	1
6180	TiO λλ6148, 6158	FW 130	Yellow	1
6386	CaH λ6382	FW 130	Yellow	1
6564	Hα	FW 130	Yellow	1
6620	Continuum	FW 130	Yellow	1
7000	Continuum	FW 130	Yellow	1
7100	TiO λ7054	FW 130	Yellow	1
7400	Continuum	FW 130	Yellow	1
		RCA 7102	Red	1
7980	Continuum	RCA 7102	Red	1
8190	Na I	RCA 7102	Red	1
8400	Continuum	RCA 7102	Red	1
8662	Ca II	RCA 7102	Red	1
8800	Continuum	RCA 7102	Red	1
8900	TiO λ8859	RCA 7102	Red	1
9200	CN(1,0) red	RCA 7102	Red	1
10300	Continuum	RCA 7102	Red	1
10700	Continuum	RCA 7102	Red	1

TABLE 2

INDICES

Number	Feature	Feature Band (λ)	Side Band(s) (λ)	r_0
1	CN	3880	4040	1 62
2	CN	4200	4040, 4500	0 94
3	Ca I	4227	4040, 4500	0 94
4	CH	4300	4040, 4500	0 95
5	Mg	5175	5000, 5300	0 86
6	D	5892	5864	1 00
7	TiO	6180	6110	1 03
8	TiO	7100	7000, 7400	0 81
9	Ca II	8662	8400, 8800	1 01
10	CN	9200	8800, 10300	0 88

Substituting equations (6) and (8) into equation (5), we obtain

$$w = 1 - \frac{(I_a + I_b)(\Delta\lambda - W_f - W)}{I_a(\Delta\lambda - W_a) + I_b(\Delta\lambda - W_b)} . \tag{9}$$

If $W_a = W_b = W_f = 0$, equation (9) reduces to

$$w = W/\Delta\lambda , \tag{10}$$

and equation (5) becomes identical with equation (3) of Price (1966*a*). In this case, w is the "blocking fraction" of the feature being measured. In the more general case, w is a "quasi-blocking fraction," still increasing monotonically with the equivalent width of the strong feature, but with both scale and zero-point differences from a hypothetical "background-free" w.[1]

The indices measured fall into three groups, according to the kinds and sizes of errors introduced by background blanketing. One includes all the indices measured longward of $\lambda 5360$; here background effects are negligible (see Price's Table 1, for example, for confirmation of this for the D-lines), and w is a genuine blocking fraction. A second includes the four blue indices, for which blanketing effects are unavoidable. As an example of the size of the errors to be expected, consider the index for $\lambda 4227$ of Ca I in the Sun; here, taking $W_a(\lambda 4040) \approx 4.2$ Å, $W_b(\lambda 4500) \approx 1.3$ Å, and $W_f \approx 3.6$ Å (from Moore, Minnaert, and Houtgast 1966) and $I(4040) \approx \frac{2}{3}I(4500)$ (as judged from scanner observations of G2 V stars), we have

$$w \approx 1.2W/\Delta\lambda + 0.09 \tag{11}$$

from equation (9) (assuming $\Delta\lambda = 15$ Å). For the range of $W/\Delta\lambda$ of interest, w will be too large by about a factor of 2, and ratios of w's (which will be used in determinations of relative abundances) will be too small because of the sign of the constant. (Neglecting the increase of the background blanketing itself as W increases does not fundamentally alter this result.) The third group consists solely of the Mg I *b*-triplet index, for which $I_a \approx I_b$ (as judged from scanner observations of K stars) and $W_f \approx \frac{1}{2}(W_a + W_b)$ (as judged from Wildey *et al.*); in this special case, equation (8) reduces to

$$w \approx W/(\Delta\lambda - W_f) . \tag{12}$$

Since W_f is of order 1–2 Å, w will be too large by 7–15 percent (for $\Delta\lambda = 15$ Å). Ratios of w's, however, will be considerably less in error. Let us assume that W_f is composed equally of lines on the curve of growth in the linear portion (changing linearly with abundance) and the flat portion (insensitive to abundance changes). Then, for two stars differing in overall abundance by a factor of 2, we might have typically $W_{f,1} = 1.5$ Å, $W_{f,2} = 2.2$ Å, and

$$\frac{w_2}{w_1} \approx \frac{W_2}{W_1}\frac{\Delta\lambda - W_{f,1}}{\Delta\lambda - W_{f,2}} \approx \frac{13.5}{12.8}\frac{W_2}{W_1} \approx 1.05\frac{W_2}{W_1} . \tag{13}$$

The nature of the errors of the latter two groups will be utilized in the discussion in § XVI.

III. THE DAMPING-LINE THEORY

The accuracy to which we measure equivalent widths does not warrant a detailed theoretical treatment of the results. We therefore derive relative abundance for our stars from the appropriate simple relations between abundance, equivalent width, and surface grav-

[1] This discussion supplants the assumption previously made (Taylor 1967, 1968) that $w = W/\Delta\lambda$ in all cases.

ity given by Deutsch (1966). Deutsch's equations indicate that equivalent width varies as the square root or the cube root of the abundance and (to first order) is not a function of surface gravity in K giants if the metal abundances vary in lockstep (i.e., in direct proportion); the derivation of these results is discussed (and given explicitly for the case of λ4227 of Ca I) by Deutsch. In order to test this assertion and to investigate the consequences of removing the lockstep restriction, Dr. Stephen Strom has kindly computed for us a series of model atmospheres in which the equivalent widths of the lines measured by us are calculated by numerical integration through the atmosphere. These confirm Deutsch's relations for the lockstep case (which is the one most frequently encountered) and provide similar relations as needed for cases of independent variation in abundance. With respect to surface-gravity sensitivity, they indicate that variation in surface gravity becomes important for damping lines in K stars only for $\log g > 3$ (luminosity classes IV and V).

IV. OBSERVATIONS AND REDUCTIONS

All observations were secured with the Wampler photoelectric spectrum scanner at the prime foci of the Crossley and 120-inch telescopes at Lick Observatory. A detailed description of this scanner has been given elsewhere (Wampler 1966). Two photomultipliers—an FW 130 (S20 surface) and an RCA 7102 (S1 surface)—were used, the former for λλ3880–7400, the latter for λλ7400–10700. An exit slot of 1 mm, corresponding to 15 Å in the second order, was used throughout. For all but the faintest stars, a dwell time was selected which would yield at least 2000 pulses ("counts") per dwell at almost all wavelengths; an observation then consisted (with occasional exceptions) of at least three dwells at each of the wavelengths observed with the photomultiplier being used that night. If inspection of the scanner output revealed that the number of counts per dwell at a given wavelength was fluctuating more than usual, the number of dwells per wavelength was increased. For the faintest stars, a compromise dwell time and a number of dwells per wavelength sufficient to obtain total counts of about $6\text{–}10 \times 10^3$ were used. Since until recently the scanner was exclusively a single-channel instrument, sky readings were obtained separately, when necessary, by offsetting the telescope; the number of dwells per wavelength used was roughly 1 for each 7–8 percent of sky contribution. The times needed to carry out a complete observation at the 120-inch (exclusive of telescope-setting time) ranged from about 8 minutes for stars with $V \lesssim 8.0$ mag to 45–50 minutes for stars with $V \approx 13.0$ mag; the Crossley was used almost exclusively for stars with $V \lesssim 6.5$ mag, for which 10–12 minutes per observation were required. Most stars were observed at 1.3 air masses or less; the only exceptions were some southern stars (which were almost always observed with $\pm\frac{1}{2}$ hour of the meridian) and a few stars near the north celestial pole, notably those in NGC 188. Care was taken to avoid observing through the haze layer which is often present over the Santa Clara Valley to the west. Several standard stars were observed each night; three such observations were regarded as an irreducible minimum, and five to seven were almost always secured.

After the raw data, consisting of numbers of counts and identifying wavelengths printed on paper tape, had been transferred to punched cards, they were put through two reduction programs. Originally the first of these programs (generously supplied to us by Dr. Kuhi) averaged dwells and computed percentage standard deviations at each wavelength and corrected the observations for extinction, by the use of the standard coefficients mentioned in § II, while the second (written by B. J. T.) transformed observations to the standard stystem, reduced the intensities to colors, averaged different observations and computed percentage standard deviations, corrected for reddening (again as mentioned in § II), and computed second-level quantities (T's, r's, w's). Later a second two-program set (written by B. J. T.) was used; in this pair, transformation to the standard system was effected by the first program. The only one of these steps needing special comment is that of transformation: coefficients for this step were computed by averaging ratios of intensities, a process equivalent to averaging magnitude differences if the range averaged over is sufficiently small. All reductions were carried out on the IBM 7094 computer of the University of California at Berkeley.

V. THE STANDARD SYSTEM

The standard system used in this investigation was set up from observations of twelve stars on selected 120-inch nights. Because the system was set up after the observational program had been begun, the stars were selected chiefly because they had been observed on previous nights, although position in the sky and (in three cases) membership in the absolute system of Oke (1964) also played a factor. Only nights free of wavelength-dependent differences in response (as revealed by inspection of the reduced observations) were used. The intensities obtained were averaged in a straightforward manner (ignoring the wavelength-independent differences in scale factor between nights) except at λ4900

TABLE 3

NIGHTS USED TO SET UP STANDARD SYSTEM

Date	Cell	Stars Observed
Jan. 24/25, 1966	RCA 7102	ε CrB, 109 Vir, τ Boo
May 17/18, 1966	RCA 7102	τ Boo, ω Ser, HR 6806, 61 Cyg A, 61 Cyg B, 55 Peg
June 11/12, 1966	RCA 7102	ε CrB, 109 Vir, τ Boo, ω Ser
June 12/13, 1966	FW 130	ε CrB, 58 Aql, 109 Vir, τ Boo
July 18/19, 1966	FW 130	ε CrB, 58 Aql, τ Boo, 55 Peg
July 19/20, 1966	FW 130	ε CrB, 58 Aql, 109 Vir, τ Boo, ω Ser, θ Psc, HR 6806, δ Psc, 61 Cyg A, 61 Cyg B, 55 Peg
July 20/21, 1966	FW 130	58 Aql, 29 Psc, 109 Vir, ω Ser, θ Psc, HR 6806, δ Psc, 61 Cyg A, 61 Cyg B, 55 Peg
July 21/22, 1966	RCA 7102	ε CrB, 58 Aql, 29 Psc, 109 Vir, ω Ser, θ Psc, HR 6806, δ Psc, 61 Cyg A, 61 Cyg B, 55 Peg
August 22/23, 1966	RCA 7102	ε CrB, 58 Aql, 29 Psc, θ Psc, HR 6806, δ Psc, 61 Cyg A, 61 Cyg B, 55 Peg

(yellow filter), where the response of the filter used is slightly temperature dependent; this was removed by forcing $I(4900)$ to be equal to $I(5000)$ in the K5 III standard, δ Psc, for each of the nights used, and by scaling all other observations accordingly. Other standards were subsequently set up as needed from observations tied into this system. Judging from transformation coefficients, no closure error as large as 1 percent exists, and our system is consistent to the same accuracy with the Hayes revision of the Oke system (Hayes 1967), with the possible exception of the common standard star 29 Psc.

Table 3 lists the nights used to set up the original twelve-star standard system and the stars observed during each. The system itself is given in Table 4 as an instrumental intensity system in number of counts per second; since only colors are relevant to this investigation, the formation of this intensity system will be discussed elsewhere.

It is our opinion that other observers who wish to reproduce our observations will be constrained to use 15 Å resolution shortward of λ5360 and 30 Å resolution longward of this limit, and to observe these standard stars on a regular basis.

VI. PHOTOELECTRIC PRECISION AND DATA TABLES

Tables 5 and 6 give the colors (§ II, step 2) for each of the stars observed (except at λ5360, for which I always equals 1000), while Tables 7 and 8 list the computed w's (§ II, step 4), identified by the numbers given in Table 2. In essentially all cases, each value listed is the average of two or more observations. The average precision of the colors is

Table 4

ABSOLUTE SYSTEM

λ(Å)	εCrB	58 Aql	29 Psc	109 Vir	τ Boo	ω Ser	θ Psc	HR 6806	δ Psc
3880	3.81(+4)	1.29(+5)	2.94(+5)	7.80(+5)	2.05(+5)	2.65(+4)	5.18(+4)	1.17(+4)	1.62(+4)
4040	1.41(+5)	2.29(+5)	4.53(+5)	1.40(+6)	3.58(+5)	8.23(+4)	1.71(+5)	3.11(+4)	5.93(+4)
4100	1.63(+5)	1.15(+5)	2.85(+5)	6.99(+5)	2.93(+5)	8.93(+4)	1.87(+5)	3.61(+4)	7.21(+4)
4200	1.54(+5)	2.22(+5)	4.26(+5)	1.34(+6)	3.79(+5)	8.51(+4)	1.77(+5)	3.65(+4)	7.61(+4)
4227	1.72(+5)	2.16(+5)	4.16(+5)	1.30(+6)	3.72(+5)	9.42(+4)	1.99(+5)	3.19(+4)	6.24(+4)
4300	1.50(+5)	1.97(+5)	3.82(+5)	1.18(+6)	3.15(+5)	7.16(+4)	1.56(+5)	2.74(+4)	7.82(+4)
4340	2.37(+5)	9.99(+4)	2.37(+5)	6.01(+5)	2.86(+5)	1.08(+5)	2.50(+5)	4.19(+4)	1.34(+5)
4500	2.74(+5)	1.58(+5)	2.90(+5)	9.41(+5)	3.41(+5)	1.22(+5)	2.81(+5)	4.69(+4)	1.75(+5)
4715	2.57(+5)	1.19(+5)	2.09(+5)	6.97(+5)	2.70(+5)	1.07(+5)	2.48(+5)	3.98(+4)	1.74(+5)
4900	2.12(+5)	7.73(+4)	1.35(+5)	4.49(+5)	1.92(+5)	8.50(+4)	2.01(+5)	3.00(+4)	1.47(+5)
4900	1.50(+5)	5.42(+4)	9.60(+4)	3.14(+5)	1.35(+5)	6.00(+4)	1.43(+5)	2.13(+4)	1.05(+5)
5000	1.59(+5)	5.94(+4)	1.02(+5)	3.46(+5)	1.46(+5)	6.38(+4)	1.47(+5)	2.17(+4)	1.05(+5)
5175	1.43(+5)	5.87(+4)	9.83(+4)	3.36(+5)	1.44(+5)	6.22(+4)	1.40(+5)	1.61(+4)	8.44(+4)
5300	1.57(+5)	4.66(+4)	7.48(+4)	2.64(+5)	1.27(+5)	6.15(+4)	1.45(+5)	2.10(+4)	1.20(+5)
5360	1.59(+5)	4.11(+4)	6.57(+4)	2.32(+5)	1.15(+5)	5.89(+4)	1.41(+5)	1.98(+4)	1.24(+5)
5360	8.16(+5)	2.26(+5)	3.56(+5)	1.21(+6)	6.09(+5)	3.15(+5)	7.34(+5)	1.07(+5)	6.49(+5)
5864	8.28(+5)	1.71(+5)	2.50(+5)	8.98(+5)	5.19(+5)	3.02(+5)	7.04(+5)	1.02(+5)	6.73(+5)
5892	7.79(+5)	1.66(+5)	2.48(+5)	8.79(+5)	5.04(+5)	2.90(+5)	6.66(+5)	9.14(+4)	5.96(+5)
6110	8.59(+5)	1.60(+5)	2.30(+5)	8.31(+5)	5.04(+5)	3.06(+5)	7.12(+5)	1.01(+5)	7.51(+5)
6180	8.27(+5)	1.50(+5)	2.16(+5)	7.85(+5)	4.79(+5)	2.94(+5)	6.87(+5)	9.78(+4)	6.73(+5)
6386	7.46(+5)	1.21(+5)	1.71(+5)	6.31(+5)	4.07(+5)	2.61(+5)	6.02(+5)	8.48(+4)	6.61(+5)
6564	5.99(+5)	7.22(+4)	1.10(+5)	3.73(+5)	2.82(+5)	2.05(+5)	4.78(+5)	6.62(+4)	5.48(+5)
6620	5.92(+5)	8.68(+4)	1.20(+5)	4.48(+5)	3.03(+5)	2.03(+5)	4.69(+5)	6.51(+4)	5.36(+5)
7000	3.05(+5)	4.02(+4)	5.29(+4)	2.05(+5)	1.45(+5)	1.02(+5)	2.37(+5)	3.29(+4)	2.95(+5)
7100	2.46(+5)	3.13(+4)	4.09(+4)	1.60(+5)	1.16(+5)	8.14(+4)	1.88(+5)	2.62(+4)	2.18(+5)
7400	9.49(+4)	1.13(+4)	1.44(+4)	5.70(+5)	4.16(+4)	3.08(+4)	7.21(+4)	9.83(+3)	9.68(+4)
7400	4.21(+4)	4.75(+3)	6.21(+3)	2.43(+4)	1.81(+4)	1.35(+4)	3.23(+4)	4.36(+3)	4.37(+4)
7980	3.40(+4)	3.34(+3)	4.19(+3)	1.63(+4)	1.34(+4)	1.07(+4)	2.55(+4)	3.43(+3)	3.68(+4)
8190	3.11(+4)	2.95(+3)	3.64(+3)	1.43(+4)	1.18(+4)	9.70(+3)	2.35(+4)	3.10(+3)	3.43(+4)
8400	2.82(+4)	2.50(+3)	3.05(+3)	1.21(+4)	1.05(+4)	8.72(+3)	2.10(+4)	2.77(+3)	3.14(+4)
8662	2.47(+4)	2.13(+3)	2.55(+3)	1.03(+4)	8.72(+3)	7.66(+3)	1.82(+4)	2.38(+3)	2.78(+4)
8800	2.65(+4)	2.51(+3)	2.80(+3)	1.18(+4)	9.21(+3)	8.04(+3)	1.93(+4)	2.42(+3)	3.01(+4)
8900	2.68(+4)	2.36(+3)	2.66(+3)	1.11(+4)	8.92(+3)	8.01(+3)	1.94(+4)	2.48(+3)	3.09(+4)
9200	2.11(+4)	1.83(+3)	2.04(+3)	8.64(+3)	7.45(+3)	6.46(+3)	1.52(+4)	2.08(+3)	2.50(+4)
10300	1.24(+4)	8.78(+2)	8.96(+2)	3.99(+3)	3.60(+3)	3.61(+3)	8.70(+3)	1.07(+3)	1.53(+4)
10700	7.22(+3)	4.84(+2)	4.88(+2)	2.13(+3)	1.94(+3)	2.07(+3)	5.06(+3)	6.17(+2)	9.11(+3)

1969ApJ...157.1279S

Table 4 (cont.)

ABSOLUTE SYSTEM

λ(Å)	61 Cyg A	61 Cyg B	55 Peg	ν And	λ Aur	32 Per	ϕ^2 Ori	π^2 Ori	ω Gem	36 UMa A	μ Leo	21 LMi
3880	1.78(+4)	7.19(+3)	1.36(+4)	5.03(+5)	1.26(+5)	2.01(+5)	9.80(+4)	4.41(+5)			4.50(+4)	2.84(+5)
4040	5.16(+4)	1.89(+4)	4.44(+4)	7.63(+5)	2.54(+5)	4.55(+5)	2.65(+5)	8.24(+5)			1.78(+5)	5.72(+5)
4100	6.17(+4)	2.20(+4)	5.82(+4)	4.83(+5)	2.32(+5)	1.93(+5)	2.85(+5)	3.89(+5)			1.96(+5)	2.89(+5)
4200	6.78(+4)	2.51(+4)	6.23(+4)	7.15(+5)	2.67(+5)	4.37(+5)	2.90(+5)	7.82(+5)			1.82(+5)	5.61(+5)
4227	4.12(+4)	1.32(+4)	4.11(+4)	7.07(+5)	2.59(+5)	4.22(+5)	2.92(+5)	7.53(+5)			2.04(+5)	5.43(+5)
4300	5.71(+4)	2.27(+4)	6.74(+4)	6.48(+5)	2.00(+5)	3.61(+5)	2.13(+5)	6.64(+5)			1.81(+5)	4.70(+5)
4340	9.41(+4)	3.43(+4)	1.14(+5)	4.03(+5)	2.33(+5)	1.73(+5)	3.21(+5)	3.41(+5)			3.20(+5)	2.61(+5)
4500	1.17(+5)	4.53(+4)	1.46(+5)	4.84(+5)	2.65(+5)	3.10(+5)	3.66(+5)	5.51(+5)			3.55(+5)	4.30(+5)
4715	1.08(+5)	4.39(+4)	1.49(+5)	3.45(+5)	2.15(+5)	2.30(+5)	3.19(+5)	4.05(+5)			3.15(+5)	3.26(+5)
4900	7.84(+4)	3.25(+4)	1.25(+5)	2.25(+5)	1.58(+5)	1.44(+5)	2.48(+5)	2.61(+5)			2.68(+5)	2.07(+5)
4900	5.53(+4)	2.30(+4)	9.14(+4)	1.61(+5)	1.13(+5)	1.02(+5)	1.79(+5)	1.84(+5)			1.95(+5)	1.47(+5)
5000	5.25(+4)	2.18(+4)	8.72(+4)	1.70(+5)	1.17(+5)	1.13(+5)	1.89(+5)	2.00(+5)			1.93(+5)	1.62(+5)
5175	3.54(+4)	1.63(+4)	7.07(+4)	1.65(+5)	1.13(+5)	1.09(+5)	1.76(+5)	1.93(+5)			1.70(+5)	1.60(+5)
5300	5.78(+4)	2.56(+4)	1.11(+5)	1.25(+5)	1.04(+5)	8.60(+4)	1.76(+5)	1.50(+5)			2.06(+5)	1.29(+5)
5360	5.80(+4)	2.60(+4)	1.17(+5)	1.10(+5)	9.54(+4)	7.51(+4)	1.66(+5)	1.32(+5)			2.07(+5)	1.13(+5)
5360	3.09(+5)	1.42(+5)	6.15(+5)	5.94(+5)	5.12(+5)	4.07(+5)	8.90(+5)	7.14(+5)			1.07(+6)	6.13(+5)
5864	3.26(+5)	1.54(+5)	5.88(+5)	4.09(+5)	4.40(+5)	2.99(+5)	8.32(+5)	5.16(+5)			1.05(+6)	4.69(+5)
5892	2.65(+5)	1.20(+5)	4.85(+5)	4.10(+5)	4.30(+5)	2.93(+5)	8.12(+5)	5.11(+5)			9.20(+5)	4.61(+5)
6110	3.38(+5)	1.72(+5)	7.26(+5)	3.78(+5)	4.32(+5)	2.75(+5)	8.41(+5)	4.74(+5)			1.07(+6)	4.40(+5)
6180	3.26(+5)	1.65(+5)	5.74(+5)	3.54(+5)	4.14(+5)	2.59(+5)	8.15(+5)	4.49(+5)			1.05(+6)	4.18(+5)
6386	2.91(+5)	1.48(+5)	6.36(+5)	2.79(+5)	3.52(+5)	2.07(+5)	7.13(+5)	3.56(+5)			9.11(+5)	3.37(+5)
6564	2.47(+5)	1.35(+5)	5.40(+5)	1.81(+5)	2.51(+5)	1.17(+5)	5.64(+5)	2.16(+5)			7.30(+5)	2.00(+5)
6620	2.39(+5)	1.29(+5)	5.25(+5)	1.95(+5)	2.62(+5)	1.45(+5)	5.55(+5)	2.52(+5)			7.10(+5)	2.42(+5)
7000	1.22(+5)	6.69(+4)	3.10(+5)	8.75(+4)	1.28(+5)	6.72(+4)	2.82(+5)	1.15(+5)			3.60(+5)	1.14(+5)
7100	9.88(+4)	5.34(+4)	2.05(+5)	6.75(+4)	1.02(+5)	5.18(+4)	2.26(+5)	8.96(+4)			2.85(+5)	8.89(+4)
7400	3.87(+4)	2.26(+4)	1.07(+5)	2.37(+4)	3.71(+4)	1.86(+4)	8.59(+4)	3.23(+4)			1.13(+5)	3.23(+4)
7400	1.68(+4)	1.01(+4)	4.82(+4)						1.29(+4)	1.89(+4)		
7980	1.39(+4)	8.59(+3)	4.07(+4)						1.01(+4)	1.42(+4)		
8190	1.25(+4)	7.72(+3)	3.88(+4)						9.09(+3)	1.27(+4)		
8400	1.14(+4)	7.26(+3)	3.53(+4)						8.11(+3)	1.11(+4)		
8662	1.00(+4)	6.44(+3)	3.06(+4)						6.81(+3)	9.44(+3)		
8800	1.03(+4)	6.61(+3)	3.44(+4)						7.47(+3)	9.68(+3)		
8900	1.05(+4)	6.71(+3)	3.45(+4)						7.25(+3)	9.46(+3)		
9200	9.03(+3)	5.90(+3)	2.87(+4)						5.90(+3)	7.91(+3)		
10300	4.80(+3)	3.18(+3)	1.78(+4)						3.27(+3)	3.84(+3)		
10700	2.82(+3)	1.89(+3)	1.07(+4)						1.82(+3)	2.11(+3)		

TABLE 5

PROGRAM STAR COLORS

WAVELENGTH		3880	4040	4100	4200	4227	4300	4340	4500	4715	4900	5000
BS	3	287	925	1010	980	1050	780	1280	1460	1290	1030	1060
BS	45	88	282	362	405	263	425	690	901	921	785	709
BS	165	140	535	640	617	641	641	1060	1220	1150	942	946
BS	224	93	340	414	437	358	449	769	1000	1000	844	844
BS	258	296	951	1060	1020	1080	842	1390	1540	1340	1040	1070
BS	271	384	1110	1160	1130	1270	979	1410	1550	1350	1060	1090
BS	337	82	286	358	394	305	418	680	911	968	823	777
BS	464	136	542	622	592	643	593	995	1170	1080	921	941
BS	489	128	482	561	567	554	571	933	1150	1110	918	935
BS	495	257	873	951	916	1060	858	1330	1450	1250	1030	1020
BS	617	221	765	866	829	909	721	1180	1370	1260	1010	1040
BS	882	171	630	703	697	732	630	1070	1260	1160	960	992
BS	911	78	247	310	351	242	370	609	801	867	757	708
BS	941	311	1020	1070	1010	1170	901	1370	1510	1300	1050	1080
BS	947	232	824	897	823	964	765	1230	1370	1250	1020	1030
BS	951	280	936	1010	952	1080	843	1330	1470	1280	1030	1060
BS	1015	179	610	671	657	706	652	1050	1210	1120	934	969
BS	1052	123	478	557	563	568	568	925	1110	1110	922	948
BS	1136	389	1100	1200	1210	1210	900	1440	1650	1370	1080	1110
BS	1457	86	305	387	409	318	438	719	943	961	820	807
BS	1551	128	466	540	547	563	536	880	1080	1070	899	945
BS	1726	186	650	713	733	710	657	1080	1300	1210	968	981
BS	1773	105	404	472	459	447	501	881	1040	1030	868	876
BS	1805	108	445	506	480	516	532	930	1110	1070	918	916
BS	1907	426	1150	1240	1260	1270	926	1400	1590	1390	1080	1140
BS	2012	232	829	891	824	948	752	1230	1400	1270	1020	1040
BS	2219	312	1020	1090	1050	1130	841	1310	1500	1320	1060	1100
BS	2429	277	928	966	938	1020	803	1360	1510	1340	1040	1050
BS	2478	208	765	838	791	873	747	1180	1330	1210	992	1020
BS	2600	204	749	796	789	820	677	1090	1300	1230	1000	998
BS	2649	118	450	530	518	525	532	906	1120	1080	904	930
BS	2697	148	576	640	609	687	633	1050	1200	1110	940	943
BS	2805	184	672	716	661	801	646	1070	1230	1170	974	979
BS	2821	309	1010	1060	1020	1130	842	1330	1500	1320	1060	1080
BS	2985	400	1200	1230	1180	1290	992	1470	1640	1410	1110	1120
BS	2990	315	1020	1080	1030	1120	849	1370	1520	1340	1060	1080
BS	3145	175	640	731	726	733	665	1070	1270	1180	988	1010
BS	3149	219	771	847	809	883	732	1190	1360	1230	997	1020
BS	3249	96	367	446	451	418	498	794	1000	1020	862	884
BS	3366	154	587	681	655	682	641	1090	1260	1150	955	973
BS	3369	301	1010	1060	990	1140	893	1380	1500	1330	1050	1050
BS	3905	152	604	664	629	701	637	1110	1240	1140	955	949
BS	3994	295	1010	1020	965	1110	815	1370	1500	1310	1040	1060
BS	4171	411	1160	1210	1180	1270	956	1430	1560	1360	1060	1110
BS	4301	308	896	918	917	1040	859	1210	1390	1250	1010	1050
BS	4517	111	331	404	449	347	470	716	914	943	810	788
BS	4737	211	738	822	764	899	753	1210	1330	1200	978	1010
BS	4932	377	1070	1150	1080	1250	982	1390	1500	1300	1020	1070
BS	5154	84	252	328	369	262	399	615	810	864	746	717
BS	5159	232	723	828	754	859	699	1150	1290	1150	947	989
BS	5200	89	313	393	410	335	445	730	943	951	805	827
BS	5201	110	394	487	495	482	505	829	1030	1020	863	914
BS	5227	191	671	747	739	747	662	1110	1290	1170	951	983
BS	5247	105	390	463	471	463	496	818	1000	1020	858	897
BS	5370	154	591	683	643	723	653	1070	1230	1100	925	961
BS	5429	138	517	625	592	626	590	977	1160	1090	915	960
BS	5480	376	1000	1080	1020	1180	920	1310	1450	1290	1020	1070
BS	5502	333	1040	1120	1060	1200	958	1350	1480	1280	1030	1100
BS	5582	153	558	624	572	664	605	1060	1170	1090	911	937
BS	5600	93	329	428	432	386	474	780	978	984	823	862
BS	5601	299	899	1020	971	1040	817	1260	1410	1270	994	1060
BS	5602	383	1090	1160	1110	1260	953	1370	1510	1320	1040	1100
BS	5616	162	578	685	649	711	615	1020	1190	1120	928	992
BS	5681	392	1090	1200	1170	1250	949	1370	1520	1320	1040	1110
BS	5739	77	252	320	352	262	397	622	826	883	763	747
BS	5777	307	941	1050	1010	1080	862	1320	1480	1280	1020	1060
BS	5826	78	277	358	365	291	423	696	884	915	787	800

TABLE 5--CONTINUED

5175	5300	5864	5892	6110	6180	6386	6564	6620	7000	7100	7400	REMARK
985	1030	954	904	966	936	822	657	638	320	258	98	
572	967	905	773	1210	859	1070	912	877	555	333	201	
799	978	1020	885	1060	1010	900	722	720	365	291	113	
679	962	1040	919	1160	1040	1020	844	824	453	335	149	
913	1030	946	876	959	931	803	630	626	313	249	92	
1080	1040	919	883	931	902	784	610	606	300	242	90	
641	940	979	854	1200	965	1070	887	872	517	349	177	
813	992	1000	909	1030	991	892	714	703	359	283	112	
810	994	1030	939	1080	1040	950	775	759	400	314	126	
918	1030	950	856	965	921	794	635	628	308	244	91	
965	1010	978	937	1010	980	862	690	680	349	280	108	
899	1010	1000	934	1040	1000	888	717	702	357	285	112	
589	946	940	800	1240	887	1080	911	898	579	346	209	
1050	1050	939	893	939	899	780	618	605	298	238	90	
1010	1030	954	908	975	936	817	654	639	322	255	98	
1020	1030	943	897	963	922	810	633	623	317	246	95	
855	999	1010	915	1050	1010	900	719	707	361	287	111	
809	984	1040	964	1110	1060	966	781	764	402	317	126	
970	1050	938	878	933	907	787	614	607	303	241	91	R
647	951	1020	891	1180	1000	1040	872	857	490	344	169	
848	992	1060	975	1120	1080	988	796	790	421	332	133	
819	1010	1010	946	1060	1020	922	736	723	377	296	116	R
730	952	1020	864	1090	1030	935	759	753	390	298	124	R
777	972	1000	889	1060	1010	901	730	718	367	284	116	R
1060	1060	934	912	944	915	801	633	623	316	253	96	R
1010	1030	959	912	981	948	833	661	650	329	259	100	
1070	1050	947	919	953	919	811	640	634	319	254	97	R
920	1040	959	874	965	933	812	643	632	311	247	94	
962	1010	979	913	1000	968	860	679	671	342	270	103	R
918	1020	991	948	1030	995	889	705	694	362	287	112	
809	974	1030	934	1080	1040	944	761	750	386	306	123	
871	982	987	894	1030	985	876	702	682	348	270	106	
993	1010	974	910	1010	971	845	673	665	335	264	104	
1050	1040	941	905	954	919	800	633	619	312	249	94	
1110	1060	922	882	927	894	777	601	601	300	236	89	
1050	1040	927	888	931	901	784	627	614	307	246	94	
889	1010	1010	965	1070	1010	924	735	724	380	299	116	
940	1020	961	901	990	952	836	665	653	331	261	101	
756	957	1050	941	1140	1070	1010	824	808	430	335	139	
845	1010	994	909	1040	1000	888	714	700	355	281	110	
1040	1010	938	896	947	912	801	623	615	307	245	93	
819	997	978	863	1010	974	850	684	670	334	265	104	
1020	1030	928	870	933	897	771	611	600	290	233	87	R
1090	1040	914	879	921	886	775	607	590	289	233	87	
1040	1030	967	913	996	957	848	665	665	335	270	103	R
625	967	992	888	1210	956	1080	905	885	534	357	183	
934	1020	978	891	996	956	849	669	661	329	264	100	
1080	1020	936	893	942	909	793	613	619	304	245	91	R
591	945	959	827	1270	912	1120	947	935	595	362	212	
896	989	987	916	998	969	852	679	674	332	272	101	
664	957	1050	909	1210	1040	1060	881	870	486	351	164	
768	971	1060	977	1140	1080	1010	822	809	427	337	136	
804	1010	995	921	1030	1000	890	709	697	352	282	109	
761	970	1060	961	1140	1080	1010	824	810	427	337	136	
824	994	1010	919	1040	997	894	716	705	355	282	109	
839	998	1040	964	1080	1050	947	765	752	385	311	123	
1090	1030	952	909	965	929	816	638	635	312	254	94	R
1070	1040	944	903	956	911	808	627	623	311	250	93	
807	989	1000	865	1050	1010	893	711	707	350	279	109	
710	953	1070	941	1190	1080	1050	860	852	461	351	150	
1020	1030	988	932	1010	973	860	680	670	336	273	103	
1130	1050	930	899	942	903	790	607	608	305	244	91	
896	1010	1030	972	1070	1040	936	757	741	382	309	121	
1090	1050	957	921	961	929	816	635	633	321	258	97	R
624	936	992	852	1250	975	1110	919	916	545	360	187	
939	1030	957	904	977	940	833	655	647	322	261	97	
662	929	1030	853	1190	1040	1050	866	863	475	344	158	

TABLE 5--CONTINUED

WAVELENGTH		3880	4040	4100	4200	4227	4300	4340	4500	4715	4900	5000
BS	5854	174	652	744	687	819	716	1150	1280	1150	942	972
BS	5888	317	986	1070	1020	1130	858	1300	1460	1280	1020	1080
BS	5889	649	1420	1430	1520	1530	1170	1560	1690	1450	1100	1180
BS	5901	302	930	1060	1010	1080	871	1340	1460	1280	1010	1060
BS	5940	209	714	807	774	829	717	1170	1320	1190	964	998
BS	5947	169	626	724	684	762	665	1050	1220	1140	940	998
BS	5966	357	1040	1130	1070	1180	874	1330	1500	1310	1030	1080
BS	6014	329	939	1090	1080	1060	856	1330	1530	1310	1030	1070
BS	6018	295	937	1060	1010	1110	858	1330	1480	1310	1020	1070
BS	6103	328	1010	1080	1020	1170	903	1360	1490	1280	1010	1080
BS	6220	404	1160	1240	1200	1350	1040	1430	1570	1360	1060	1130
BS	6623	585	1450	1470	1560	1630	1240	1580	1790	1430	1110	1160
BS	6770	371	1090	1150	1110	1240	963	1380	1540	1330	1050	1100
BS	6791	424	1140	1200	1190	1320	1170	1470	1560	1340	1040	1090
BS	6817	375	1070	1170	1140	1190	929	1410	1580	1340	1050	1090
BS	6869	378	1080	1200	1190	1270	983	1400	1560	1340	1050	1110
BS	6872	196	692	771	722	830	692	1140	1280	1160	963	998
BS	7149	274	866	932	875	991	730	1240	1420	1240	996	1050
BS	7176	263	871	930	858	1010	804	1290	1440	1270	1010	1040
BS	7373	596	1480	1460	1550	1570	1130	1590	1820	1470	1100	1150
BS	7405	107	363	425	465	351	474	772	1030	1020	841	785
BS	7429	188	662	759	741	777	693	1130	1290	1160	950	989
BS	7430	320	878	912	898	1030	784	1180	1350	1210	954	1020
BS	7576	136	531	595	570	616	610	1060	1190	1110	929	917
BS	7602	482	1230	1360	1380	1390	991	1480	1670	1410	1080	1120
BS	7670	619	1490	1520	1610	1600	1180	1620	1850	1500	1120	1160
BS	7806	126	465	575	568	567	589	949	1150	1090	899	937
BS	7831	213	731	809	749	879	706	1180	1340	1200	992	1010
BS	7949	283	918	1030	982	1090	849	1270	1430	1260	1020	1070
BS	7957	420	1190	1270	1280	1290	929	1460	1660	1430	1080	1130
BS	8082	323	978	1070	1010	1090	841	1320	1480	1320	1020	1090
BS	8255	252	844	912	858	993	753	1240	1400	1240	1000	1040
BS	8317	233	803	872	816	936	752	1250	1390	1250	1000	1020
BS	8448	496	1160	1290	1280	1340	1040	1440	1610	1360	1060	1090
BS	8551	317	924	1050	1030	1070	817	1290	1470	1310	1040	1080
BS	8841	266	846	918	883	950	714	1200	1410	1240	991	1030
BS	8857	250	857	946	899	1000	810	1300	1450	1290	1020	1040
BS	8924	212	769	835	806	866	749	1280	1420	1240	997	997
BS	8974	272	914	1010	974	1030	820	1330	1500	1310	1030	1050
HD	29038	162	617	695	680	711	659	1100	1270	1130	947	948
HD	122563	843	1310	1330	1470	1450	1300	1420	1460	1330	996	1160
HD	165195	522	953	1040	1130	1170	1050	1200	1300	1220	952	1100
BS	1346	345	1050	1110	1050	1240	960	1400	1530	1340	1060	1080
BS	1373	331	1040	1110	1040	1230	934	1400	1530	1340	1060	1080
BS	1409	310	1000	1070	1000	1190	912	1390	1520	1340	1050	1070
BS	1411	398	1130	1180	1140	1280	991	1460	1610	1390	1070	1100
M13	59	134	374	443	472	559	515	697	889	964	828	949
FAG	84	262	935	1000	934	1050	823	1320	1470	1300	1050	1050
FAG	105	183	659	741	723	762	674	1140	1320	1200	980	983
FAG	108	134	505	572	583	567	568	970	1160	1110	919	949
FAG	141	264	948	1010	947	1070	821	1360	1520	1330	1060	1070
FAG	151	286	979	1030	975	1070	866	1380	1530	1360	1060	1090
FAG	170	136	526	623	610	640	607	1000	1200	1140	937	971
FAG	193	392	1150	1230	1180	1250	984	1480	1670	1400	1090	1120
FAG	224	246	863	928	865	985	838	1320	1440	1290	1020	1040
MUR	1465	88	309	392	405	333	445	750	954	975	816	827
I	1	370	979	964	999	1060	836	1240	1440	1290	1010	1070
I	69	201	660	701	693	755	613	1130	1320	1220	963	1010
I	105	255	846	870	834	959	736	1250	1420	1280	1030	1050
II	75	203	691	767	791	764	677	1100	1310	1220	986	991
II	181	225	688	729	702	749	620	1070	1290	1170	929	958
III	4	285	906	974	962	982	809	1290	1470	1270	1010	1030
III	18	96	359	421	434	382	479	787	1000	997	846	865
BD+	37418	345	1050	1100	1080	1190	912	1370	1520	1320	1050	1080
BD+	37432	343	1060	1120	1090	1190	908	1360	1520	1320	1060	1090
BD+	37448	321	1000	1050	1010	1140	865	1340	1480	1310	1030	1060
K	751	74	272	331	375	269	385	644	856	902	771	767

TABLE 5—CONTINUED

5175	5300	5864	5892	6110	6180	6386	6564	6620	7000	7100	7400	REMARK
879	998	969	885	997	968	856	679	674	334	267	103	
1060	1040	959	919	971	934	828	649	643	324	258	97	
1160	1090	903	879	907	870	764	584	582	288	231	85	
945	1020	963	902	976	937	825	646	640	320	259	97	
848	1020	988	912	1020	972	870	692	679	342	276	105	
900	985	1010	953	1050	1010	913	732	724	373	300	116	
1090	1050	952	914	958	927	820	637	632	319	256	96	
882	1040	954	882	961	932	816	639	630	315	253	95	
974	1030	964	915	981	939	830	651	645	326	262	98	
1030	1030	950	894	956	913	801	621	620	309	249	92	
1110	1050	920	894	929	891	780	614	609	307	244	92	
1100	1060	886	855	880	841	726	552	560	276	218	81	
1110	1060	940	899	952	908	796	611	612	304	240	91	
1080	1040	931	876	938	897	785	608	609	306	244	92	R
994	1050	942	893	948	913	801	623	613	307	247	92	
1050	1030	930	897	947	908	797	629	623	312	251	95	
946	1010	979	910	1000	974	855	681	672	336	268	103	
998	1050	952	904	964	936	816	646	639	311	254	95	R
977	1030	952	887	966	932	817	644	635	316	254	96	R
1080	1070	898	847	883	852	728	545	556	269	216	79	
623	1000	939	829	1150	906	1030	849	824	487	323	163	R
812	1010	1000	910	1020	983	876	699	687	349	279	108	R
1050	1020	994	923	1020	979	860	682	678	343	273	105	
763	979	1000	858	1050	1010	890	714	708	354	279	109	R
1070	1050	917	883	922	889	779	600	597	299	239	91	
1050	1060	894	854	887	848	732	545	560	269	217	78	
815	973	1020	930	1070	1020	915	752	738	382	302	121	R
919	1020	978	908	1000	961	850	670	667	333	266	104	
1040	1030	946	922	969	931	822	657	646	331	264	101	
1060	1060	928	889	930	900	786	614	610	305	247	92	R
1060	1050	957	919	965	930	815	638	634	321	256	96	
997	1040	956	904	979	945	827	654	640	320	255	96	R
954	1020	964	892	988	948	833	656	650	323	259	98	
1010	1040	949	883	946	910	808	632	617	310	248	94	R
974	1050	964	920	973	950	838	683	648	329	266	100	
962	1020	974	924	978	945	837	656	647	326	264	100	
952	1040	962	896	977	943	829	654	642	322	259	96	
816	1020	979	845	994	960	834	666	652	323	256	98	
928	1020	947	891	967	943	818	648	638	318	256	96	
788	991	991	892	1040	988	883	703	691	348	276	107	
1270	1100	965	954	1010	977	868	688	674	349	280	107	R
1210	1090	1000	980	1050	1010	899	729	706	371	297	114	R
1060	1020	930	878	937	904	778	608	602	297	237	89	1
1070	1030	929	880	941	909	781	611	605	300	240	90	1
1060	1020	930	880	941	908	784	613	608	300	241	91	1
1070	1040	920	869	930	896	778	599	598	294	236	88	1
1060	1020	1110	1060	1180	1170	1080	881	856	473	376	157	R
1000	1030	935	876	940	914	794	619	608	299	239	89	2
866	1000	990	905	1000	978	857	688	676	334	267	103	2
791	985	1020	911	1060	1010	915	732	724	361	289	113	2
1000	1030	941	882	954	913	802	621	614	303	237	88	2
1030	1050	929	866	946	904	793	620	608	299	233	87	2
826	992	1010	921	1050	1000	906	719	712	360	282	111	2
987	1050	936	877	925	904	780	615	607	300	238	89	2
938	1010	948	861	969	936	813	641	628	310	246	93	2
659	947	1030	874	1170	1010	1030	843	828	458	327	152	2
974	1050	949	894	975	942	824	655	652	314	251	99	3
854	1010	992	886	1020	981	861	703	686	344	262	107	3
991	1060	949	879	961	919	813	645	636	308	245	94	3
823	1010	989	912	1020	976	885	704	689	358	288	112	3
837	1010	981	906	1030	983	877	692	677	343	276	107	3
882	1030	968	893	977	951	815	654	638	322	255	97	3
674	965	1040	893	1140	1030	997	811	805	420	321	138	3
1080	1040	939	905	949	912	800	628	618	307	246	94	4
1090	1040	941	908	950	918	795	627	610	307	243	91	4
1050	1040	941	910	957	918	811	632	621	313	247	93	4
658	930	1040	894	1230	1020	1080	906	885	509	356	168	5

TABLE 6

SURVEY STAR COLORS

WAVELENGTH		3880	4040	4100	4200	4227	4300	4340	4500	4715	4900	5000
BS	6136	97	360	442	436	415	484	824	986	985	835	867
BS	6148	406	1150	1200	1150	1330	1010	1400	1550	1350	1060	1100
BS	6154	78	263	341	358	282	402	660	851	908	778	764
BS	6159	98	337	429	459	387	484	767	999	989	849	838
BS	6228	81	290	375	390	307	435	717	922	944	796	796
BS	6239	516	1300	1250	1330	1460	1170	1430	1620	1390	1060	1100
BS	6258	78	265	340	365	294	414	644	864	899	778	794
BS	6287	382	1090	1180	1130	1240	956	1380	1530	1330	1040	1100
BS	6292	421	1160	1270	1240	1330	1010	1440	1580	1360	1050	1120
BS	6293	108	406	505	500	475	533	873	1090	1050	874	887
BS	6299	210	722	805	755	844	685	1150	1340	1180	964	993
BS	6305	486	1250	1360	1330	1420	1070	1510	1660	1440	1090	1140
BS	6307	249	830	906	856	987	772	1230	1360	1210	970	1030
BS	6325	150	539	613	569	692	592	958	1130	1080	922	961
BS	6342	300	909	1050	989	1070	861	1270	1440	1290	1000	1070
BS	6364	152	548	618	607	609	597	1010	1210	1130	924	952
BS	6390	300	896	1040	983	1080	854	1270	1430	1250	1020	1070
BS	6393	100	300	374	402	348	426	641	840	880	766	761
BS	6443	356	1050	1170	1090	1220	945	1400	1530	1330	1050	1090
BS	6452	76	268	324	354	306	391	617	853	891	776	731
BS	6476	183	609	708	640	816	747	1040	1150	1070	906	944
BS	6526	108	393	486	474	467	505	848	1040	1030	869	903
BS	6542	323	973	1050	1010	1120	850	1300	1440	1270	1010	1070
BS	6575	329	966	1050	1000	1150	895	1320	1460	1280	1010	1040
BS	6590	193	610	697	655	767	646	1000	1160	1120	928	982
BS	6602	103	377	458	472	404	498	831	1030	997	857	850
BS	6603	185	676	770	730	838	712	1170	1310	1170	973	986
BS	6608	757	1670	1590	1770	1810	1330	1610	1840	1490	1110	1190
BS	6644	210	707	781	754	858	728	1140	1290	1150	962	999
BS	6654	246	839	935	884	1020	811	1220	1380	1240	995	1030
BS	6665	339	994	1090	1050	1160	907	1340	1460	1270	1010	1080
BS	6687	153	573	656	624	695	615	1020	1180	1100	920	973
BS	6703	394	1120	1190	1140	1300	1020	1430	1580	1350	1060	1100
BS	6763	163	596	682	668	700	609	1040	1210	1130	920	979
BS	6765	78	250	325	353	232	383	595	754	825	717	635
BS	6800	189	664	768	730	785	669	1100	1270	1160	954	983
BS	6820	107	399	473	490	466	478	830	1050	1050	868	911
BS	6868	79	262	338	363	265	396	659	873	894	772	738
BS	6882	74	262	329	361	296	383	635	861	924	786	788
BS	6885	176	610	699	683	712	621	1050	1230	1160	953	989
BS	6895	206	708	791	774	815	677	1140	1330	1210	974	1010
BS	6966	96	363	453	445	429	472	815	1010	1010	860	883
BS	6980	318	1010	1080	1020	1180	908	1370	1510	1310	1040	1060
BS	7064	191	651	752	733	783	679	1100	1270	1160	948	991
BS	7112	222	733	828	764	898	700	1130	1270	1160	958	1000
BS	7132	120	456	555	548	545	543	913	1120	1080	892	923
BS	7181	184	640	715	714	719	618	1060	1270	1170	941	979
BS	7918	174	625	722	721	739	664	1110	1280	1180	955	988
BS	7923	420	1130	1240	1190	1300	954	1400	1540	1350	1050	1100
BS	7939	194	680	793	735	853	707	1110	1270	1160	955	997
BS	7995	547	1320	1390	1380	1490	1130	1510	1660	1410	1080	1150
BS	8008	96	353	447	443	426	480	803	1010	1010	850	872
BS	8011	269	799	914	859	982	790	1200	1380	1250	1010	1040
BS	8030	422	1120	1230	1190	1290	1000	1410	1560	1350	1050	1090
BS	8032	109	399	494	491	472	505	862	1060	1040	863	897
BS	8066	73	259	320	323	303	368	636	838	890	787	796
BS	8163	80	251	319	361	264	389	607	820	877	754	722
BS	8173	248	808	910	857	941	739	1230	1410	1240	993	1030
BS	8197	281	890	1000	923	1070	821	1280	1430	1260	1020	1040
BS	8225	79	264	343	367	254	410	669	874	924	779	736
BS	8277	297	928	1030	954	1080	799	1280	1450	1260	1010	1070
BS	8287	105	395	486	465	496	501	829	1010	1030	877	913
BS	8325	171	621	721	697	744	651	1090	1250	1160	944	963
BS	8390	151	564	663	644	702	640	1040	1210	1150	945	971
BS	8393	97	374	459	454	427	485	857	1020	1000	856	880
BS	8413	99	357	435	431	386	468	813	1010	980	836	846
BS	8415	157	576	677	658	704	616	1040	1210	1140	939	983

TABLE 6—CONTINUED

5175	5300	5864	5892	6110	6180	6386	6564	6620	7000	7100	7400	REMARK
713	955	1050	859	1150	1060	994	813	805	420	326	136	
1130	1040	940	905	938	904	803	613	613	307	244	92	
634	937	1040	871	1240	1020	1100	911	907	527	360	178	
675	985	1050	942	1180	1050	1060	867	854	474	345	155	
635	937	1030	873	1210	1020	1070	883	874	492	344	163	
1140	1060	931	888	926	890	783	597	609	302	239	90	
652	941	1050	907	1240	1030	1090	903	901	523	361	174	
1070	1030	952	908	952	921	813	628	627	314	252	96	
1100	1060	942	909	943	904	801	615	614	310	250	93	
718	968	1050	939	1130	1060	1000	809	804	423	329	136	
900	1010	990	920	1000	972	860	677	675	336	269	104	
1140	1090	940	900	944	903	797	618	613	308	247	92	
966	1020	980	932	994	962	845	666	661	335	268	101	
924	995	1030	942	1060	1010	913	718	728	364	290	115	
994	1040	968	936	985	949	851	666	659	333	267	103	
814	1020	1010	927	1070	1040	927	753	739	378	303	118	
988	1040	967	924	979	949	838	664	655	330	267	102	
635	949	986	868	1260	949	1120	938	926	572	362	201	
1080	1040	949	906	951	920	802	632	624	315	251	95	
606	946	985	867	1240	953	1120	919	902	544	349	186	
951	982	1030	942	1060	1010	879	727	723	371	294	113	
767	974	1050	948	1120	1070	978	795	789	412	325	130	
1040	1020	945	908	963	934	814	668	631	313	253	93	
1030	1040	969	915	987	946	841	656	651	327	261	97	
962	979	1020	943	1070	1020	911	737	727	370	298	117	
667	967	1020	897	1140	1030	994	817	799	436	324	140	
885	1010	982	899	1010	974	859	690	672	337	268	105	
1180	1070	886	859	875	832	713	521	538	264	207	75	
866	1000	986	916	1030	971	869	682	671	344	270	104	
975	1020	959	907	990	964	842	662	651	332	263	100	
1060	1030	941	899	950	924	802	624	626	311	246	95	
889	996	1010	932	1050	1010	896	720	708	363	289	112	
1100	1050	927	880	938	905	785	603	600	302	239	89	
879	996	1020	942	1080	1030	925	735	719	376	300	118	
538	937	859	717	1310	810	1130	963	924	677	358	252	
929	985	1010	938	1050	1000	888	699	688	353	282	108	
768	991	1070	983	1180	1100	1020	833	817	446	348	143	
607	952	1000	855	1260	982	1090	914	890	533	355	183	
649	954	1070	940	1270	1080	1140	945	941	549	383	186	
901	1000	1020	947	1050	1020	915	729	720	373	299	114	
890	1030	990	922	1030	994	869	694	686	348	281	108	
766	958	1060	964	1170	1080	1010	821	813	435	341	138	
1060	1030	942	890	974	917	806	626	613	309	248	93	
893	1010	998	929	1030	992	885	704	692	354	283	110	
1010	1010	986	928	1030	985	873	688	680	347	277	107	
786	978	1050	961	1110	1060	959	778	767	401	317	126	
869	986	1020	950	1060	1020	917	730	711	373	300	115	
870	1010	1020	945	1040	1010	907	724	719	365	293	113	
1110	1050	939	915	956	913	801	622	628	314	252	94	
928	990	983	927	1010	972	870	688	680	348	278	106	
1150	1050	910	886	910	873	762	579	583	289	232	87	
746	965	1070	937	1140	1080	997	816	811	427	334	139	
1020	1020	972	926	993	959	847	666	664	336	265	104	
1070	1040	933	897	942	900	792	614	611	305	245	92	
763	969	1040	943	1110	1060	972	791	786	413	326	132	
699	925	1080	922	1220	1100	1060	873	886	474	358	161	
593	937	970	853	1260	931	1130	938	937	579	364	208	
958	1030	973	925	982	953	843	665	658	327	264	102	
1010	1020	953	918	966	929	813	639	632	317	254	95	
596	937	939	803	1220	939	1070	897	883	527	340	186	
1020	1030	956	917	961	928	817	636	635	315	255	96	
814	956	1070	968	1130	1090	994	809	802	417	335	136	
852	990	1000	924	1000	991	880	713	695	355	286	113	
875	999	1010	941	1060	1020	916	737	716	372	296	116	
736	958	1050	932	1130	1070	986	812	793	418	325	136	
681	974	1020	872	1120	1030	960	795	780	411	314	136	
882	1000	1020	940	1050	1020	910	740	721	371	300	117	

TABLE 6—CONTINUED

TABLE 6—CONTINUED

WAVELENGTH		3880	4040	4100	4200	4227	4300	4340	4500	4715	4900	5000	5175	5300	5864	5892	6110	6180	6386	6564	6620	7000	7100	7400	REMARK
BS	8458	80	273	356	384	262	407	681	881	925	776	739	589	949	971	826	1230	934	1090	917	890	541	342	189	
BS	8461	348	1050	1170	1140	1240	951	1410	1550	1330	1060	1080	1020	1050	943	878	943	910	793	622	611	306	244	92	
BS	8482	188	679	795	761	828	719	1190	1340	1210	990	1000	862	1020	993	897	1010	975	860	689	676	341	271	103	
BS	8562	85	300	376	400	322	417	697	912	950	807	818	673	949	1040	922	1190	1050	1050	866	859	478	352	156	
BS	8564	169	619	706	653	762	658	1090	1220	1170	956	979	936	993	989	914	1020	983	868	697	683	346	278	108	
BS	8618	419	1180	1240	1200	1340	1020	1400	1560	1360	1060	1100	1100	1040	938	903	945	914	790	622	607	305	248	92	
BS	8642	278	790	901	873	948	743	1200	1370	1200	986	1010	961	1010	974	911	978	964	838	665	657	332	268	102	
BS	8660	284	922	1030	966	1110	810	1290	1450	1280	1040	1070	1040	1030	955	905	958	929	812	642	628	321	256	96	
BS	8703	266	781	886	854	935	817	1190	1350	1210	980	1000	930	989	986	907	1000	997	857	684	676	345	272	106	
BS	8730	221	807	887	816	969	765	1240	1370	1220	1010	1020	982	1020	977	910	989	953	836	659	653	327	265	101	
BS	8742	322	1040	1090	1020	1210	927	1420	1510	1330	1050	1070	1040	1030	935	863	938	910	779	607	601	297	238	90	
BS	8751	124	484	583	560	579	581	968	1140	1100	914	936	794	980	1040	932	1090	1050	944	763	748	390	306	126	
BS	8785	368	1160	1150	1110	1240	925	1420	1520	1320	1040	1100	1070	1030	931	887	935	896	780	601	604	294	239	89	
BS	8795	85	278	364	390	257	422	713	913	933	782	746	605	947	934	797	1190	944	1040	887	862	509	336	175	
BS	8824	130	479	588	567	584	580	975	1140	1100	912	924	815	968	1020	934	1070	1030	931	747	739	380	306	121	
BS	8833	342	1040	1120	1070	1170	837	1340	1510	1330	1050	1090	1070	1040	943	914	954	921	803	628	620	313	253	94	
BS	8842	586	1370	1370	1410	1540	1180	1480	1630	1380	1080	1140	1210	1060	919	883	916	874	752	571	579	289	232	85	
BS	8852	484	1250	1320	1300	1360	979	1430	1620	1410	1080	1160	1120	1070	938	910	936	909	791	620	613	308	250	95	
BS	8878	229	727	814	821	861	731	1100	1290	1220	982	1030	929	1020	1010	967	1050	1010	910	723	714	373	305	117	
BS	8893	131	510	602	586	609	593	993	1170	1110	928	979	826	983	1030	931	1060	1020	908	730	720	373	297	117	
BS	8912	323	968	1060	999	1120	843	1300	1440	1280	1020	1090	1060	1050	940	910	954	921	813	640	630	314	253	96	
BS	8916	262	866	945	897	1010	788	1270	1420	1260	1010	1040	992	1030	958	907	969	935	820	650	638	322	256	98	
BS	8922	252	853	973	911	1050	786	1260	1440	1260	1030	1070	1020	1050	958	918	973	942	836	655	644	330	265	102	
BS	8923	395	1130	1170	1150	1250	961	1430	1580	1370	1060	1090	1090	1030	931	884	888	896	773	602	597	298	235	91	
BS	8991	78	263	314	362	285	387	602	848	899	786	725	618	958	959	841	1250	921	1120	938	909	573	357	199	
BS	8997	416	1170	1230	1200	1340	1010	1450	1600	1380	1080	1120	1110	1040	934	905	939	904	788	610	606	305	242	91	
BS	9035	81	264	342	370	259	406	661	860	897	779	705	574	952	923	789	1220	880	1090	908	863	554	334	194	
BS	9055	78	266	339	370	263	405	655	862	909	780	720	579	949	940	792	1220	888	1090	920	889	562	343	199	

1 percent (s.d.) in the blue and 0.7 percent (s.d.) in the yellow and red, except for the $\lambda 3880$ and $\lambda 4300$ points (for which the standard deviation is 1.5 percent) and for all wavelengths in all stars in NGC 188 (for which the error bars are twice as large as usual). We expect that the errors in the indices will be of the same order, yielding in most cases errors in w of about ± 0.01.

VII. THE SELECTION OF THE STARS OBSERVED

The stars observed during the course of this investigation are all of MK luminosity classes III, III–IV, and IV, and, for the most part, have spectral types ranging from about G7 to M2 ($370 \leq T \leq 720$). The temperature-class boundaries are somewhat arbitrary, since some hotter subgiants and cooler giants were also observed. Since the values of w for the strongest damping lines are about 0.1 at $T \approx 390$ (G8) and continue to increase with decreasing T, the lower boundary of T generally restricts the uncertainties in the equivalent widths to 10 percent or less (for 1 percent photometric accuracy). The upper boundary of T was chosen to avoid the complications found in the atmospheres of middle- and late-type M giants.

Some of the program stars were chosen because prior work on them, as reported in the literature, indicated normalcy. Most, however, either are members of clusters or are objects of of interest for spectroscopic, kinematic, or other reasons. The cluster stars include one or more members of M13, M67, NGC 188, NGC 752, NGC 7789, and the Hyades; the NGC 188 stars scanned include two (III-18 and II-75) tentatively rejected from membership by Greenstein and Keenan (1964) but regarded by us as members, while the M67 stars scanned include two (Murray 1339 and Murray 1465) classified as members by Murray (1967) from his proper-motion work on the cluster. These stars, together with broad-band photometric data (when available), are listed in Table 9. The field stars were selected for such reasons as having high velocities (e.g., HD 29038 [Roman 1955]), being below the NGC 188 giant or subgiant branches in the standard color-magnitude diagram (e.g., 18 Lib A [Bidelman 1958]), having spectroscopically determined abundances (e.g., δ Eri [Pagel 1963]), or being strong- or weak-lined as determined photoelectrically (e.g., θ UMi [Griffin 1961]).

One particular star—the abundance standard—deserves special mention. The G8 giant ϵ Vir was chosen for this purpose. This star has been compared directly with the Sun by Cayrel and Cayrel (1963), who find that it has almost precisely solar-normal abundances except for an Na overabundance of a factor of 2.

Some time after the outset of the work, it was realized that an adequate standard of reference could not be derived from the relatively few normal giants observed. Therefore, in the summer of 1967, we conducted a survey of 100 stars listed in the *Bright Star Catalogue* (Hoffleit 1964). The object of this survey was to secure a sample of K giants unbiased by spectroscopic or kinematic considerations. The survey included stars of catalogued types G7–M2 in the right-ascension and declination intervals $16^{h}20^{m}$–24^{h} and 0°–+30°, respectively, except for those stars for which $b^{II} < 10°$; the last of these restrictions was added because of the undesirable possibility of reddening near the galactic plane. Two observations were secured with the Crossley for each star, and ninety-six of the original 100 were deemed to have suitably accurate photometry. The Survey, as it will henceforth be called, is probably a quite representative sample of the K giants in the solar neighborhood. We do not at present have a similar sample of subgiants.

VIII. DISCUSSION OF THE SCANNER DATA: THE YELLOW-RED TEMPERATURE INDEX

In order for our yellow-red color T to serve as a temperature index, it must be independent of blanketing. As a check on this, we have compared it with other red and infrared colors for our brighter stars. The first comparison, in which T_{IR} was used,

TABLE 7

PROGRAM STAR BLOCKING FRACTIONS

		1	2	3	4	5	6	7	8	9	10	T
BS	3	0.50	0.23	0.17	0.38	0.19	0.05	0.00	0.00			415
BS	45	0.49	0.36	0.58	0.32	0.41	0.15	0.27	0.29	0.10	-0.00	757
BS	165	0.57	0.34	0.31	0.31	0.29	0.13	0.02	0.01			482
BS	224	0.56	0.39	0.50	0.37	0.35	0.11	0.08	0.10	0.09	0.03	606
BS	258	0.50	0.23	0.19	0.36	0.25	0.07	0.00	0.00	0.08	0.03	403
BS	271	0.44	0.20	0.10	0.30	0.13	0.04	0.00	-0.00	0.09	0.02	388
BS	337	0.53	0.38	0.52	0.34	0.36	0.13	0.17	0.18	0.09	0.04	693
BS	464	0.59	0.35	0.30	0.34	0.28	0.09	0.01	0.03			477
BS	489	0.57	0.35	0.36	0.33	0.28	0.09	0.01	0.03			525
BS	495	0.52	0.26	0.15	0.30	0.23	0.10	0.02	0.01	0.08	0.03	401
BS	617	0.53	0.27	0.20	0.36	0.19	0.04	-0.00	0.01	0.09	0.02	453
BS	882	0.56	0.31	0.27	0.37	0.23	0.07	0.01	0.02			469
BS	911	0.49	0.37	0.57	0.33	0.39	0.15	0.26	0.29			788
BS	941	0.50	0.25	0.13	0.32	0.15	0.05	0.01	0.00			389
BS	947	0.54	0.30	0.17	0.34	0.16	0.05	0.01	0.02			424
BS	951	0.51	0.26	0.16	0.33	0.16	0.05	0.01	0.03			412
BS	1015	0.52	0.32	0.27	0.32	0.25	0.09	0.01	0.02			474
BS	1052	0.58	0.33	0.33	0.32	0.28	0.08	0.02	0.03			525
BS	1136	0.43	0.17	0.18	0.38	0.23	0.06	-0.00	0.01	0.08	0.01	388
BS	1457	0.54	0.38	0.52	0.33	0.37	0.13	0.12	0.15			661
BS	1551	0.55	0.33	0.31	0.34	0.25	0.08	-0.00	0.03			548
BS	1726	0.53	0.29	0.31	0.36	0.29	0.07	0.01	0.03			488
BS	1773	0.58	0.40	0.42	0.34	0.31	0.15	0.03	0.06			525
BS	1805	0.61	0.42	0.37	0.35	0.29	0.11	0.02	0.05	0.09	0.08	500
BS	1907	0.40	0.14	0.13	0.36	0.17	0.02	0.00	0.00	0.07	-0.02	402
BS	2012	0.55	0.30	0.20	0.36	0.16	0.05	0.01	0.02			433
BS	2219	0.50	0.22	0.15	0.37	0.14	0.03	0.01	0.01			412
BS	2429	0.52	0.28	0.21	0.37	0.24	0.09	0.00	0.01	0.07	0.07	408
BS	2478	0.56	0.29	0.22	0.32	0.19	0.07	0.01	0.02			446
BS	2600	0.56	0.27	0.25	0.37	0.22	0.04	0.00	0.02			469
BS	2649	0.57	0.38	0.37	0.36	0.27	0.09	0.01	0.02			516
BS	2697	0.58	0.35	0.27	0.32	0.22	0.09	0.02	0.04			462
BS	2805	0.56	0.35	0.21	0.36	0.14	0.07	0.01	0.03			448
BS	2821	0.50	0.24	0.16	0.36	0.15	0.04	0.01	0.01			405
BS	2985	0.46	0.22	0.14	0.34	0.13	0.04	0.01	0.02			388
BS	2990	0.50	0.24	0.17	0.36	0.15	0.04	0.00	0.01	0.09	0.03	401
BS	3145	0.56	0.28	0.28	0.34	0.24	0.05	0.03	0.02			489
BS	3149	0.54	0.29	0.22	0.35	0.21	0.06	0.01	0.02			433
BS	3249	0.58	0.38	0.43	0.31	0.29	0.11	0.04	0.04	0.08	0.05	571
BS	3366	0.57	0.33	0.31	0.34	0.27	0.09	0.01	0.02			470
BS	3369	0.52	0.26	0.15	0.32	0.14	0.05	0.01	0.01			402
BS	3905	0.59	0.36	0.28	0.34	0.28	0.12	0.01	0.02	0.10	0.09	449
BS	3994	0.53	0.28	0.17	0.38	0.16	0.06	0.01	0.00			383
BS	4171	0.43	0.18	0.12	0.33	0.13	0.04	0.01	-0.00			376
BS	4301	0.44	0.25	0.14	0.29	0.14	0.06	0.01	0.00			434
BS	4517	0.45	0.32	0.48	0.28	0.39	0.10	0.19	0.19	0.09	-0.01	703
BS	4737	0.54	0.31	0.18	0.31	0.21	0.09	0.01	0.01			434
BS	4932	0.43	0.21	0.09	0.28	0.11	0.05	0.01	-0.00	0.09	0.04	393
BS	5154	0.46	0.35	0.54	0.29	0.39	0.14	0.26	0.27	0.10	0.02	808
BS	5159	0.48	0.30	0.20	0.34	0.22	0.07	0.00	-0.02			436
BS	5200	0.54	0.39	0.50	0.33	0.36	0.13	0.11	0.12	0.09	0.04	652
BS	5201	0.54	0.35	0.36	0.33	0.30	0.08	0.02	0.03			558
BS	5227	0.54	0.29	0.28	0.36	0.31	0.07	-0.00	0.01	0.08	0.03	460
BS	5247	0.56	0.37	0.38	0.32	0.30	0.10	0.02	0.03			563
BS	5370	0.58	0.34	0.25	0.32	0.28	0.09	0.01	0.02			469
BS	5429	0.57	0.33	0.30	0.33	0.26	0.07	0.01	0.01			508
BS	5480	0.39	0.22	0.09	0.29	0.11	0.04	0.01	-0.01			403
BS	5502	0.48	0.21	0.11	0.28	0.14	0.04	0.02	-0.00			400
BS	5582	0.56	0.38	0.28	0.34	0.28	0.14	0.01	0.02			471
BS	5600	0.54	0.38	0.45	0.31	0.33	0.12	0.06	0.07	0.08	0.05	612
BS	5601	0.46	0.21	0.16	0.33	0.16	0.06	0.00	-0.01			432
BS	5602	0.43	0.20	0.09	0.30	0.09	0.03	0.01	0.00			392
BS	5616	0.55	0.31	0.24	0.34	0.23	0.06	0.00	0.00			499
BS	5681	0.41	0.16	0.10	0.31	0.13	0.04	0.00	0.00			408
BS	5739	0.50	0.39	0.54	0.30	0.36	0.14	0.20	0.20	0.09	0.04	733
BS	5777	0.47	0.21	0.16	0.32	0.23	0.06	0.01	-0.01	0.06	0.01	414
BS	5826	0.54	0.41	0.53	0.31	0.34	0.18	0.10	0.12	0.12	0.07	641

TABLE 7—CONTINUED

		1	2	3	4	5	6	7	8	9	10	T
BS	5854	0.57	0.33	0.20	0.30	0.23	0.09	-0.00	0.01	0.07	0.09	444
BS	5888	0.48	0.21	0.13	0.33	0.15	0.04	0.01	0.01	0.08	0.02	416
BS	5889	0.26	0.08	0.08	0.28	0.12	0.03	0.01	-0.00	0.09	-0.02	374
BS	5901	0.47	0.21	0.15	0.31	0.22	0.06	0.01	-0.01	0.07	0.04	412
BS	5940	0.53	0.28	0.23	0.33	0.28	0.08	0.01	0.00	0.09	0.04	447
BS	5947	0.56	0.30	0.22	0.31	0.22	0.06	0.01	0.00	0.09	0.04	486
BS	5966	0.44	0.21	0.13	0.35	0.12	0.04	0.00	0.00			410
BS	6014	0.43	0.18	0.20	0.34	0.28	0.08	0.00	0.00			403
BS	6018	0.49	0.21	0.14	0.32	0.20	0.05	0.01	0.00	0.05	0.05	419
BS	6103	0.47	0.23	0.12	0.31	0.16	0.06	0.02	-0.00			400
BS	6220	0.43	0.17	0.07	0.28	0.13	0.03	0.01	0.01	0.07	0.02	393
BS	6623	0.35	0.09	0.05	0.28	0.15	0.03	0.02	0.01	0.09	-0.02	357
BS	6770	0.45	0.21	0.12	0.30	0.12	0.04	0.02	0.01			392
BS	6791	0.40	0.17	0.08	0.18	0.13	0.06	0.01	0.01			393
BS	6817	0.43	0.19	0.15	0.33	0.20	0.05	0.01	-0.00			394
BS	6869	0.43	0.16	0.10	0.29	0.16	0.04	0.01	0.00	0.08	0.02	399
BS	6872	0.54	0.31	0.21	0.33	0.19	0.07	0.00	0.01			443
BS	7149	0.49	0.28	0.18	0.39	0.18	0.05	-0.00	-0.01			410
BS	7176	0.51	0.30	0.18	0.34	0.19	0.07	0.01	0.00	0.09	0.07	418
BS	7373	0.34	0.11	0.11	0.35	0.16	0.06	0.01	-0.00	0.10	-0.00	349
BS	7405	0.52	0.37	0.52	0.35	0.40	0.12	0.19	0.19			648
BS	7429	0.54	0.29	0.25	0.33	0.30	0.09	0.01	0.01	0.08	0.06	456
BS	7430	0.41	0.24	0.13	0.33	0.11	0.07	0.01	0.01			442
BS	7576	0.58	0.38	0.33	0.33	0.31	0.14	0.02	0.02	0.10	0.07	475
BS	7602	0.37	0.10	0.10	0.35	0.15	0.04	0.01	0.01	0.08	-0.01	380
BS	7670	0.33	0.09	0.10	0.33	0.19	0.04	0.01	-0.01	0.10	-0.01	348
BS	7806	0.56	0.34	0.34	0.30	0.27	0.09	0.01	0.03	0.09	0.04	504
BS	7831	0.53	0.32	0.20	0.35	0.22	0.07	0.01	0.01	0.07	0.07	442
BS	7949	0.50	0.21	0.12	0.31	0.15	0.02	0.01	0.01	0.09	-0.01	426
BS	7957	0.43	0.16	0.15	0.38	0.17	0.04	0.00	-0.01	0.08	-0.00	390
BS	8082	0.46	0.23	0.17	0.35	0.15	0.04	0.01	0.00			414
BS	8255	0.51	0.28	0.17	0.36	0.17	0.05	0.01	0.01			419
BS	8317	0.53	0.30	0.20	0.35	0.19	0.07	0.01	0.01	0.09	0.07	426
BS	8448	0.30	0.13	0.09	0.28	0.19	0.07	0.01	0.01			394
BS	8551	0.44	0.19	0.16	0.35	0.22	0.05	-0.01	-0.00			421
BS	8841	0.49	0.26	0.21	0.40	0.19	0.05	0.00	-0.00	0.08	0.04	426
BS	8857	0.53	0.27	0.18	0.33	0.21	0.07	0.01	-0.00	0.08	0.05	419
BS	8924	0.55	0.31	0.26	0.35	0.30	0.14	0.01	0.01	0.08	0.06	426
BS	8974	0.52	0.24	0.19	0.35	0.23	0.06	-0.01	-0.00			412
HD	29038	0.57	0.32	0.29	0.34	0.30	0.10	0.02	0.02			459
HD	122563	-0.04	0.00	0.02	0.11	0.03	0.01	0.00	0.00	0.05	-0.01	433
HD	165195	0.11	0.06	0.02	0.11	0.05	0.02	0.00	0.01			461
BS	1346	0.46	0.23	0.09	0.29	0.13	0.06	0.01	0.00	0.09	0.03	386
BS	1373	0.48	0.24	0.10	0.31	0.12	0.05	0.00	0.00	0.09	0.04	391
BS	1409	0.50	0.25	0.11	0.31	0.13	0.05	0.01	0.00	0.10	0.04	394
BS	1411	0.43	0.22	0.12	0.31	0.14	0.05	0.01	-0.00	0.09	0.02	382
M13	59	0.42	0.30	0.17	0.23	0.08	0.04	-0.02	0.03			613
FAG	84	0.55	0.27	0.18	0.35	0.17	0.06	-0.00	0.00			392
FAG	105	0.55	0.31	0.28	0.35	0.25	0.09	-0.00	0.01			442
FAG	108	0.57	0.34	0.36	0.35	0.30	0.11	0.01	0.01	0.09	0.04	479
FAG	141	0.55	0.28	0.18	0.37	0.18	0.06	0.01	0.02			396
FAG	151	0.53	0.27	0.19	0.34	0.17	0.07	0.02	0.02			390
FAG	170	0.58	0.34	0.30	0.33	0.28	0.09	0.01	0.03	0.10	0.07	475
FAG	193	0.45	0.21	0.17	0.34	0.22	0.06	-0.01	0.01			388
FAG	224	0.54	0.29	0.20	0.31	0.22	0.09	0.00	0.01			408
MUR	1465	0.54	0.40	0.50	0.33	0.36	0.15	0.11	0.13			615
I	1	0.39	0.22	0.17	0.34	0.21	0.06	0.00	0.02			410
I	69	0.51	0.34	0.28	0.41	0.27	0.11	0.01	0.06			458
I	105	0.51	0.31	0.20	0.38	0.19	0.07	0.02	0.01			410
II	75	0.52	0.26	0.28	0.36	0.29	0.08	0.01	0.01			463
II	181	0.47	0.33	0.29	0.40	0.27	0.08	0.01	0.01			456
III	4	0.49	0.24	0.22	0.35	0.26	0.08	-0.00	0.01			417
III	18	0.56	0.40	0.47	0.33	0.37	0.14	0.07	0.07			565
BD+	37418	0.47	0.21	0.12	0.32	0.13	0.04	0.01	0.01	0.09	0.02	398
BD+	37432	0.47	0.20	0.13	0.33	0.12	0.03	0.00	0.01			395
BD+	37448	0.48	0.24	0.14	0.34	0.14	0.03	0.01	0.02			405
K	751	0.56	0.38	0.55	0.35	0.33	0.14	0.14	0.15			677

1969ApJ...157.1279S

TABLE 8

SURVEY STAR BLOCKING FRACTIONS

		1	2	3	4	5	6	7	8	9	10	T
BS	6136	0.56	0.39	0.42	0.32	0.33	0.18	0.05	0.05			560
BS	6148	0.43	0.20	0.07	0.29	0.09	0.04	0.01	0.01			394
BS	6154	0.52	0.39	0.52	0.31	0.36	0.16	0.15	0.17			708
BS	6159	0.52	0.35	0.45	0.31	0.36	0.10	0.09	0.11			625
BS	6228	0.54	0.39	0.52	0.32	0.37	0.16	0.13	0.15			659
BS	6239	0.36	0.15	0.06	0.24	0.09	0.05	0.01	0.01			385
BS	6258	0.52	0.39	0.51	0.30	0.35	0.13	0.14	0.16			699
BS	6287	0.43	0.19	0.12	0.31	0.13	0.05	0.00	0.00			404
BS	6292	0.41	0.15	0.09	0.30	0.13	0.03	0.01	-0.00			395
BS	6293	0.57	0.37	0.40	0.32	0.33	0.11	0.03	0.05			560
BS	6299	0.53	0.31	0.23	0.37	0.23	0.07	0.00	0.01			444
BS	6305	0.37	0.14	0.08	0.30	0.12	0.04	0.01	-0.00			391
BS	6307	0.51	0.27	0.15	0.33	0.19	0.05	0.00	0.01			435
BS	6325	0.55	0.36	0.22	0.33	0.19	0.08	0.01	0.02			486
BS	6342	0.47	0.21	0.14	0.30	0.19	0.03	0.01	0.01			429
BS	6364	0.55	0.35	0.35	0.35	0.29	0.08	-0.00	0.01			500
BS	6390	0.46	0.21	0.13	0.30	0.20	0.04	0.00	-0.00			425
BS	6393	0.46	0.34	0.43	0.29	0.36	0.12	0.23	0.24			774
BS	6443	0.45	0.20	0.11	0.31	0.13	0.05	0.00	0.01			405
BS	6452	0.54	0.40	0.49	0.34	0.38	0.12	0.21	0.23			731
BS	6476	0.51	0.31	0.13	0.19	0.15	0.08	0.02	0.02			483
BS	6526	0.55	0.38	0.39	0.33	0.30	0.10	0.02	0.03			545
BS	6542	0.46	0.21	0.13	0.33	0.14	0.04	0.00	-0.01			403
BS	6575	0.45	0.22	0.10	0.30	0.15	0.06	0.01	0.01			420
BS	6590	0.49	0.30	0.19	0.31	0.16	0.07	0.01	0.01			485
BS	6602	0.56	0.37	0.46	0.33	0.37	0.12	0.07	0.09			577
BS	6603	0.56	0.31	0.21	0.32	0.24	0.08	0.00	0.02	0.08	0.07	445
BS	6608	0.26	0.05	0.03	0.28	0.10	0.03	0.02	0.01			339
BS	6644	0.52	0.29	0.19	0.31	0.25	0.07	0.03	0.02			448
BS	6654	0.52	0.25	0.14	0.31	0.18	0.05	-0.00	0.01			429
BS	6665	0.45	0.20	0.11	0.30	0.13	0.04	-0.00	0.02			402
BS	6687	0.57	0.33	0.26	0.33	0.22	0.08	0.01	0.02			478
BS	6703	0.43	0.20	0.09	0.28	0.12	0.05	0.01	0.01			389
BS	6763	0.56	0.31	0.27	0.36	0.23	0.07	0.02	0.02			491
BS	6765	0.49	0.34	0.56	0.28	0.41	0.16	0.36	0.38			929
BS	6800	0.54	0.29	0.24	0.34	0.19	0.07	0.02	0.01			460
BS	6820	0.56	0.37	0.40	0.37	0.31	0.08	0.04	0.04			587
BS	6868	0.51	0.40	0.56	0.34	0.38	0.15	0.20	0.20			720
BS	6882	0.54	0.40	0.50	0.35	0.36	0.12	0.12	0.16			736
BS	6885	0.53	0.30	0.27	0.36	0.22	0.07	0.01	0.01			484
BS	6895	0.53	0.29	0.25	0.37	0.25	0.07	0.01	0.00			456
BS	6966	0.57	0.39	0.41	0.35	0.29	0.09	0.05	0.04			577
BS	6980	0.49	0.24	0.12	0.32	0.13	0.06	0.03	0.00			402
BS	7064	0.53	0.28	0.24	0.33	0.23	0.07	0.01	0.01			461
BS	7112	0.51	0.28	0.16	0.34	0.14	0.06	0.02	0.01			452
BS	7132	0.57	0.34	0.35	0.34	0.29	0.08	0.02	0.03			526
BS	7181	0.53	0.30	0.29	0.38	0.24	0.07	0.02	0.00			485
BS	7918	0.55	0.29	0.27	0.34	0.25	0.07	0.00	0.01			475
BS	7923	0.40	0.16	0.08	0.32	0.11	0.03	0.02	0.00			400
BS	7939	0.54	0.29	0.18	0.31	0.20	0.06	0.01	0.01			454
BS	7995	0.33	0.13	0.06	0.28	0.10	0.03	0.01	0.00			377
BS	8008	0.56	0.39	0.41	0.33	0.30	0.12	0.03	0.04			570
BS	8011	0.45	0.26	0.15	0.31	0.15	0.05	0.00	0.02			438
BS	8030	0.39	0.17	0.10	0.29	0.14	0.04	0.02	-0.00			391
BS	8032	0.56	0.37	0.39	0.34	0.30	0.10	0.02	0.03			546
BS	8066	0.54	0.45	0.48	0.36	0.30	0.14	0.07	0.09			654
BS	8163	0.48	0.37	0.54	0.31	0.39	0.12	0.24	0.25			787
BS	8173	0.50	0.27	0.20	0.37	0.20	0.05	0.00	0.00			430
BS	8197	0.49	0.25	0.13	0.33	0.16	0.04	0.01	0.00			412
BS	8225	0.51	0.39	0.58	0.32	0.39	0.14	0.21	0.23			716
BS	8277	0.48	0.25	0.15	0.36	0.16	0.04	0.01	-0.00			411
BS	8287	0.57	0.38	0.34	0.32	0.25	0.09	0.01	0.02			555
BS	8325	0.55	0.30	0.25	0.34	0.25	0.08	-0.02	0.01			467
BS	8390	0.57	0.32	0.26	0.31	0.24	0.07	0.01	0.02			487
BS	8393	0.58	0.39	0.42	0.34	0.31	0.11	0.03	0.05			558
BS	8413	0.55	0.41	0.47	0.35	0.36	0.14	0.05	0.07			556
BS	8415	0.56	0.31	0.26	0.35	0.24	0.08	0.00	0.00			486
BS	8458	0.52	0.37	0.57	0.33	0.40	0.15	0.22	0.24			731
BS	8461	0.46	0.18	0.11	0.30	0.18	0.07	0.01	0.01			393
BS	8482	0.55	0.29	0.23	0.32	0.27	0.10	0.00	0.01			446
BS	8562	0.54	0.38	0.50	0.35	0.34	0.12	0.09	0.10			635
BS	8564	0.56	0.33	0.22	0.32	0.18	0.08	0.00	0.01			459
BS	8618	0.42	0.18	0.08	0.29	0.12	0.04	0.00	-0.01			392
BS	8642	0.43	0.24	0.17	0.35	0.18	0.06	-0.02	-0.00			430
BS	8660	0.50	0.23	0.12	0.35	0.15	0.05	0.00	0.01			415
BS	8703	0.45	0.24	0.17	0.27	0.20	0.08	-0.02	0.02			446
BS	8730	0.56	0.30	0.16	0.33	0.17	0.07	0.01	-0.00			432
BS	8742	0.50	0.25	0.11	0.31	0.15	0.08	0.00	0.00			389
BS	8751	0.59	0.35	0.33	0.32	0.29	0.11	0.00	0.04			518
BS	8785	0.48	0.22	0.12	0.34	0.14	0.05	0.01	-0.01			383
BS	8795	0.51	0.38	0.59	0.33	0.39	0.15	0.18	0.20	0.11	0.03	685
BS	8824	0.56	0.34	0.32	0.32	0.26	0.08	0.00	0.01			503
BS	8833	0.47	0.21	0.14	0.38	0.14	0.03	0.01	-0.01			403
BS	8842	0.31	0.12	0.04	0.25	0.06	0.04	0.02	-0.00			374
BS	8852	0.37	0.15	0.11	0.35	0.14	0.03	0.00	-0.00			395
BS	8878	0.49	0.24	0.20	0.31	0.22	0.04	0.01	-0.01			478
BS	8893	0.58	0.35	0.32	0.33	0.28	0.09	0.00	0.02			493
BS	8912	0.46	0.22	0.12	0.34	0.15	0.03	0.01	0.00			407
BS	8916	0.51	0.26	0.17	0.35	0.18	0.05	0.01	0.01	0.09	0.04	420
BS	8922	0.52	0.25	0.14	0.35	0.17	0.04	0.00	0.01			430
BS	8923	0.43	0.21	0.13	0.33	0.12	0.05	-0.04	0.02			387
BS	8991	0.52	0.39	0.52	0.34	0.37	0.12	0.24	0.25			772
BS	8997	0.42	0.18	0.09	0.31	0.12	0.03	0.01	0.01			392
BS	9035	0.50	0.38	0.57	0.31	0.40	0.14	0.26	0.28			748
BS	9055	0.25	0.13	0.27	0.00	0.00	0.00	0.52	0.56			762

TABLE 8A

INFRARED COLORS

WAVELENGTH		7980	8190	8400	8662	8800	8900	9200	10300	10700	T (IR)
BS	45	169.8	164.0	149.0	130.0	144.0	146.0	126.0	76.6	45.8	267.0
BS	224	125.6	117.0	107.0	94.9	103.0	105.0	85.3	52.1	31.1	186.0
BS	258	74.2	67.0	59.6	51.5	53.9	54.8	42.8	24.0	14.2	92.1
BS	271	70.9	63.4	57.3	49.5	51.9	51.9	41.5	22.5	13.0	87.4
BS	337	152.3	141.0	129.0	116.0	127.0	129.0	106.0	67.4	39.5	234.0
BS	495	71.9	65.2	58.1	50.2	52.7	53.6	42.0	23.8	13.7	90.3
BS	617	87.2	80.0	72.6	63.2	67.6	68.2	54.6	30.6	18.1	116.0
BS	1136	71.5	64.1	57.5	49.5	51.3	52.0	41.2	22.2	12.7	86.2
BS	1805	93.4	83.8	77.6	68.8	75.3	76.2	58.2	36.2	21.4	133.0
BS	1907	77.3	70.1	62.6	55.0	57.1	56.5	48.0	25.3	14.8	97.2
BS	2429	74.6	66.9	59.0	52.6	55.0	56.0	41.6	24.1	14.0	93.1
BS	2990	74.7	68.1	61.3	52.8	55.7	56.3	44.5	24.8	14.3	94.8
BS	3249	118.1	108.0	97.7	87.7	94.9	95.9	77.0	47.9	27.9	171.0
BS	3905	83.6	75.6	69.2	60.3	66.0	67.0	49.7	30.3	17.8	114.0
BS	4517	155.1	149.0	133.0	119.0	130.0	130.0	113.0	66.6	39.9	237.0
BS	4932	72.3	65.5	58.3	49.8	52.7	53.6	41.4	23.1	12.8	88.7
BS	5154	185.0	174.0	160.0	142.0	159.0	159.0	136.0	84.2	50.1	293.0
BS	5200	136.4	126.0	116.0	103.0	114.0	115.0	93.7	57.2	33.9	205.0
BS	5227	86.9	79.2	72.1	63.4	66.3	68.4	53.5	30.6	18.0	115.0
BS	5600	124.1	115.0	105.0	94.4	102.0	104.0	82.6	51.2	30.4	184.0
BS	5739	158.3	149.0	136.0	122.0	135.0	138.0	112.0	71.8	42.9	250.0
BS	5777	77.1	70.0	63.2	55.8	56.2	57.8	46.2	26.3	15.0	97.4
BS	5826	132.0	122.0	113.0	97.2	109.0	112.0	86.8	55.1	33.0	197.0
BS	5854	81.8	74.1	66.0	58.9	62.2	64.7	47.5	29.1	16.5	108.0
BS	5888	77.6	70.2	63.2	55.5	58.2	58.0	46.8	26.2	15.0	99.4
BS	5889	66.7	60.1	53.6	45.8	48.0	47.7	39.3	19.8	11.5	79.4
BS	5901	77.1	69.3	61.9	55.0	57.3	57.6	45.0	25.5	14.8	97.5
BS	5940	83.3	75.8	69.0	59.6	62.9	63.9	50.3	29.0	17.0	109.0
BS	5947	93.6	85.8	77.6	68.1	73.0	73.9	58.3	34.1	19.9	127.0
BS	6018	77.5	69.8	62.7	56.5	57.9	58.1	45.6	26.4	15.0	99.2
BS	6220	72.4	64.8	58.5	51.0	52.7	53.0	42.0	22.9	13.2	88.8
BS	6623	63.4	56.0	49.9	42.3	43.9	43.7	35.8	18.1	10.1	72.1
BS	6869	74.9	68.2	60.8	52.8	54.8	55.1	44.1	24.0	13.9	92.6
BS	7176	76.3	68.9	62.0	53.6	57.5	58.8	44.2	26.1	14.7	98.3
BS	7373	61.9	56.3	49.2	40.9	42.7	42.8	34.4	17.6	10.0	70.3
BS	7429	87.6	78.7	71.5	63.0	66.2	68.2	52.2	31.3	17.4	115.0
BS	7576	88.9	80.5	72.9	63.5	69.1	71.4	53.7	32.6	19.6	121.0
BS	7602	72.4	64.7	57.9	50.1	51.4	51.4	42.4	22.2	12.9	86.6
BS	7670	61.6	55.2	48.6	40.6	42.3	42.2	34.5	17.6	10.2	70.0
BS	7806	99.0	89.8	80.9	71.2	77.2	79.8	62.7	37.3	21.9	136.0
BS	7831	82.8	74.3	66.1	59.7	63.0	63.3	48.7	28.9	16.6	108.0
BS	7949	81.0	73.1	66.7	57.4	60.2	60.8	49.7	26.6	15.6	102.0
BS	7957	73.1	65.8	59.0	50.9	52.7	52.9	42.9	22.8	13.3	88.1
BS	8317	78.8	71.8	64.0	55.3	59.2	60.1	45.7	27.0	15.7	102.0
BS	8841	78.9	71.9	65.2	56.9	59.8	60.6	47.1	26.9	15.8	102.0
BS	8857	78.2	70.7	63.6	55.3	57.8	58.4	45.7	26.6	15.3	99.6
BS	8924	77.4	70.1	63.4	55.8	58.6	59.9	45.5	26.9	15.8	101.0
HD	122563	85.4	77.2	71.2	64.7	66.1	64.1	54.8	29.5	16.7	112.0
BS	1346	69.6	62.2	56.5	48.2	50.7	52.0	40.3	22.5	13.0	86.3
BS	1373	70.6	63.4	57.3	49.2	52.3	53.1	41.2	22.9	13.3	88.5
BS	1409	71.7	64.6	58.4	49.7	53.0	54.2	41.6	23.3	13.5	89.8
BS	1411	69.3	62.7	56.0	48.2	50.8	50.5	40.5	22.0	12.7	85.5
FAG	108	92.8	85.0	76.7	68.0	74.8	76.0	60.7	36.4	20.8	132.0
FAG	170	90.2	83.2	74.1	65.0	72.0	72.0	56.1	34.6	20.0	127.0
BD+	37418	74.6	68.0	60.1	52.1	55.4	56.1	44.8	24.8	14.0	94.2
BS	6603	84.0	75.8	68.7	60.6	63.7	66.1	49.3	30.0	17.1	111.0
BS	8795	148.6	141.0	129.0	112.0	126.0	127.0	105.0	65.0	39.0	230.0
BS	8916	77.5	71.4	64.0	55.5	58.7	59.0	46.3	26.5	15.4	101.0

REMARKS TO TABLES 5, 6, 7, 8, 8a

BS/HD	Name	Estimated $E(B-V)$ (mag)	Abundance Analysis or Other Comment
1136 .	δ Eri	. . .	Pagel (1963)
1726 . . .	16 Aur	0 03	
1773	σ Aur	04	
1805.	Φ Aur	04	Cayrel (1966)
1907 .	Φ^2 Ori		Schwarzschild *et al.* (1957); Helfer and Wallerstein (1968)
2219. .	κ Aur	. .	Helfer and Wallerstein (1968)
2478	30 Gem	02	
3994	λ Hya		Helfer and Wallerstein (1968)
4301 . .	α UMa		Helfer and Wallerstein (1968); unresolvable double; companion F star
4932 . .	ϵ Vir	.	Cayrel and Cayrel (1963)
5480	31 Boo	.	Helfer and Wallerstein (1968)
5681 .	δ Boo		Helfer and Wallerstein (1968)
6791		. . .	Helfer and Wallerstein (1968)
7149 .	η Sct	02	
7176. .	ϵ Aql	02	
7405. . . .	α Vul	03	
7429 .	μ Aql	01	Helfer and Wallerstein (1968)
7576 .	20 Cyg	. .	Helfer and Wallerstein (1968)
7806	39 Cyg	03	
7957	η Cep		Hazelhurst (1963)
8255	72 Cyg		Helfer and Wallerstein (1968)
8448 . .	AR Lac		Observed during primary eclipse
122563		. .	Wallerstein *et al.* (1963)
165195	. . .	25	Wallerstein *et al.* (1963); reddening from same paper
	M13 #59	0 06	Helfer *et al.* (1959); reddening from Sandage (private communication)

Remark No	Remark
1	. Hyad
2	Member of M67; $E(B-V) = 0.06$ mag (Eggen and Sandage, 1964)
3	Member of NGC 188; $E(B-V) = 0.10$ mag (Sandage, private communication)
4	Member of NGC 752; $E(B-V) = 0.02$ mag (Eggen 1963; Johnson 1953)
5	Member of NGC 7789; $E(B-V) = 0.25$ mag (Burbidge and Sandage 1958; Arp 1962)

exhibited a small but definite anomaly correlated with stellar CN strength. The anomaly was in the sense that the stars with particularly strong CN bands had T's too blue (small numerically) for their T_{IR}'s, and vice versa; the size of this anomaly never exceeded 5 percent. The physical explanation of the problem is the presence of the red CN system in the $\lambda\lambda$6800–7500 region (cf. Davis and Phillips 1963); these bands, while but weakly present in the solar spectrum, reach significant strengths in late G and K giants. (There is little or no CN blanketing in the passbands defining T_{IR}.) To correct this anomaly, the T residuals were compared with residuals from a mean relation between the λ4200 CN index and T for a moderate-sized group of stars (Fig. 1), and the resulting correlation was then used to correct T for all stars. The corrected values of T correlate well with T_{IR} (for stars not used for the original correlation; see Fig. 2) and also with independent infrared measures such as those made in the standard broad-band system of Johnson (Johnson *et al.* 1966; Mendoza V. 1967; see Figs. 3–5) and Argue's (1967) $(r-i)$ system (Fig. 6).

TABLE 9

Cluster Stars, Supplementary Data

Star	M_v	V	$(B-V)_0$	$(U-B)_0$	$E(B-V)$	Notes
	a) The Hyades (Johnson *et al* 1966)					
θ^1 Tau	+0 80	3.85	0 96	0 74	0 00	
γ Tau	68	3 66	0 99	81	00	
δ Tau	66	3 77	0 99	82	00	
ϵ Tau	+0 54	3 52	1 01	0 87	0 00	
	b) M67 (Johnson and Sandage 1955; Eggen and Sandage 1964; Sandage 1968)					
Murray 1465	−0 9	8 83	1 50	1 88	0 06	
Fagerholm 170	+0 1	9 69	1 30	1 44	06	
Fagerholm 108	+0 2	9 72	1 32	1 50	06	
Fagerholm 105	+0 8	10 30	1 20	1 28	06	
Fagerholm 141	+0 9	10 48	1 05	0 94	06	
Fagerholm 151	+0 9	10 49	1 04	0 94	06	
Fagerholm 84	+1 0	10 59	1 06	0 91	06	
Fagerholm 224	+1 2	10 76	1 07	1 05	06	
Fagerholm 193	+2 7	12 26	0 94	0 80:	0 06	Subgiant
	c) M13 (Arp and Johnson 1955)					
M13 #59	−2 7:	12 03	1 52	1 77	0 06	M_v here assumes RR Gap at M_v=+0 5
	d) NGC 752 (Eggen 1963; Johnson 1953)					
+37° 418	+1 20	8 95	0 99	0 75	0 02	=Heinemann 75
+37° 432	+1 26	9 01	0 97	0 73	0 02	=Heinemann 213
+37° 448	+1 30	9 05	1 02	0 80	0 02	=Heinemann 311
	e) NGC 7789 (Burbidge and Sandage 1958)					
Küstner #751	−1 2	10 84	1 59		0 25	
	f) NGC 188 (Sandage 1962; Eggen and Sandage 1968)					
III-18*	0 0	11 34	1 49:	1 79:	0 10	Membership from anomalous line strengths
(III-4)	+ 3	11 66	1 04	1 01	10	Composite? member?
(II-75*†)	− 7	10 84	1 18	1 27	10	
I-69	+ 9	12 26	1 20	1 28	10	
I-105	+ 9	12 30	1 07	1 00	10	
II-181†	+ 7	12 09	1 14	. . .	10	
I-1	+0 5	11 88	1 04	0 75	0 10	Member; composite; H- and K-emission (Greenstein and Keenan 1964)

* Greenstein and Keenan (1964) weakly suggest III-18 and II-75 to be nonmembers from examination of low-dispersion spectra.

† Sandage (1962) only. Also, stars enclosed in parentheses are likely nonmembers on the basis of new proper-motion data by R Cannon

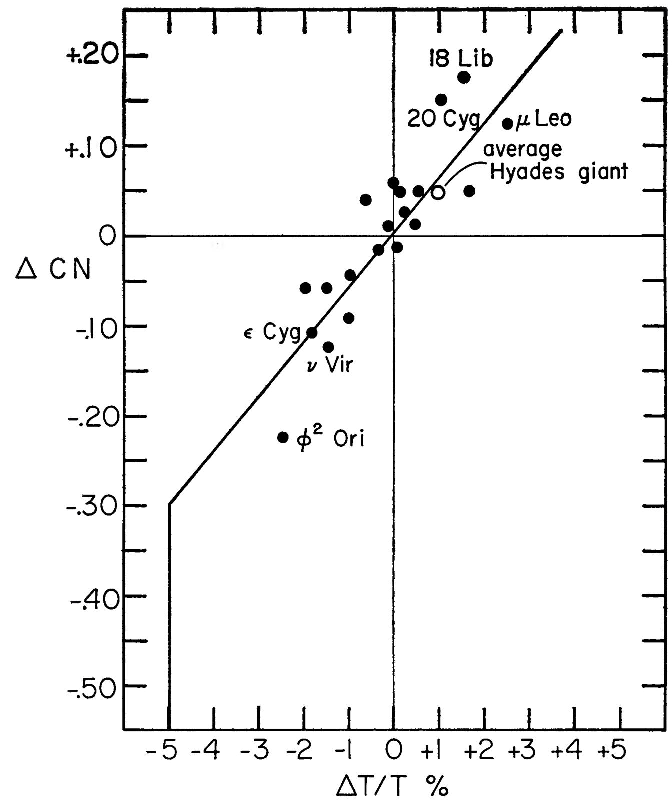

FIG. 1 —Correlation between residuals of individual program K-giant blue (λ4200) CN-band indices and residuals in an uncorrected red color T, compared with T_{IR} Positive correlation is due to the presence of numerous weak lines of the red CN system in the T-defining passbands λλ7000 and 7400 In practice we use ΔCN to determine the small percentage residual in T which is then used to correct T (see discussion in text).

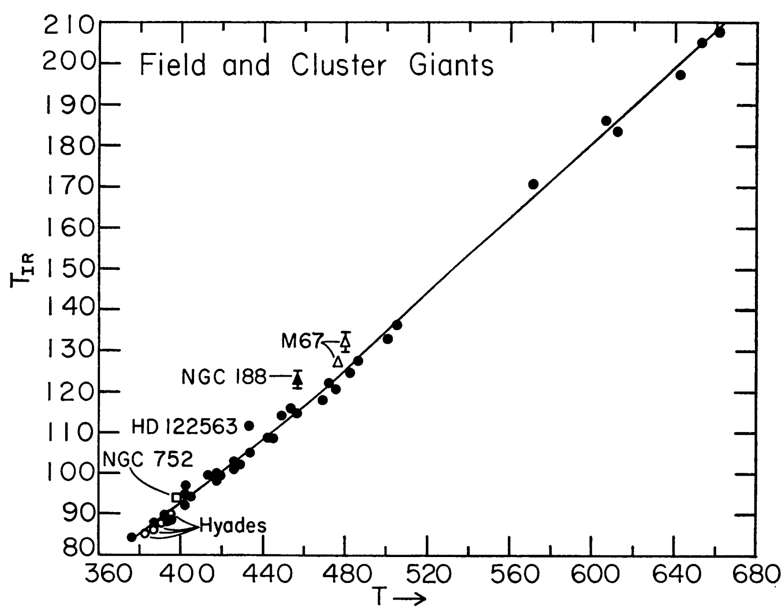

FIG. 2.—Correlation between T_{IR} (λλ8800, 10300, 10700) and T (corrected) for field and cluster program stars. The CN correction has now removed residuals which are systematic with abundance; we note a very tight correlation for the apparently bright stars

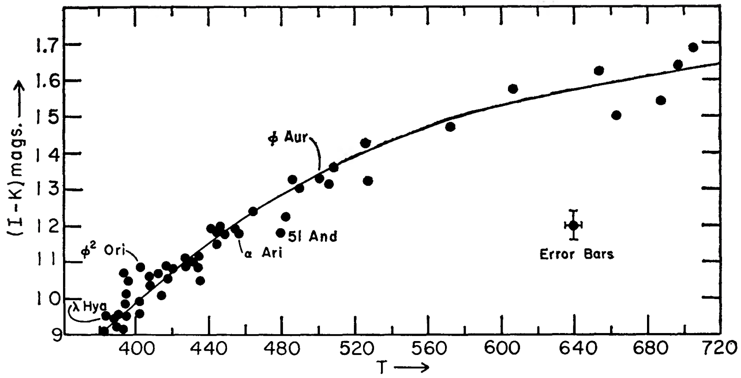

FIG 3 —Correlation between T and the $(I - K)$ broad-band infrared color of Johnson *et al.* (1966). Estimated photometric error bars are shown The Φ Aur data are due to recent unpublished photometry communicated to us by Dr. R Mitchell.

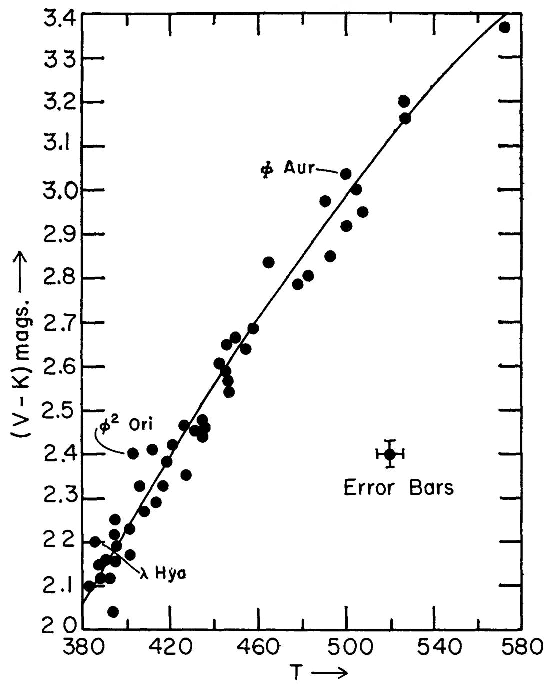

FIG 4.—Correlation between T and $(V - K)$ of Johnson *et al.* (1966)

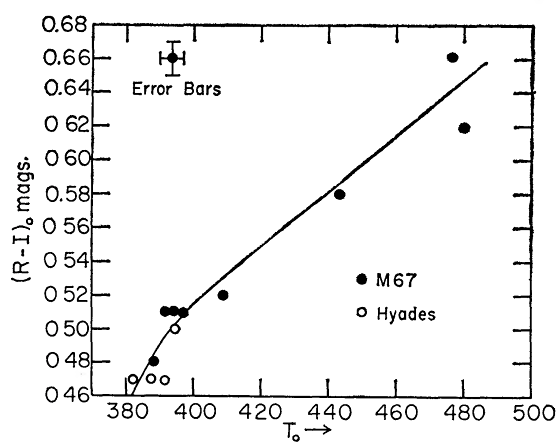

FIG. 5.—Correlation of T and $(R - I)$ on the Johnson system for M67 and Hyades cluster stars observed by Mendoza V. (1967)

Comparisons of T with unpublished six-color photometry by Kron (1968) have also proven satisfactory. The tightness of these correlations, together with the insensitivity of T to differential back warming and variation of convective efficiency (see R. Cayrel 1968), indicates that T is an excellent temperature parameter; we emphasize this point in view of the fact that it has been disputed (G. Cayrel 1967).

We note that the T base line is close enough to the $B - V$ base line (in $1/\lambda$) that interstellar reddening has a similar effect on both colors.

We may attempt to establish a rough correlation between effective temperature and T by using the comparison of cool-star continua in the λλ7800–11000 region with

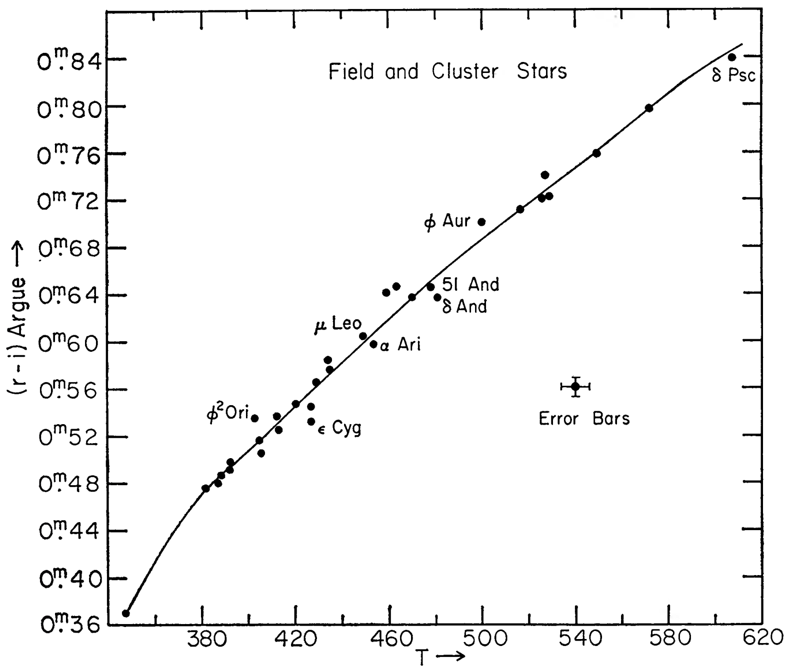

FIG. 6 —Correlation of T and the broad-band $(r - i)$ colors of Argue (1967). In this and the preceding three figures we find T correlates well with published broad-band red and infrared colors There are no systematic deviations with abundance We conclude T is quite free from differential blanketing effects for G8–M1 III stars.

Planckian energy distributions made by Wing (1967), who utilized the calibration of Hayes. Wing's temperatures agree quite well with the few directly measured for cool stars (as derived from the diameter measures of Pease and Michelson [Pettit and Nicholson 1928]). The relation between T and Wing's temperatures (T_e) is given in Figure 7; Table 10 lists T_e values for those of our values of T which correspond to certain spectral types, together with those types. A comparison of Table 10 with the tabulation of Johnson (1966) and with the temperature 4940° ± 100° K derived by the Cayrels for ε Vir from their study of the star's Hα profile indicates excellent agreement. These temperatures are given solely for illustrative purposes and are not used in any of the discussion which follows.

IX. A COMPARISON OF T'S AND MK SPECTRAL TYPES

A comparison of the T's and the MK spectral types of a number of the stars observed reveals inconsistencies between the two methods of assigning temperature parameters. Table 11 lists some of the outstanding examples. All MK classifications listed are from

Johnson and Morgan (1953) or the *Bright Star Catalogue*, with the following exceptions: γ, δ, ϵ, and θ^1 Tau (Morgan and Hiltner 1965); Fagerholm 151 in M67 (Burbidge and Burbidge 1959); and ϵ Vir (Keenan 1963). The first star or stars in each of the three lists of Table 10 have abnormal line strengths, as indicated by the scanner measurements; ω Ser, δ Boo, and Φ^2 Ori are generally weak-lined, 55 Peg has strong Ca I λ4227, and the first five stars in the third list belong to high-abundance clusters (the Hyades and M67; see § X). In each list (and for all other cases found), the inconsistency is of such a nature

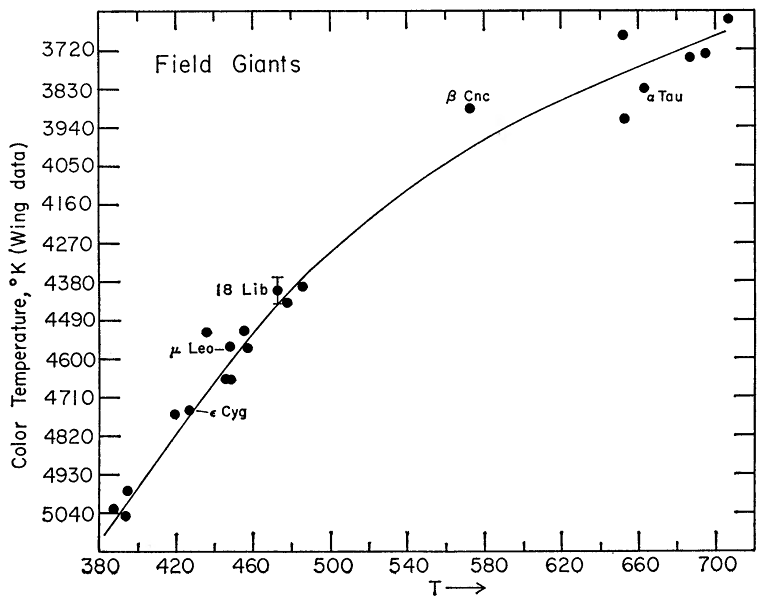

FIG. 7.—Correlation of T with the infrared color-temperature scale of Wing (1967) derived from the unpublished calibration of Vega given by Hayes (1967).

TABLE 10

T VERSUS T_e (WING)

T	Approximate MK Spectral Type	T_e(° K)
390	G8 III	5000
420	K1 III	4800
450	K2 III	4600
480	K3 III	4400
540	K4 III	4100
660	K5 III	3800

that stars of progressively higher abundances with a given T are assigned progressively later spectral types. The obvious explanation of these inconsistencies is that abundance-induced variations in line strength influence the parameters used to assign MK spectral types; in particular, such variations will cause misinterpretations of a straightforward kind when line strengths themselves are used as temperature parameters. (Note that Ca I λ4227 is used in just such a manner in early M giants, thus neatly explaining the spectral class assigned to 55 Peg.) That some such effect might exist is reasonable a priori, since the MK system uses two parameters (spectral type and luminosity class) to describe a system with three free variables (temperature, luminosity, abundance). A similar effect has been noted in recent work on late-type dwarfs (Whiteoak 1967; Pagel 1962). It appears that variations in line strength at a given temperature, the existence of which was used by Morgan and Hiltner as an argument for the usefulness of MK classification, actually provide a compelling reason to avoid exclusive dependence on such work for basic information about a star.

We maintain that MK-classification work on stars cooler than the Sun should be accompanied whenever possible by reddening-corrected red and infrared photometry, in order to check temperature classifications and to permit the identification of possible abundance anomalies. Without resorting to a detailed discussion (which would be beyond the scope of this paper), we also conjecture that a similar procedure may be necessary for hotter stars as well.

X. DISCUSSION OF THE SCANNER DATA: THE *w*-*T* DIAGRAMS

We now address ourselves to the task of assessing the abundances of our program stars from their photometric-abundance parameters (*w* for each feature and *T*). Since we can directly compare stars only if they have identical or nearly identical temperatures, and since we wish to compare stars having different temperatures with each other

TABLE 11

T VERSUS MK SPECTRAL CLASS FOR GIANTS

Star	MK Class	*T*	Star	MK Class	*T*	Star	MK Class	*T*
δ Boo	G8	409	55 Peg	M2	685	γ Tau	K0	387
ω Ser	G8	417	β And	M0	694	δ Tau	K0	391
Φ^2 Ori	G8p	402	χ Peg	M2	757	ϵ Tau	K1	394
ϵ Vir	G8	393				θ^1 Tau	G9	382
β Gem	K0	401				Fag 151 (M67)	K0	391
θ Psc	K1	420				ϵ Vir	G8	393
						β Boo	G8	393

and with the Sun by way of our abundance standard ϵ Vir, we can accomplish our purpose only if we can devise an indirect way of making such comparisons. To accomplish this for the giants, we adopt the following approach. The Survey data are plotted in diagrams of blocking fraction versus temperature index (*w*-*T*), and mean lines are drawn in these diagrams by eye estimate. These lines, which are assumed to be isoabundance trajectories, are then placed in corresponding *w*-*T* diagrams for the program stars. Comparison across temperature differences may be made by reference to these lines; moreover, they may be calibrated in terms of solar abundances by comparison with the abundance standard and then used to effect the desired comparisons of the program stars to the Sun. This approach, as may be seen, stands or falls with the validity of the one assumption; we shall see later that there is encouraging internal evidence that this assumption is indeed a good one. As for the subgiants, we must be content with using means derived from the program stars themselves; these will admittedly yield somewhat less precise results.

The *w*-*T* plots for the Survey stars, together with the adopted means, are given in Figures 8–10. We note in passing that these diagrams are of some interest in their own right. Note the relatively small scatter about the means; note also the degree of symmetry, which extends even to the outlying stars. For the most part, these K giants appear to be quite uninteresting in the pathological sense.

Figures 11–14 contain the *w*-*T* plots for the program giants. The first five of these (CN, Ca I λ4227, CH [G band], Mg [*b*-triplet], and Na [D-lines]) are quite similar to each other. Our comparison star ϵ Vir falls on the Survey mean lines in all the plots except those for the CN bands and the D-lines, in which it is somewhat above the mean lines; since it is known to be overabundant with respect to the Sun only in Na, this indicates that the mean lines represent solar abundance in each plot. This is further confirmed by the positions of the Hyades, which are also significantly above the lines

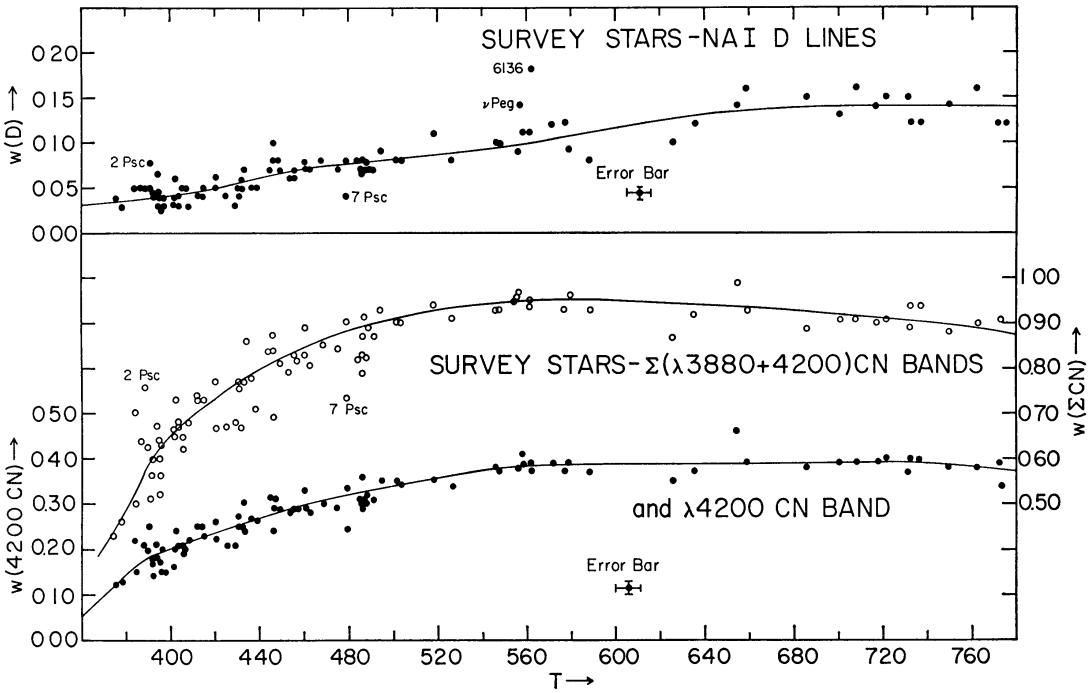

FIG. 8.—The Survey w-T (blocking fraction) diagrams for the Na I D-lines, the *sum* of the w's for the two blue CN bands (λλ3880 and 4200), and the blue CN band at λ4200 The mean line in each relation is hand-drawn and is used as a definition of normalcy Note the positions of the stars 2 Psc and 7 Psc.

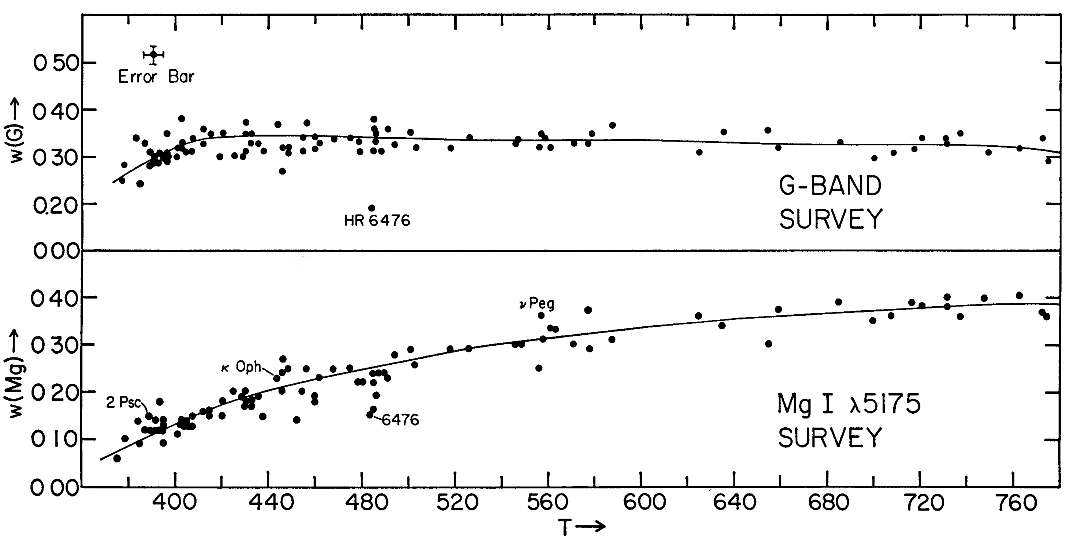

FIG. 9—The Survey w-T diagrams in the b-triplet of Mg I and the G-band of CH. Note the rather small dispersion in each parameter, especially CH. HR 6476 is apparently C-poor, and also has rather weak Mg I lines.

only in the CN (Griffin and Redman) and Na (Helfer and Wallerstein 1964) plots. The members of NGC 752 and NGC 7789 fall on or near the lines, a fact which indicates that their abundances are essentially solar. The independent abundance information available for some of the stars below the means, such as Φ^2 Ori (Schwarzschild *et al.* 1957), HD 122563 and HD 165195 (Wallerstein *et al.* 1963), and M13 No. 59 (Arp and Johnson 1955; Morgan 1956), indicates that the straightforward interpretation of underabundance is correct for this group of stars. The equivalent interpretation of the stars above the Survey lines is that they are *over*abundant with respect to the Sun and

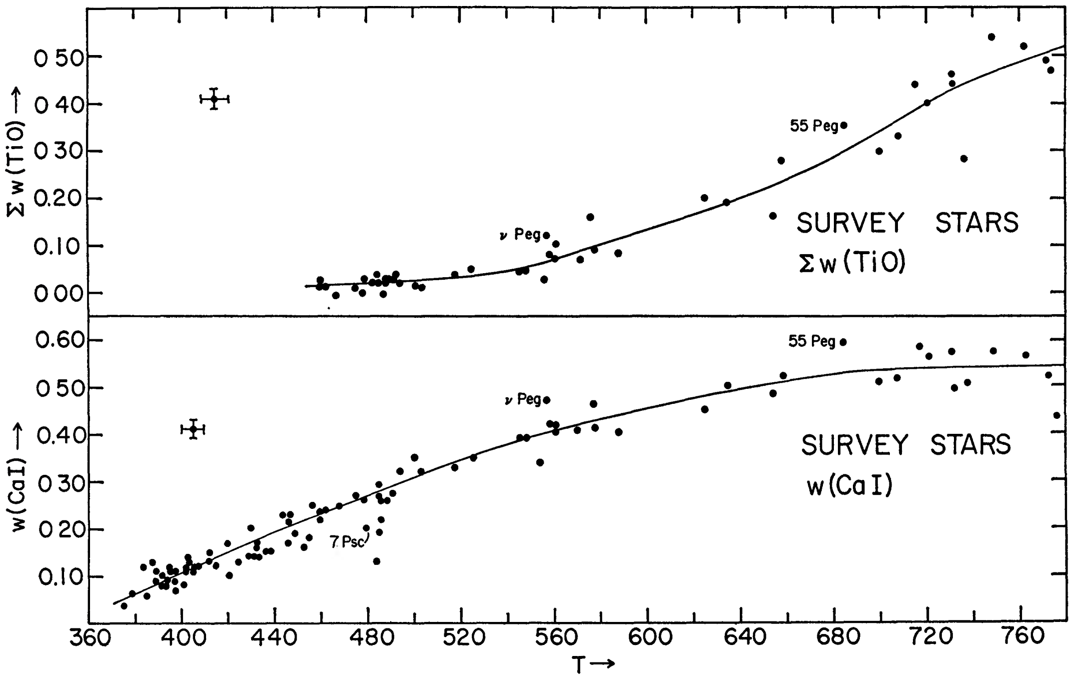

FIG. 10.—The Survey *w*-*T* diagrams for Ca I λ4227 and the sum of the blocking fractions for the red TiO bands with heads near λλ6148 and 7054. TiO is measured confidently at about type K4 III ($T \sim 540$), and we note a modest dispersion in the *w*-*T* diagram for TiO. The Ca I figure is rather similar to that of *w*(Na D) in Fig. 8; note some decrease in the dispersion of the stars around the mean line in Ca I with increasing red color *T*. ν Peg (K4 III) has anomalously strong TiO and Ca I λ4227. Approximate photometric error bars are indicated.

(in many cases, notably those of M67 and NGC 188) even overabundant with respect to the Hyades themselves; since this interpretation is in flat contradiction to current astrophysical mythology, we shall consider the matter further below.

The *w*-*T* diagrams for TiO (Fig. 13) and Ca II λ8662 (Fig. 14) require separate mention. There is no possibility of comparing the TiO strengths of most of the clusters or of referring comparisons to ε Vir, since we usually begin to measure TiO satisfactorily only at spectral type K4 ($T \approx 540$). However, we note that, as in the other five diagrams, M13 No. 59 falls far below the Survey mean and the cooler M67 and NGC 188 stars fall above it, an observation which suggests that this plot is fundamentally similar to the others. The λ8662 line is the only one from an ion measured; the *w*-*T* plot is almost devoid of scatter, with $w = 0.09 \pm 0.01$ for above 80 per cent of the thirty-five stars plotted. There is no systematic displacement of the cluster stars.

The *w*-*T* diagrams for the subgiants are given in Figures 15–18. As far as one can tell, they are quite similar to the corresponding plots for the giants. Note particularly the positions of the M67 star.

There are a number of particularly interesting field program stars which deserve special mention. We refer the reader to Table 12 for details concerning these stars.

We now return to the matter of interpreting the positions of the stars above the adopted means in the various *w-T* diagrams. The alternative explanation given first consideration by other investigators who have encountered this phenomenon (cf. Pagel

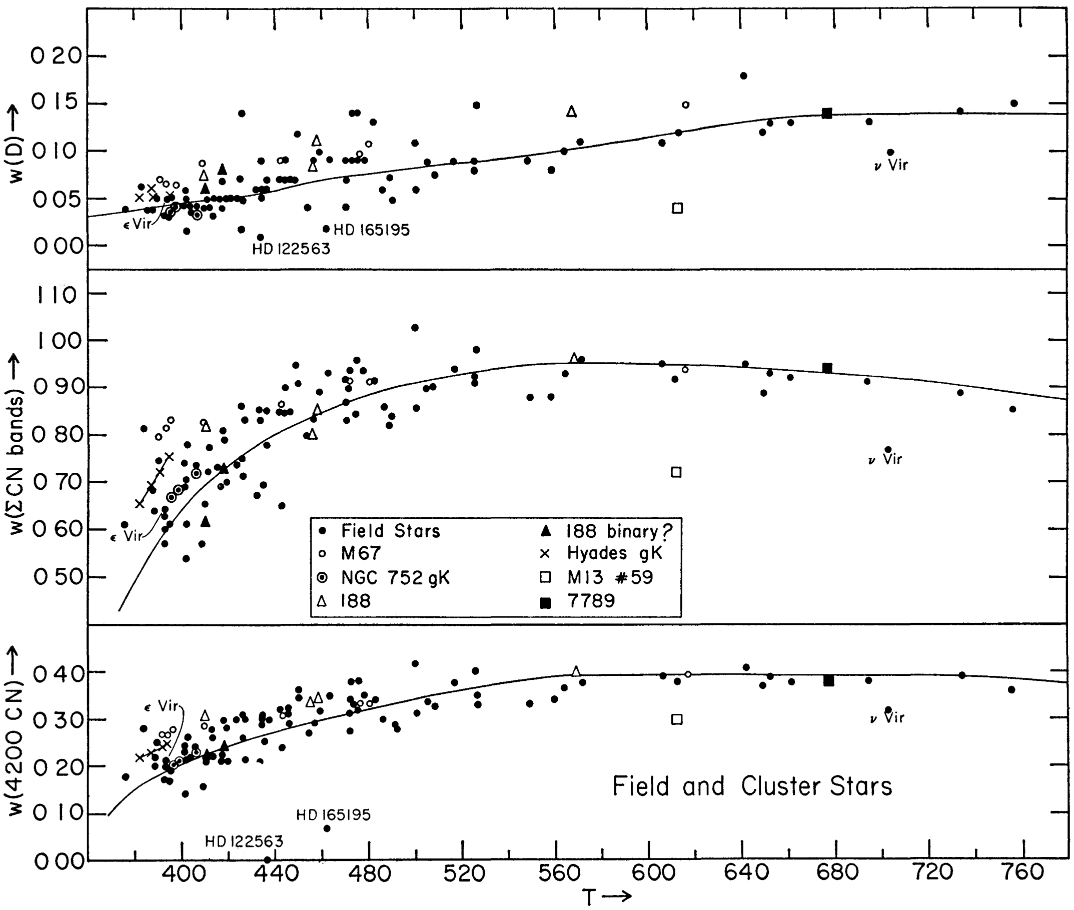

FIG. 11.—Program-star (field and cluster) *w-T* diagrams for CN (both the λ4200 CN band and the *sum* of the *w*'s for the two blue bands) and the Na I D-lines. *Solid lines*, Survey mean relations from Fig. 8. Blocking fractions for program stars show a large dispersion, as both metal-rich and metal-poor stars were observed. Many of the interesting stars are cited in Table 12 of the text, but note the weakness of CN and D in the halo giants HD 122563 and HD 165195 and M13 No. 59. The Hyades G8 III stars ($T \simeq 390$) are above normal in these three parameters; however, note the presence of NGC 188 and M67 stars higher yet in each subsection of the figure. ε Vir lies very slightly above the Survey means in CN and Na. Note the approximate normalcy of the stars in NGC 752 and the M0 III in NGC 7789. The dispersion in the CN measures decreases toward greater *T*-values; this is mainly a side-band absorption effect (see discussion in text).

1966; Johnson, MacArthur, and Mitchell 1968) is that of surface-gravity effects; others include microturbulence effects (on the bands; the other features measured are damping lines) and interstellar contributions (in the case of the D-lines). Microturbulence effects may be dismissed by noting that the strengths of the various bands do not vary in lock-step (Taylor 1967). Interstellar contributions are quite negligible; in the case of the D-lines, we note that the equivalent widths of interstellar lines rarely exceed 500 mÅ in stars at moderate galactic latitude which lack intrinsic D-lines (cf. Greenstein 1968), and

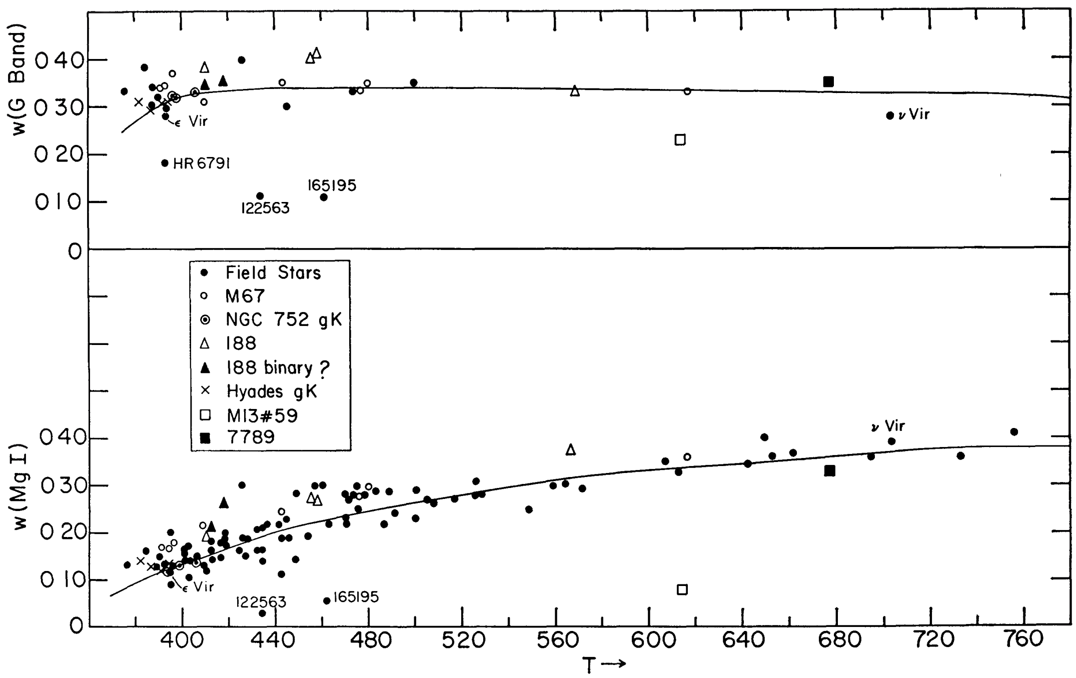

FIG. 12.—Program-star w-T diagram for Mg I b and the G-band of CH. Our abundance standard star, ϵ Vir, is Survey-normal in both parameters. Note the weakness of CH in the metal-poor giants HD 122563 and 165195 and the C-poor star HR 6791 (cf. Helfer and Wallerstein 1968). The Mg I blocking-fraction diagram is rather similar to that shown for Na; note that the NGC 188 (triangular) and the M67 (open circle) symbols are parallel to and well above the Survey mean line, and lie above the Hyades near $T \simeq 390$.

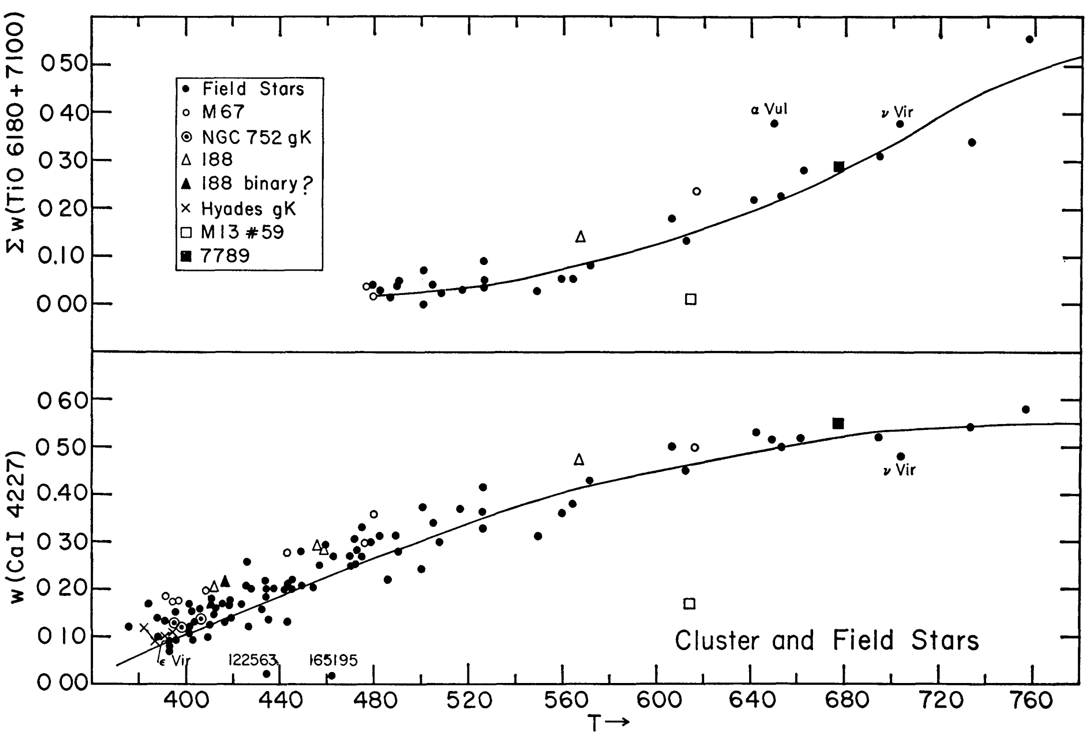

FIG. 13.—Program star w-T diagrams for Ca I λ4227 and the sum of the two red TiO bands (heads near $\lambda\lambda$6148, 7054). TiO is anomalously strong in α Vul and ν Vir, a pair of high-velocity, CN-weak stars which are likely to have large O/C ratios (see the text). TiO is also stronger than normal in the coolest stars observed in M67 (M1465) and NGC 188 (III-18), which have strong CN. The Ca I plot shows ϵ Vir normal, the Hyades stars slightly strong (especially θ^1 Tau, the hottest, at $T = 382$), and the M67 and NGC 188 stars very high. Note again the constriction of the w(Ca) range at large T-values.

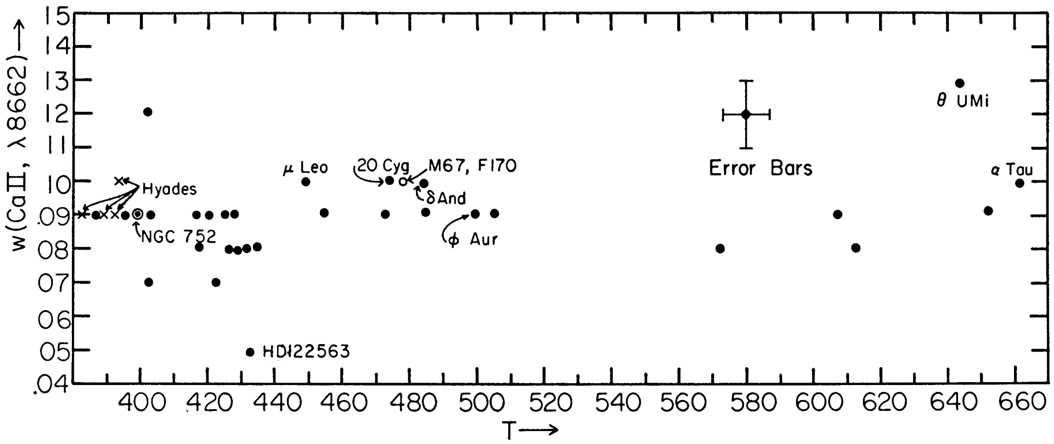

FIG 14.—Program star w-T diagram for Ca II λ8662. Note approximate constancy at $w = 0.09 \pm 0.01$ for all giants observed, except HD 122563. Contrast with the behavior of Ca I λ4227 in Fig. 13.

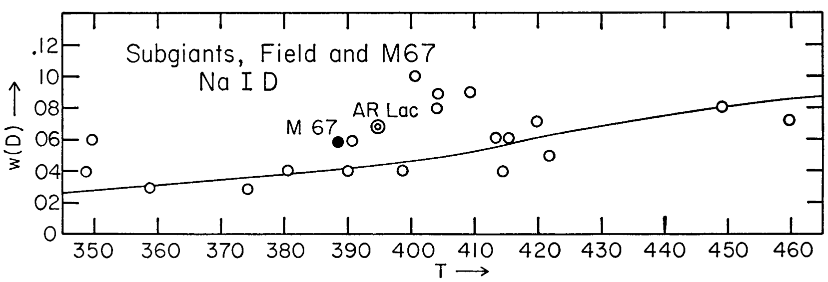

FIG 15.—Subgiant w-T diagram for the Na I D-lines. Range in T is equivalent to spectral types G6 IV–K3 IV. Note unusual strength of the D-lines in the M67 star, F193 ($M_V = +2\ 7$) and in the secondary component of the eclipsing system AR Lac The AR Lac observations refer to the minimum light phase in the total eclipse. Solid line in this graph and the other *subgiant* diagrams of blocking fraction versus T are *internal* means and were not derived from an independent Survey. See Table 12 for interesting field stars in this diagram.

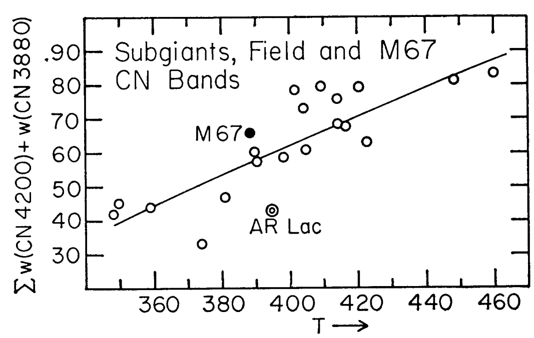

FIG. 16.—Subgiant w-T diagram for the two blue CN bands. Note the CN weakness of the AR Lac secondary; this result confirms earlier work by Miner (1966) and Hall (1967) on the CN deficiency of some subgiant components of close binary systems. The M67 star has strong CN bands and resembles the more luminous M67 giants in this anomaly.

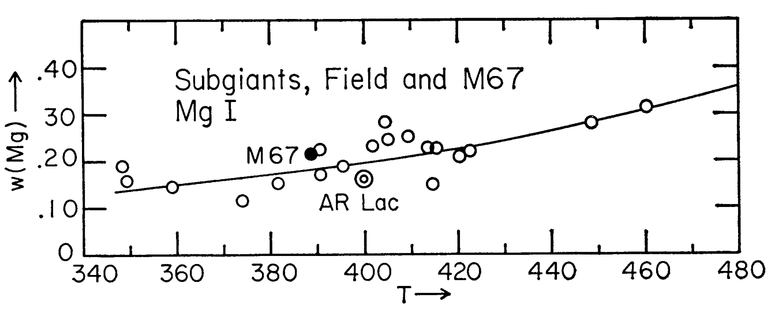

FIG. 17.—Subgiant w-T diagram for the Mg b-triplet lines (probably plus MgH). Note four stars with strong Mg lines—they are M67 F 193, γ Cep ($T = 413$), ν^2 CMa ($T = 409$), and HR 7670 ($T = 348$).

that the interstellar lines will fall at or near the bottom of the stellar lines in low-velocity K stars, thus greatly reducing the equivalent widths of the former. Distant high-velocity stars ($\rho > 40$ km sec^{-1}) could have w(D) increased by one or two hundredths in some cases, which would be significant in our context only for metal-poor stars such as No. 59 in M13. As for gravity effects, the available luminosity data for the giants studied indicate that most, if not all, have above the same intrinsic luminosities; there is little scatter in the w-T plot for the Ca II lines, which is well known to be luminosity sensitive (cf. Sharpless 1956); and, as we shall see in § XII, there is a strong positive correlation between CN-band and D-line anomalies, which is exactly opposite to what would be expected from gravity effects. We conclude that the stars above the Hyades in the w-T plots for the giants and significantly above the means in the corresponding plots for the subgiants have higher metal abundances than the Hyades, in accord with our previously published conclusions (Spinrad and Taylor 1967; Taylor 1967).

Before terminating discussion of the w-T diagrams, we should comment on the success of the approach used for giants to make comparisons across temperature differences. The fact that all of the Survey means which can be compared to ϵ Vir appear to represent solar abundance is an indication that the approach has succeeded for the hotter stars. For the cooler stars, the convergence of the lines defined by the M67 and NGC 188 stars toward the mean Survey lines as T increases might appear to indicate that these

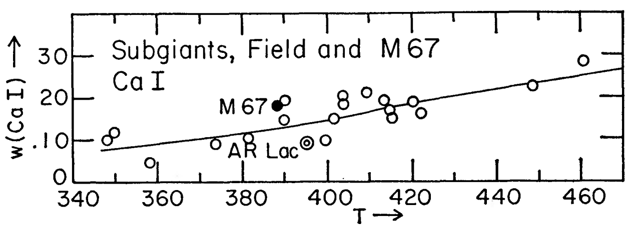

FIG. 18.—Subgiant w-T diagram for Ca I λ4227. This graph is similar in most respects to that for Mg (Fig. 17).

lines depart from true isoabundance trajectories. Further examination reveals, however, that there is a general decrease in amount of departure from the Survey means with decreasing temperature for all the stars plotted; moreover, the amount of collapse is a function of the feature that is being discussed, and is greatest for those in the blue and quite small for those in the yellow and red. This strongly suggests that the effect is primarily due to progressively increasing side-band blanketing; if this is admitted to be the case, then there is no evidence that the Survey means are not isoabundance trajectories over the entire temperature range considered.

XI. DISCUSSION OF THE SCANNER DATA: CONTINUUM-BLANKETING MEASURES

Another method of utilizing the scanner data is to compare overall blanketing in the blue ($\lambda \lesssim 5000$ Å) at a given red color. Since such blanketing is dominated by weak and partially saturated lines, this approach provides a valuable check on the strong-feature data. Here we use three blanketing index–temperature index pairs: (1) published $U - B$'s and our T's; (2) our pseudocontinuum color at λ4040, called I(4040), and our T's; (3) all of our pseudocontinuum blue colors, together with our continuum colors in the yellow and red.

We anticipated that a useful new ultraviolet residual could be defined by using $U - B$'s and our yellow-red colors. This expectation is amply confirmed; we find enormous $U - B$ blanketing differences between strong- and weak-lined stars. As with the w-T diagrams, we compare the program giants with the Survey mean (Figs. 19 and 20) and the program subgiants with an internally defined mean (Fig. 21). The results are strikingly similar to the strong-feature data. Let us define the parameter $\Delta(U-B)$ as $(U-B)_{\text{observed}} - (U_r-B)_{\text{mean},T}$, the latter quantity in the expression being the $(U-B)$ of the adopted mean relation at the star's T. (Note that positive $\Delta(U-B)$ implies a metallicity *excess*.) We see that $\Delta(U-B)$ is about 0.00 mag for ϵ Vir and the stars in NGC 752 and NGC 7789, +0.14 mag (on the average) for the Hyades, +0.21 mag for the hottest M67 giants, and +0.15 mag for star I-105 in NGC 188, all as we would expect from the data in § X; similar agreement is found for the field giants of interest and the subgiants (Tables 12 and 13). The influence of microturbulence on $\Delta(U-B)$ is

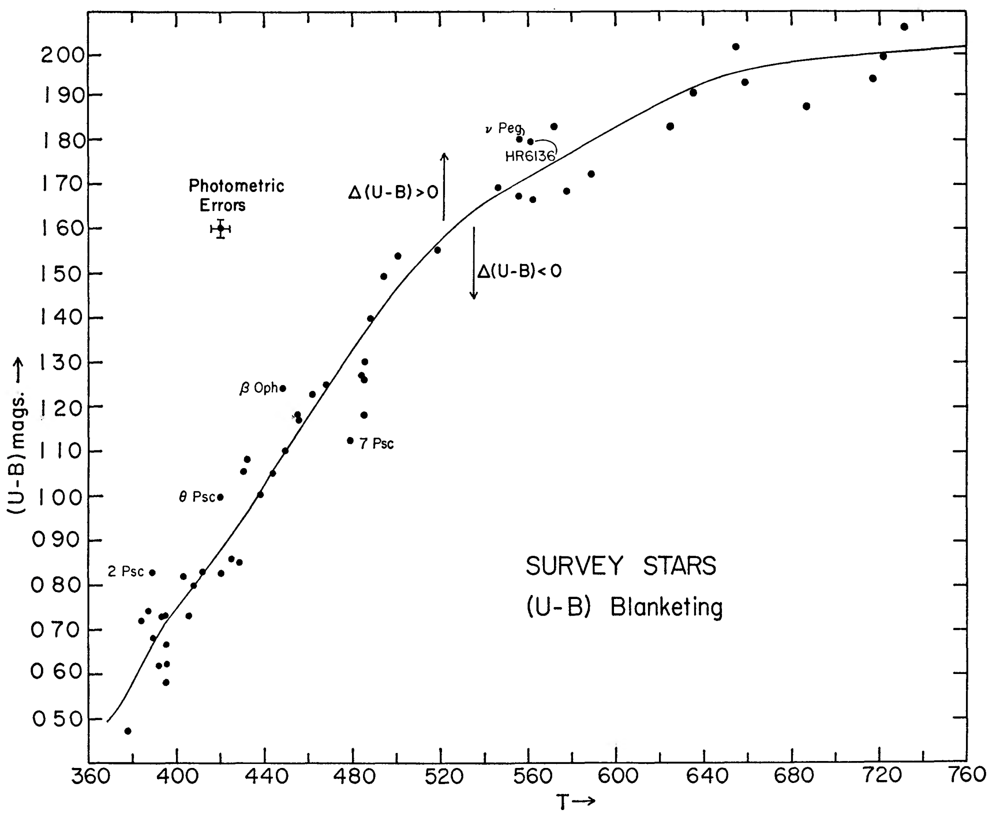

FIG. 19.—Published broad-band $(U-B)$ colors for Survey giants versus T. We have used photometry from Eggen (1966), Johnson *et al* (1966), and Argue (1963, 1966). The relatively minute sizes of the expected photometric errors are indicated by error flags. We define $\Delta(U-B)$ as the deviation from the hand-drawn mean line in the diagram, with positive $\Delta(U-B)$ indicating a blanketing excess—usually associated with a metal-rich star. Note that 2 Psc (rich) and 7 Psc (poor) have rather large blanketing anomalies. These stars have already been mentioned with regard to the w-T diagrams for CN and Na (cf. Fig. 8).

apparently unimportant, in conformity with the results of Barry (1967), McNamara (1967), and Kraft, Kuhi, and Kuhi (1968). Eggen (1964), Pagel (1966), and Johnson *et al.* (1968) have successfully used this general technique to study abundances in G and K dwarfs; evidently it is highly useful for K giants as well.

The intensity $I(4040)$ is measured at a local blanketing minimum; the only strong lines in the λ4040 passband are Fe I λ4045 and Mn I $\lambda\lambda$4033, 4034, and 4035. In the solar spectrum, the remaining blanketing in the band comes equally from lines on the linear portion ($W < 60$ mÅ) and the flat portion ($60 \text{ mÅ} \leq W \leq 300$ mÅ) of the curve of growth (Minnaert *et al.* 1940). This color correlates well with $B-V$ for the Survey stars (Fig. 22)—a circumstance, we note parenthetically, which illustrates the inade-

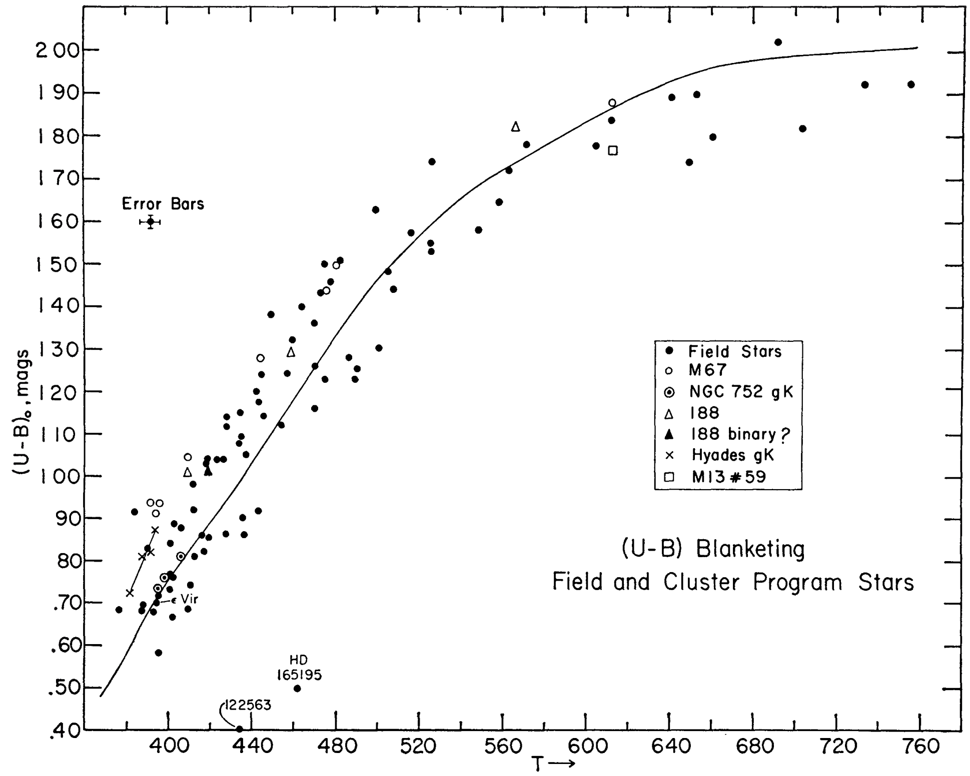

FIG. 20.—$(U - B)$ versus T for field and cluster program giants. *Solid line*, mean Survey relationship (Fig. 19). Note the large ultraviolet excesses for HD 122563 and 165195 ($\Delta(U - B) \simeq -0.6$), and the large $(U - B)$ deficiencies (Δ positive) for the very strong-line stars in the clusters M67 and NGC 188. The range in $\Delta(U - B)$ seems somewhat contracted for the coolest stars ($T > 550$). See Table 13.

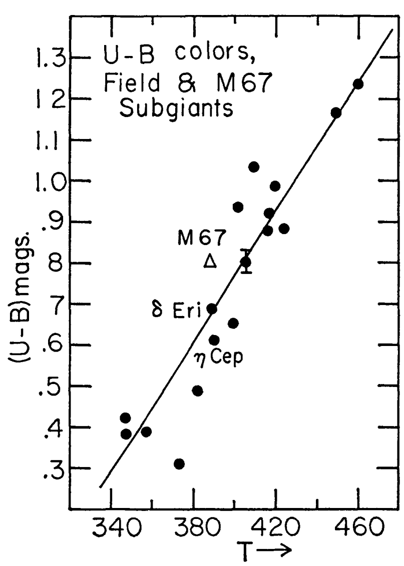

FIG. 21.—$(U - B)$ versus T for subgiants. Note the intermediate position of normal-abundance star δ Eri (Hazelhurst 1963; Pagel 1963) and the heavy blanketing in F193 in M67. See Table 13 for blanketing data on interesting field stars. Solid line is an internal mean.

quacy of $B - V$ as a temperature parameter for significantly blanketed stars. There are only three noticeably deviant stars in Figure 22—7 Psc, γ Psc, and HR 6820—and, since these stars are metal poor, low Mn/Fe ratios of the sort found by Wallerstein (1962) in metal-poor G dwarfs would neatly explain the deviation. On the whole, the data in Figure 22 indicate that $I(4040)$ is representative of blue-region blanketing as a whole. The plots of $I(4040)$ versus T for the Survey stars (Fig. 23) and the program stars (Fig. 24) have smaller excursion ranges than the corresponding plots for $U - B$, because the blanketing in the λ4040 passband is less than the mean blanketing difference between the U and B filters; otherwise, they are exactly similar to the corresponding $U - B$ plots, star by star.

In order to extract the maximum possible blanketing information from our scans, we

TABLE 12

DATA ON w-T FOR NOTEWORTHY FIELD STARS

BS/HD	Name	CN λ4200	Ca I	CH	Mg	D	TiO(λ6148+ λ7054)	T
1136	δ Eri	0 17	0 18	0 38	0 23	0 06	0 01	388
1805	Φ Aur	.42	37	35	29	11	07	500
2429	ν^2 CMa	.28	21	37	24	09	01	408
3905	μ Leo	36	28	34	28	12	03	449
4517	ν Vir	32	.48	28	39	10	38	703
4737	γ Com	31	.18	.31	.21	.09	02	434
5854	α Ser	33	.20	30	23	09	01	444
6791.	. .	17	08	18	.13	06	02	393
7405 .	α Vul	37	52	35	40	.12	38	648
7429	μ Aql	29	25	.33	30	09	02	456
7576	20 Cyg	38	33	33	31	14	04	475
7670	. .	.09	.10	33	19	04	00	348
8413	ν Peg	.41	47	35	.36	.14	12	556
8448	AR Lac	13	09	28	19	.07	02	394
8795	55 Peg	38	59	.33	39	.15	38	685
8924 .		.31	26	.35	.30	.14	02	426
122563		00	02	.11	03	01	00	433
165195		0 06	0 02	0 11	0 05	0 02	0 01	461

TABLE 13

BLANKETING DATA FOR NOTEWORTHY FIELD STARS

BS/HD	Name	$U-B$	T
1805 ..	Φ Aur	1 63	500
3905..	μ Leo	1 38	449
4517 ..	ν Vir	1 82	703
5854...	α Ser	1 24	444
6791...	.. .. .	0 68	393
7405..	α Vul	1 76	648
7429 .	μ Aql	1 25	456
7576	20 Cyg	1 50	475
8413	ν Peg	1 80	556
8795	55 Peg	1 87	685
8924 .	.	1 14	426
122563		0 38	433
165195		0 50	461

may compare the total energy distributions of weak- and strong-lined stars with those of stars having normal abundances and the same or nearly the same temperatures. We illustrate five such comparisons in Figures 25–29. These involve, in order, the Hyades δ and ϵ Tau and the M67 stars Fagerholm 84 and Fagerholm 141, which are compared with ϵ Vir; star I-105 in NGC 188, which is compared with the normal-abundance Survey star HR 8912; γ Psc and HR 6791, which are compared with ϵ Vir; Φ^2 Ori, which is compared with κ Aur; and HD 122563, which is compared to α Ari. In each case, the quantity

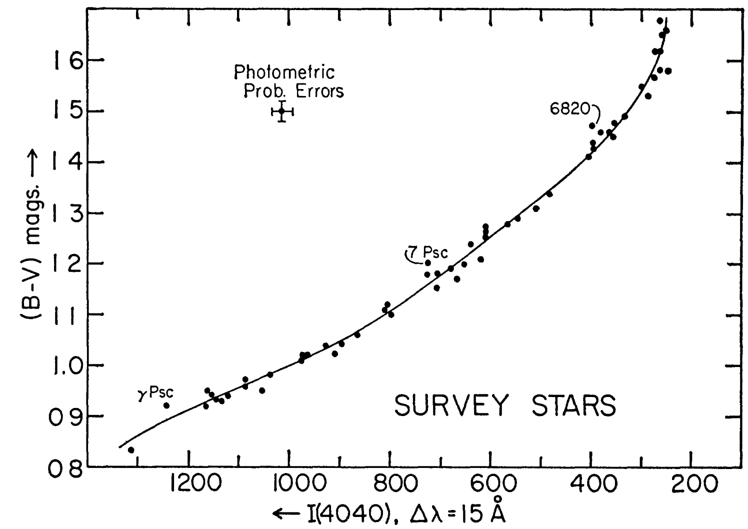

FIG. 22.—Correlation between published $(B - V)$ colors and our pseudocontinuum intensity at λ4040 for the Survey giants. $I(4040)$ is measured with an exit slot corresponding to 15 Å. Deviations from the hand-drawn line are quite small (see photometric error bars); the slightly deviant stars γ Psc, 7 Psc, and HR 6820 are discussed in the text. $I(4040)$ is apparently affected by line blanketing in much the same way as the $(B - V)$ color.

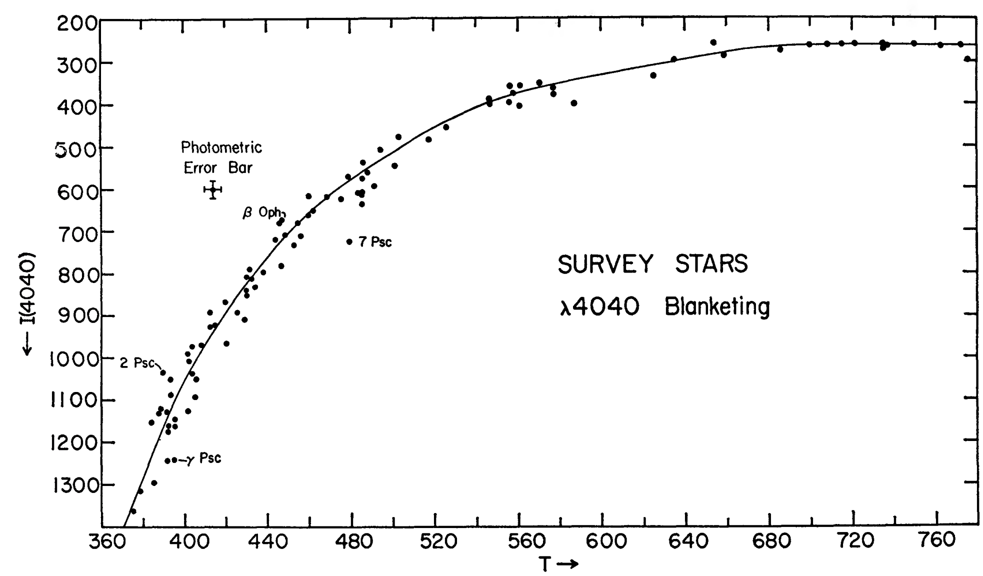

FIG. 23.—Relation between $I(4040)$ and T for the Survey stars. The mean line here, as usual, defines normalcy for the program stars. Note the λ4040 continuum flux excesses for γ and 7 Psc.

$[I(\lambda)/I(\lambda)_{\text{comparision}} - 1] \times 100$ percent is plotted as a function of λ. Progressing from short to long wavelengths in the first comparison, we note in order a depressed region due to the high blanketing in the cluster stars, ending at about $\lambda 4340$; a region of small flux *excess* extending to $\lambda 5360$ (but not including the apparently blanketed $\lambda 5000$ point), apparently due to back warming; and a region in which the continua match (except at the

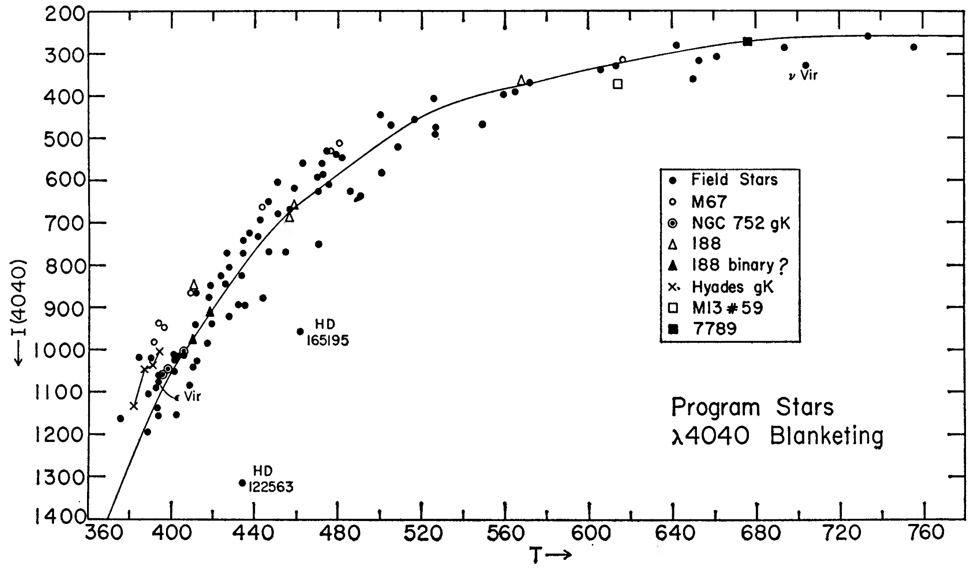

FIG. 24.—$I(4040)$ versus T for the field and cluster stars. This diagram shows $\lambda 4040$ blanketing, and is very similar in form (star by star) and in interpretation to Fig. 20, which displays $U - B$ blanketing.

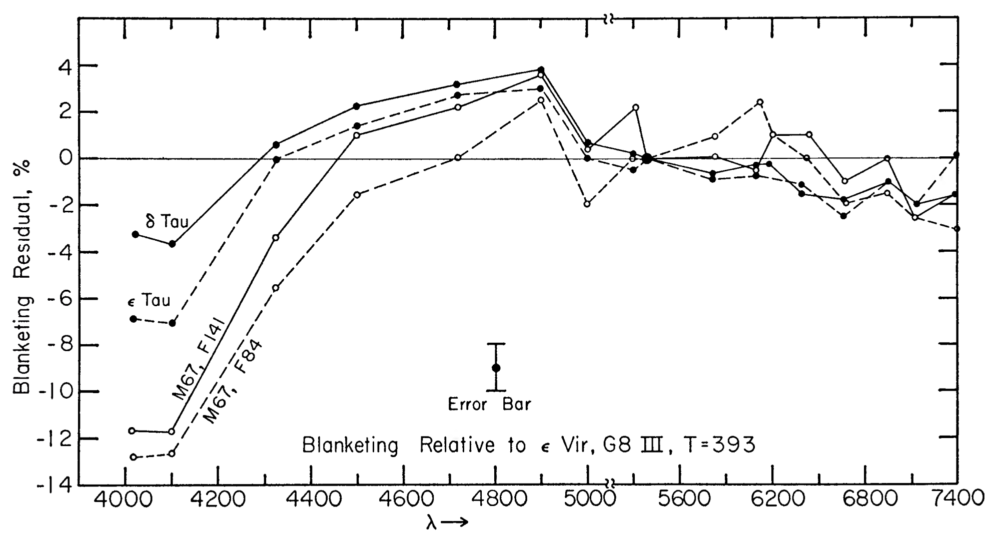

FIG. 25.—Complete *continuum* blanketing diagrams for G8 III stars ($T = 393$) F84 and F141 in M67 and the Hyades stars ϵ and δ Tau, with respect to the abundance standard ϵ Vir. Plotted is the percentage blanketing residual, $R = [I_\lambda(\text{Program Star})/I_\lambda(\epsilon\,\text{Vir}) - 1] \times 100$ percent, versus λ. Note that a negative residual implies larger blanketing than ϵ Vir, and vice versa. Note the flux deficiencies of about 12 percent for the M67 stars and 5 percent for the Hyades in the deep blue. The blanketing decreases rapidly toward longer wavelengths (except the $\lambda 5000$ point) and a small *flux excess* appears for $\lambda \geq 4500$ Å We interpret this excess in the green-yellow region as due to "back warming"—the escape of radiation blocked by the numerous lines in the ultraviolet and blue parts of the spectrum in the metal-rich and SMR stars. In the red the spectra all match well if one recalls the mild CN blanketing for $\lambda \geq 7000$ Å.

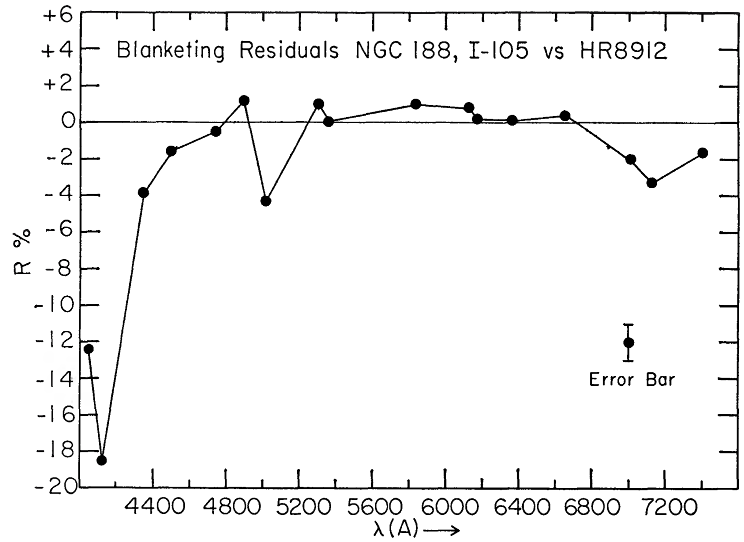

FIG 26.—A complete continuum-blanketing diagram for I-105 in NGC 188 compared with the normal Survey giant HR 8912. Both stars have $T = 410$. The features shown here are similar to those of Fig. 25.

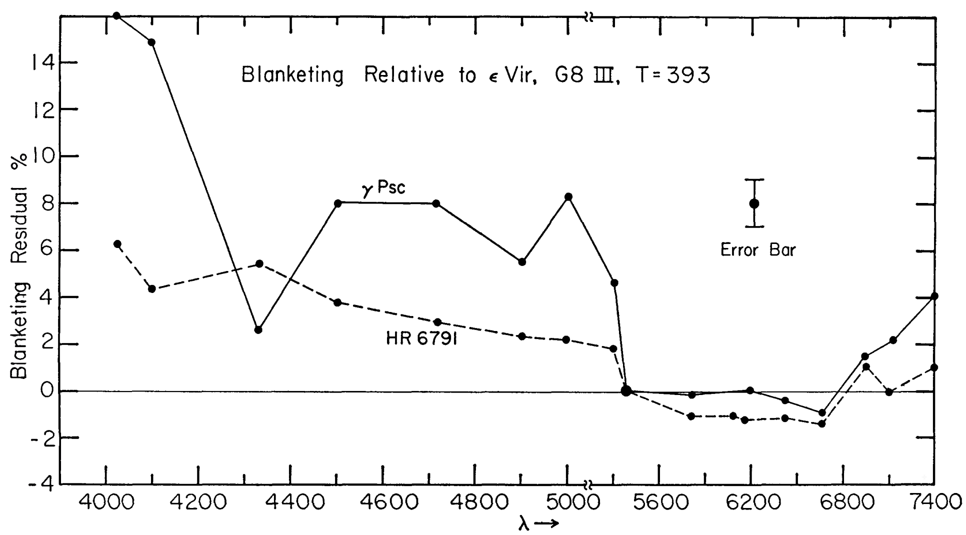

FIG. 27.—Blanketing diagrams for two metal-poor stars versus ε Vir, all with $T \simeq 393$. Note that the metal-poor stars mirror-image the continuum residuals of the metal-rich stars illustrated in the previous two figures.

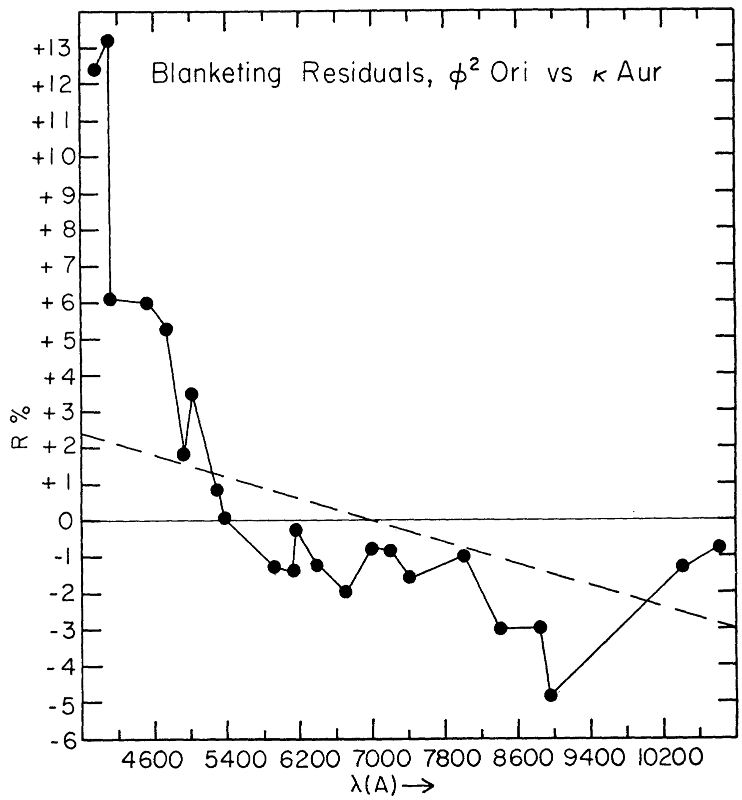

FIG. 28 —More extensive coverage in wavelength of the relative continuum blanketing of the metal-poor star Φ^2 Ori and the normal giant κ Aur. The temperature match here is imperfect; the dotted line would be a somewhat better "zero-residual" base line to take account of the slightly higher effective temperature of Φ^2 Ori. In any case, the blue excess of Φ^2 Ori is now large; the back warming of this star is less than normal, and the continuum match in the red is satisfactory to 1 μ.

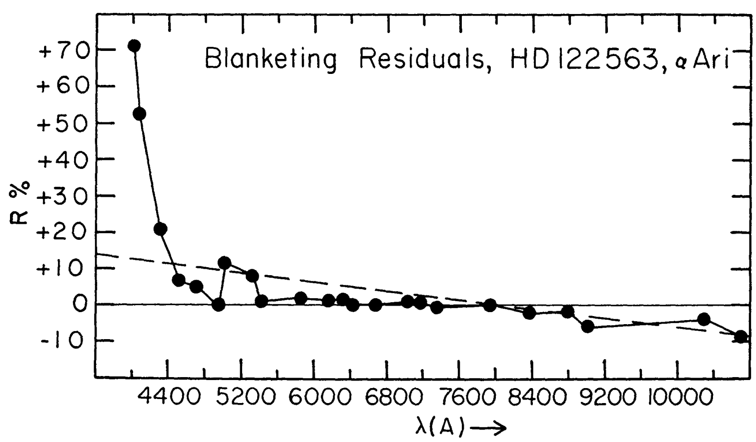

FIG 29.—Blanketing diagram for the metal-poor halo star HD 122563 as compared with the almost normal K2 III α Ari This figure is similar to the previous one in detail, but the blue flux excess of HD 122563 is very large; $R = 70$ percent at λ4040!

requires temperatures of the order of 4×10^9 ° K (Hoyle and Fowler 1960), and this is a condition extremely unlikely to be attained in the interiors of K giants. Fifth, the mechanism which supplies stars with their "intrinsic" metal contents is now required to yield well-correlated amounts of a product of the CNO cycle (nitrogen), a product of the Ne-Na cycle or a form of helium burning (sodium), and an *e*-process element (iron), while supplying α-elements (magnesium and calcium) in amounts somewhat "decoupled" from those of the first three elements mentioned (Burbidge *et al.* 1957; see Fig. 34 for the Mg-Na correlation). It is difficult to understand how this last matter can be explained, and we suspect that the pursuit of the explanation may prove to be a merry one indeed.

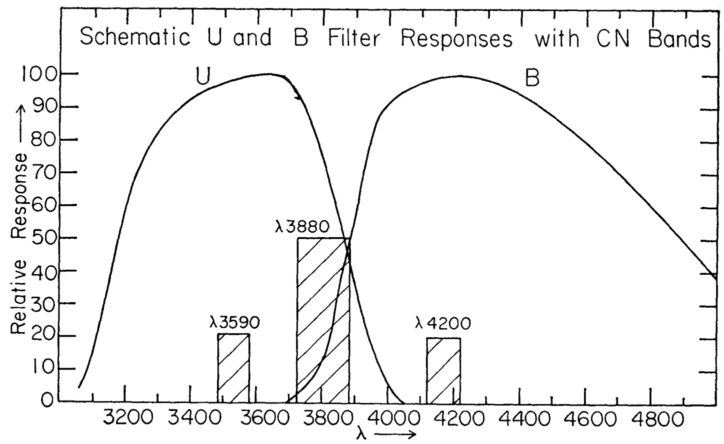

FIG. 33.—Schematic representation of the blue and ultraviolet CN bands occuring in K-star spectra, together with the equal-energy U and B filter response curves. Note approximate symmetry of the CN bands with respect to these curves; we conclude that unusual CN strength *alone cannot cause* substantial $\Delta(U - B)$ variations.

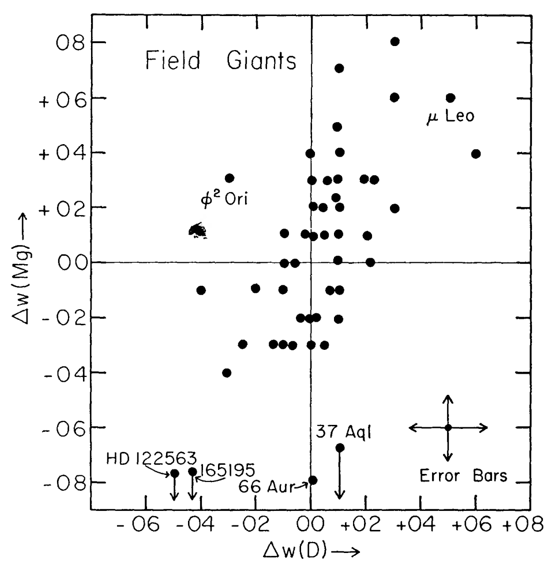

FIG. 34.—The residual correlation between Mg and Na anomalies, Δw(Mg) versus Δw(D). Here the positive correlation is somewhat less marked than those seen in Figs. 30–32. Note position of Φ^2 Ori, a star possibly rich in Mg and α-elements and with an overall metal deficiency (cf. Helfer and Wallerstein 1968).

XIII. SLIT SPECTROGRAMS

In order to spot-check the scanner strong-feature measurements, particularly for those stars with metal abundances higher than those of the Hyades (which we shall refer to hereinafter as super–metal-rich or SMR stars [Spinrad and Taylor 1967]), and also to obtain more detailed information on weak-line blanketing, we have obtained a number of slit spectrograms in the yellow and blue wavelength regions. There are two groups of these spectrograms; one was obtained at high dispersion (8 Å mm^{-1}) with the 120-inch telescope and 40-inch coudé camera, while the other was obtained at lower dispersion (39 Å mm^{-1}) with the Cassegrain spectrograph of the 84-inch telescope at Kitt Peak National Observatory. The stars observed were selected so as to be comparable in pairs or groups, each pair or group being characterized by the same value of T and containing one star with particularly interesting feature strengths. Five pairs or groups of spectrograms are illustrated in Figure 35 and Figures 36–39 (Plates 6 and 7); in each of these, one of the stars whose spectra are illustrated is SMR, according to the scanner observations. On inspecting these figures, we note the following: first, the scanner data on the strong lines

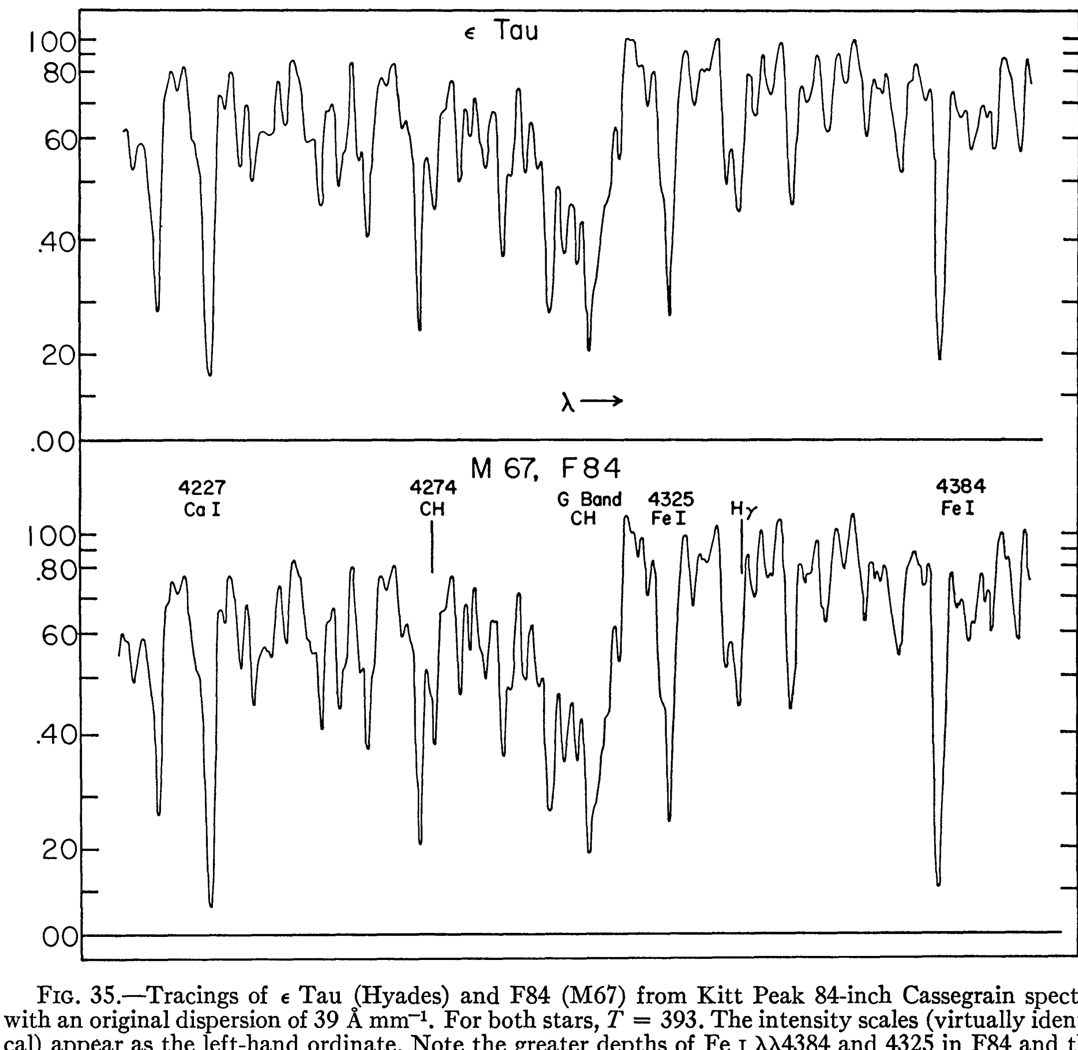

FIG. 35.—Tracings of ε Tau (Hyades) and F84 (M67) from Kitt Peak 84-inch Cassegrain spectra with an original dispersion of 39 Å mm^{-1}. For both stars, T = 393. The intensity scales (virtually identical) appear as the left-hand ordinate. Note the greater depths of Fe I λλ4384 and 4325 in F84 and the substantial strength of Ca I λ4227 in the M67 star, compared with ε Tau. CH is also slightly enhanced in the M67 giant.

1969ApJ...157.1279S

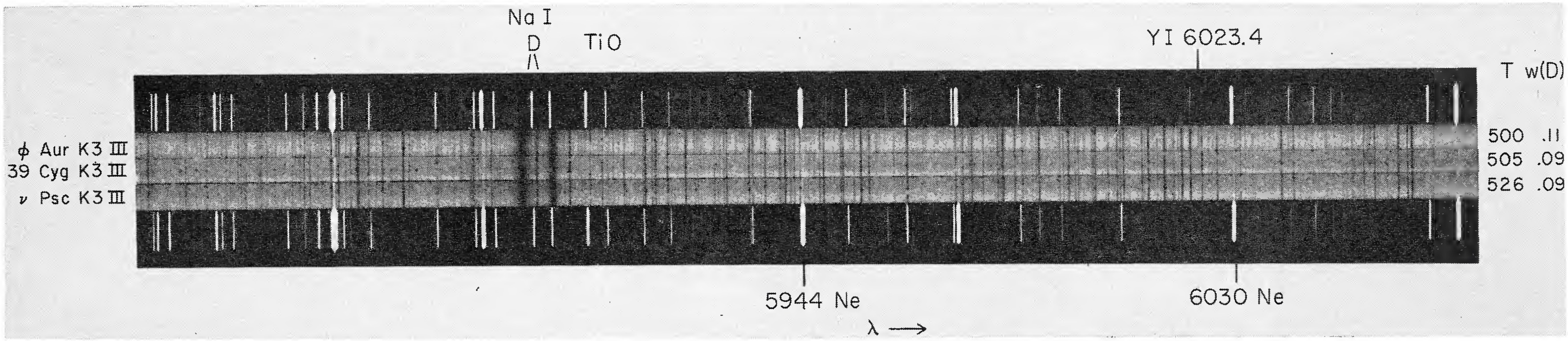

FIG. 36.—Portions of Lick 120-inch 8 Å mm^{-1} coudé spectrograms in the red region. Here we compare the SMR giant Φ Aur with the normal stars 39 Cyg and ν Psc. All stars have $T \gtrsim 500$. Note relative strengths of the D-lines and the numerous weak lines (especially Y I λ6023) in the three stars. Note probable presence of weak TiO lines near λ5900 in Φ Aur.

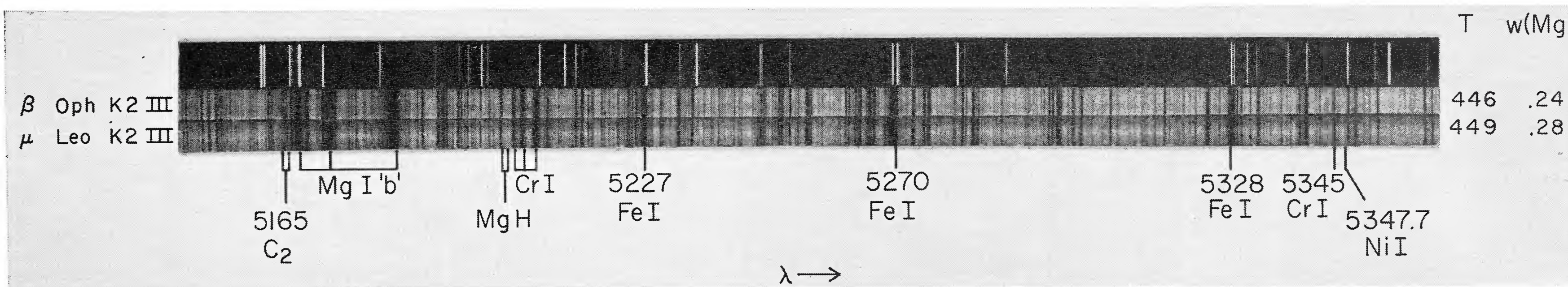

FIG. 37.—Portions of Lick 120-inch 8 Å mm^{-1} spectrograms. We compare the green spectral regions of β Oph (slightly metal rich) and μ Leo (SMR). The two stars have $T \simeq 448$. Note enhancement of Mg I λλ5167, 5175, 5184, weak MgH lines, and Fe I λ5328, Cr I λ5345, and Ni I λ5347.7 in the spectrum of μ Leo.

SPINRAD AND TAYLOR (*see* page 1323)

1969ApJ...157.1279S

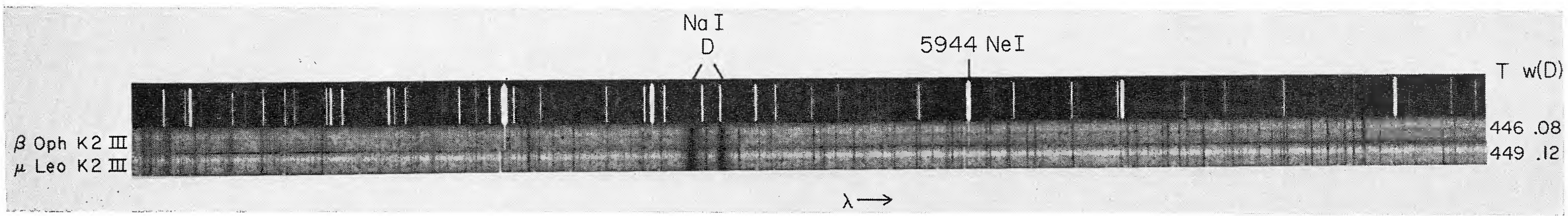

FIG. 38.—Portions of Lick 120-inch 8 Å mm^{-1} coudé spectrograms. This montage compares β Oph and μ Leo in the red region of the spectrum. Remarks generally similar to previous figures.

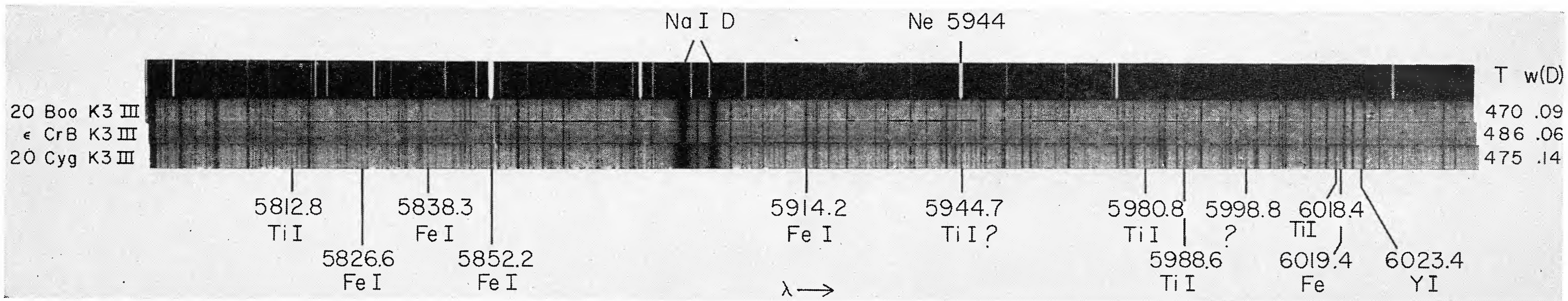

FIG. 39.—Portions of Lick 120-inch 8 Å mm^{-1} plates. Here we compare the K3 III stars 20 Boo (normal abundances), ϵ CrB (slightly metal poor), and 20 Cyg (SMR). All have $T \approx 480$. Note the wings of the D-lines in 20 Cyg and the strengths of the numerous weak lines of Ti I, Fe I, and Y I λ6023.4 in the three stars.

SPINRAD AND TAYLOR (*see* page 1323)

illustrated are in qualitative agreement with the appearances of these lines. Second, the weak lines vary from star to star in phase with the strong lines, exactly as we would expect for abundance-induced changes. Third, the line of Y I at λ6023.4 is strong in Φ Aur and 20 Cyg (Figs. 36 and 39, Pls. 6 and 7); Helfer and Wallerstein find [Y/Fe] = +0.1 in 20 Cyg. Coupling this with our overall metal-abundance excess found for this star or even with the more conservative [Fe/H] = +0.1 obtained by Mannery, Wallerstein, and Welch (1968), we obtain [Y/H] ≥ +0.2. Since Y is an *s*-process element (Burbidge *et al.* 1957), this could indicate that the enrichment process for these stars (and perhaps others as well) involved material from quite different synthesis sites, although one might also suppose that these stars simply synthesized *s*-process elements from their "primordial" supply of Fe. The first two of these points eliminate any vestiges of reasonable doubt concerning the cause of the observed feature strengths; the third indicates a direction for further investigation.

XIV. THE PROBLEM OF HELIUM ABUNDANCE

We have not yet examined the possibility that the high metal-to-hydrogen ratios found in the SMR stars observed are expressions of high helium (and correspondingly low hydrogen) content and not of high metallicity. In order to shed light on the matter, we resort to the following test. In the atmosphere of a K giant in which metals are being increased at the expense of hydrogen, the increasing electron pressure will cause the ionization equilibrium to favor neutrality by progressively greater amounts, and the ratio of the strengths of neutral lines to those of ionized lines will progressively increase. On the other hand, in a similar atmosphere in which helium is being increased at the expense of hydrogen, transparency will progressively increase because of the steady decrease of H^- opacity, and the strengths of neutral and ionized lines will increase in lockstep. In principle, one may therefore differentiate between the two possibilities by intercomparing the behavior of such lines. Figure 40 contains a plot of residuals (from the respective Survey means) of our w-values for Ca I λ4227 against similar quantities for Ca II λ8662. The solid lines represent the approximate behavior expected for the cases of "changing metals only" and "changing helium only." The large uncertainty and the quantization of the residuals involved make the test quite rough, but we see that there appears to be no indication of the lockstep behavior expected for the case of helium variation. We discuss in § XVI additional evidence concerning this question for the particular case of M67.

XV. SUPERMETALLICITY IN DWARFS AND THE QUESTION OF PRIMORDIALITY

If the abundances of our SMR giants are primordial, there should be SMR dwarfs; moreover, SMR dwarfs and giants of common origin should have the same abundances. SMR dwarfs are indeed known to exist (van den Bergh and Sackmann 1965; Pagel 1966; Taylor 1967; Greenstein and Oinas 1968). Furthermore, observations of the secondary of 18 Lib by Taylor (unpublished) indicate that the abundances of this star are similar to those of the SMR primary (Tables 5 and 6). These findings strongly support the conclusion made in § XII that the abundances of the SMR stars observed are primordial. Very recent measures of the Na D-lines in several M67 F dwarfs near the cluster turnoff indicate these unevolved stars have [Na/H] greater than in the Hyades F stars.

XVI. CALCULATIONS OF METAL ABUNDANCES AND COMPARISONS WITH PREVIOUS DETERMINATIONS

Through the use of the scanner data presented in the w-T diagrams (§ X) and the equations of Deutsch as checked by Strom's model atmospheres (§ III) we may calculate differential abundances in stars of interest for each of the three elements—Ca, Mg, and Na—whose lines we have measured. This approach requires that ratios of values of w

between two stars accurately reflect ratios of equivalent widths. Referring to the discussion of § II, we see that this requirement is well satisfied for Na and Mg, but it appears that differential Ca over- or underabundances will be consistently underestimated. In this last case, we proceed as if the systematic error did not exist, and regard the result as a lower limit. Because of this error, and because of the necessarily rough and approximate nature of the method itself, these results are probably the weakest in this paper.

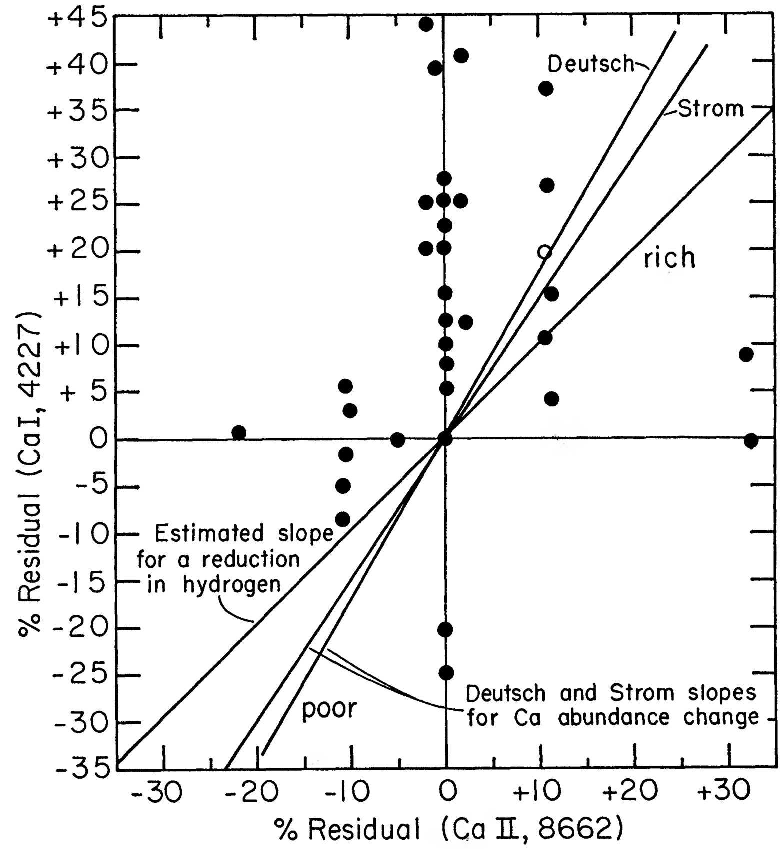

FIG. 40.—Plot of the Ca I λ4227 and the Ca II λ8662 blocking-fraction percentage residuals for the program stars. These residuals are defined as $(W_*/W_{\text{Survey}} - 1) \times 100$ percent. Expected error bars are rather large, ± 10 percent in most cases. Points are badly scattered and quantized to discrete residual levels. The two solid lines with largest slopes are the theoretically anticipated slopes for changing the Ca/H ratio as computed tby Deusch's (1966) rules and from Strom's unpublished models. The smaller-slope solid line is a relation in the residual-residual plane estimated for helium enrichment at the expense of H, with Ca/H held constant. Open circle is F170 in M67. Note that, at least for the metal-rich stars (upper right quadrant), the observations are suggestive of calcium abundance variations rather than any large He enrichment.

However, as we shall see later, they are accurate enough to be very interesting.

In Table 14, we list abundances for the most interesting of our hotter stars ($390 \leq T \leq 400$). Here the computations are straightforward and reliable, particularly since Deutsch's rules have been checked for this temperature range. For cooler stars, we encounter the scale constriction in w noted in § X; we overcome this difficulty by assuming that the M67 stars define an isoabundance trajectory in each relevant w-T diagram and adding correction factors obtained by comparing this trajectory to the Survey mean to the computations. The relatively small scatter of the M67 stars about their trajectory and the similarity of the trajectory defined by the NGC 188 stars make this assumption appear reasonable. A selection of results for the cooler stars is also given in Table 14. Note that, in all cases listed, the greatest overabundance with respect to the Sun is about a factor of 4.

It is of interest to compare abundances derived in this manner with those obtained for the same stars in previously published investigations. We direct our attention first toward results obtained using curve-of-growth and model-atmosphere techniques. Table 15 lists results (referred, as usual, to the Sun) necessary to the comparison; Part 1 is restricted to stars with spectral types G7–K1, while Part 2 lists cooler stars. Inspecting Part 1, we

TABLE 14

ABUNDANCES OF INTERESTING STARS

Star or Cluster	HR, BD, Cluster No.	Our Type	T	Ca/H*	Mg/H*	Na/H*	[M/H]†	Notes
..	495	K2 IV	401	1 0:	1 4:	4 0:	+0 3:	
γ Tau	1346	G8 III	386	....	...	...	....	
δ Tau	1373	G8 III	391	1 4	1 3	1 9	+0 2	Average of γ, δ, ϵ Tau
ϵ Tau	1409	G8 III	394	...	...	...	...	
θ^1 Tau	1411	G7 III	382	2.5	2 2	1 9	+0 35	
ν^2 CMa	2429	K0 IV	409	2 7:	1 8:	3 5:	+0 4	
μ Leo	3905	K2 III	449	3 6	4 0	4 4	+0 6	
α Ser	5854	K2 III	445	1 2	1 5	2 4	+0 2	
ϵ CrB	5947	K3 III	486	0 5	0 7	0 6	−0 2	
μ Aql	7429	K3 III–IV	457	1 5	3 3	1 7	+0 3	
20 Cyg	7576	K3 III	475	3 5	3 2	4 4	+0 55	
ϵ Cyg	7949	K1 III	427	0 5	0 5	0 2	−0 4	
γ Cep	8974	K1 IV	413	1 3:	1 5:	1 2:	+0 1:	
M13	59	...	616	0 07:	0 02:	0 1:	−1 3:	
M67	F84	G8 III	392	.	..	..	...	
M67	F141	G8 III	396	3 6	2 9	2 2	+0 45	Average of F84, F141, F151
M67.	F151	G8 III	390	..	..	..	..	
M67.	F193	K0 IV	388	2 3:	1 8:	2 3:	+0 3	
NGC 188	I-105	K0 III	410	3 4	2 4	2 2	+0 4	
NGC 752	+37°418	G9 III	398	...	...	..	....	
NGC 752	+37°432	G9 III	395	1 3	1 0	0 8	+0 05	Average of 37°418, +37°432, +37°448
NGC 752..	+37°448	G9 III	405	..	...	...	...	
NGC 7789...	K751	M0 III	677	1 5:	0 7:	1 0	+0 05	

* Ratio of stellar to solar value.

† Average of three abundance ratios, expressed in usual logarithmic form, relative to the Sun.

note substantial disagreement for λ Hya; we have no ready explanation for this, especially since the temperatures assigned by the two approaches agree rather well. Otherwise, the scatter is about what one would expect from the sizes of the internal errors (about ± 0.15 in the log for each technique). For Part 2, the situation is somewhat less satisfactory; note particularly Φ Aur (G. Cayrel 1966), 20 Cyg (Helfer and Wallerstein 1968), μ Leo, and δ Psc (Peat and Pemberton 1968). The question immediately arises: Whose is the error? The abundances quoted in the literature for the four cool stars mentioned above are compatible with our data only if a strong gradient of metal abundance with temperature exists in the two old clusters and for the average field star; for Φ Aur, the size of this gradient would approach an order of magnitude per half spectral interval. Since this is extremely unlikely, we conclude that the error lies in the previously published analyses, and we suggest that this conclusion is generally true in this temperature range (except possibly for the most underabundant stars, for which both techniques are quite imprecise). A gradient of the sort described above is implied by a comparison of observations used by Peat and Pemberton with their calculated relations between abundance and line strength (see their Figs. 3, 4, and 7); the sense of the gradient is that stars of progressively lower temperatures are assigned progressively lower abundances, and is suggestive of the existence of an unsuspected source of opacity in K giants. Our technique is not affected by such considerations because it does not involve comparisons across temperature differences.

There are three recent abundance determinations for M67 of which we also wish to take notice. The first of these is the photometric analysis of the cluster K giants made by Mannery, Wallerstein, and Welch (1968); this yields [Fe/H] = +0.4, in excellent agreement with our results ([M/H] = +0.45). The second is that of Sargent (1968), who concludes from a study of the cluster's horizontal-branch stars that M67 has normal abundances. With respect to this result, we make the following comments:

1. Sargent bases his abundance determination on a plot of equivalent width against $(B - V)$ of the Ca II K-line (Fig. 3 in his paper). The scatter in this plot is quite noticeable, as he himself remarked; according to Deutsch's equations, it corresponds to about a factor of 3 in abundance. Moreover, no correction for gravity effects is made for the

TABLE 15

COMPARISONS OF OUR ABUNDANCES WITH PUBLISHED VALUES

BS or BD	Name	T	Our Type	[M/H]	$\Delta(U-B)$	Published [Fe/H]	Reference
			PART 1. G8–K0				
1136	δ Eri	389	K0 IV	+0 1:	+0 01	0 0	1
1346	γ Tau	386	G8 III	.	..	. ... .	
1373	δ Tau	391	G8 III	+ 2	+ 15	+ .15	2
1409	ϵ Tau	394	G8 III	..	..	. .	. .
1411	θ^1 Tau	382	G7 III	+ 35	+ .12	+ 3	2
1907	Φ^2 Ori	402	K0 III	− 7:	− 10	− 5	3
2219	κ Aur	412	K0 III	0	− 01	− 3	3
3994	λ Hya	384	G7 III	+ 6:	+ 29	2	3
5480	31 Boo	403	K0 III	− 15	+ 00	0	3
5681	δ Boo	409	K0 III	− 1	− 12	− 4	3
6791	.... .	393	G8 III	+ 1	− 01	+ 2	3
8255	72 Cyg	419	K1 III	+ 1	+ 16	+ 2	3
+37°432	...	395	G9 III	+0 05	+0 01	−0 05	4
			PART 2 K2–K5				
224	δ Psc	606	K5 III	+0 1	−0 06	−1 0	5
1805	Φ Aur	500	K3 III	+0 4	+ 17	−0 4	6
3905	μ Leo	449	K2 III	+0 6	+ 26	−0 1:	5
7429	μ Aql	457	K2 III	+0 35	+ 07	+0 4	3
7576 .	20 Cyg	475	K3 III	+0 55	+ 20	+0 1	3
122563	.	434	K2p	−2 0:	− 62	−2 7:	7, 8
165195	. . .	462	K3p	−2 0:	− 68	−2 7:	7
M13 ..	#59	614	K5p	−1 3	−0 09	−1 2	9

References:
1 Hazelhurst (1963) and Pagel (1963)
2. Helfer and Wallerstein (1964)
3 Helfer and Wallerstein (1968) as corrected by Mannery *et al* (1968) and referred to the Sun using the differential Hayes abundance of 0 2 quoted by Alexander (1967).
4. Wallerstein and Conti (1964)
5. Peat and Pemberton (1968)
6. G. Cayrel (1966)
7. Wallerstein *et al* (1963)
8 Pagel (1965).
9. Helfer *et al* (1959); their analysis refers to Barnard 140

hotter stars; since the M67 stars have lower gravities, the correction would increase the equivalent widths of their K-lines. We conclude that these data do not contradict our results for M67.

2. Sargent notes that for two stars, Fagerholm 55 and Fagerholm 153, the metallic-line type is much later than the K-line type, and he concurs in Pesch's (1967) classification of them as metallic-line A stars. He also notes, however, that the ratio of K-line to hydrogen-line strengths is not abnormally low, as it is in many classical Am stars. We submit that these facts are much better explained by supposing that the two stars mentioned above simply share the cluster's intrinsic overabundances; judging from the print of Sargent's plates, they have this in common with the other cluster members he observed.

3. Sargent compares his line-strength data for Fagerholm 81, the B7 V star seen in the cluster ($[B - V]_0 = -0.13$), with the data of Searle and Sargent (1964), and concludes that both its metallic and helium abundances are normal. But "normalcy" as defined by those authors covers a broad range of abundance (see their Figs. 1 and 2), since they were interested in excluding only Ap and Am stars from the definition, and since certain of the overabundances in these stars attain two orders of magnitude. We have looked into this question in somewhat more detail; through the courtesy of Dr. Sargent, we have examined this plate and tracing of the spectrum of Fagerholm 81. Table 16 lists

TABLE 16

EQUIVALENT WIDTHS OF FAGERHOLM 81

Line (λ)	Identification	W_λ(mÅ)	[El/H]	Comparison-Star References
4471	He I	390	0 0	Searle and Sargent (1964); Williams (1936)
3862	Si II	136±20	+ .5	Wolff (1967); Searle and Sargent (1964)
4131	Si II	184±40	+ .7	Wolff (1967); Searle and Sargent (1964)
4481	Mg II	450	+ .6	Wolff (1967); Searle and Sargent (1964)
4508	Fe II	100±30	$\gtrsim$0.0	Wolff (1967)

equivalent widths of several moderately strong lines (either as measured by Spinrad or as averaged from independent measurements by Spinrad and Sargent) and abundances derived from each, relative to the Sun, by using the data of Searle and Sargent and also those of Wolff (1967). The abundances are naturally rather imprecise, but they do indicate that Fagerholm 81 has the same enhancement of metals as the cluster's cool stars. They also confirm Sargent's result for helium. If Fagerholm 81 is a cluster member (and, as Pesch points out, the only discordant datum, the radial velocity, is not discordant enough to rule it out), then these results are consistent with our own; in addition, they provide further evidence that abnormal helium abundances do not confound our line-strength interpretations (see § XIV). We conclude that Sargent's data generally support our results for M67.

The third abundance determination for M67 which we wish to compare with our results is that of Eggen and Sandage (1964). These authors derive $E(B - V) = 0.06$ mag and $\delta(U - B) = +0.03$ mag for M67 by fitting the Hyades main-sequence relation to their data in the $(U - B, B - V)$-plane. This small ultraviolet excess suggested that M67 was slightly metal-poor compared with the Hyades. With respect to this result, we make these comments:

1. The reddening of M67 derived in this manner is lower than that derived by using the observed amount of neutral hydrogen in the cluster line of sight (which, at the galactic latitude of M67 [32°] should all be in front of the cluster) and a calibration of the (N_H, E_{B-V})-relation that uses photometry of high-latitude RR Lyrae stars and reddening values derived by using the technique of Sturch (1969). A complete discussion of this

technique will be given in a subsequent paper; we note here, however, that the preliminary values of $E(B - V)$ for M67 and NGC 188 are at least 0.03 and 0.07 mag higher, respectively, than those given by Eggen and Sandage (1964) for M67 and by Eggen and Sandage (1969) for NGC 188.

2. Our photometry of the M67 giants Fagerholm 84, Fagerholm 141, and Fagerholm 151 is inconsistent with that of Eggen and Sandage if the value $E(B - V) = 0.06$ mag is used. In an appendix to their 1964 paper, these authors give a result which implies that unreddened giants of Hyades chemical composition will lie on the Hyades main sequence in the $(U - B, B - V)$-plane for $B - V$'s between about 0.63 and 1.10 mag. According to the photometry of Johnson and Knuckles (1955), this is true of the Hyades giants themselves, as consistency requires. By plotting the three M67 giants in the two-color diagram given by Eggen and Sandage (their Fig. 2) and applying their reddening, we obtain $(B - V)_{0,\mathrm{Hyades}} \approx 1.05$ mag for these stars, while our red colors (corrected for the equivalent amount of reddening) imply that these stars have the same temperature as δ and ϵ Tau, whose average $B - V$ is 1.00 mag; the latter conclusion is the same if the red photometry of Mendoza V. (1967) or Kron (1968) is used instead. This discrepancy may be removed by increasing the reddening; this decreases the $(B - V)_{0,\mathrm{Hyades}}$ assigned by both the red photometry and the *UBV* photometry, but the $(B - V)_{0,\mathrm{Hyades}}$ derived by the *UBV* photometry decreases more rapidly as the assumed reddening is increased, since its derivation involves correction along a blanketing vector whose slope is not too different from that of the Hyades main sequence. Any attempt actually to derive the interstellar reddening of M67 by comparison of the resultant $(B - V)_{0,\mathrm{Hyades}}$ derived from the red and *UBV* photometry is difficult, since the technique is very sensitive to photometric errors and also to the slope of the blanketing vector used. A rough calculation, however, suggests that $E(B - V) \geq 0.1$ mag.

3. It is physically unlikely that the M67 giants have heavy-element abundances different from those of the M67 dwarfs. Increasing the reddening removes this discrepancy; this increases the abundances derived for both giants and dwarfs, but those derived for the dwarfs (by ultraviolet excess) increase faster for the same reason as that given above.

4. The M67 *UBV* photometry is, on the whole, not inconsistent with a reddening value somewhat higher than that given by Eggen and Sandage, especially since the data of highest weight near $B - V = 0.6$ mag (see Fig. 2 of Eggen and Sandage 1964) indicate the presence of nonnegligible observational scatter.

We conclude that considerable evidence exists that the reddening—and hence the blanketing—of main-sequence stars in M67 has been underestimated by Eggen and Sandage. We have nonetheless used the reddening values given by Eggen and Sandage (1964, 1968) for M67 and NGC 188, since they yield lower limits for the abundances derived for these clusters. Increasing these reddening values does not materially affect our results.

XVII. APPLICATIONS TO GALACTIC STRUCTURE

We now turn to an examination of possible correlations between metallicity and kinematic properties for as many of our stars as have published space motions. Most of the space motions used here were taken from lists given by Eggen (1962, 1966),[2] although other sources were also used (Roman 1955, 1967; Wallerstein *et al.* 1963); all of these vectors have been computed with respect to the Sun. For the sake of convenience, we use $\Delta(U - B)$ as the abundance parameter throughout. We first compare this parameter with $Q = \sqrt{(U^2 + V^2 + W^2)}$ (Fig. 41), position in the Haas-Bottlinger dia-

[2] We are aware of the criticism recently directed at the 1962 paper (Weller, Crull, and Hynek 1968). However, our stars are bright and therefore reasonably close to the Sun; moreover, the space motions given for those of our stars found in both papers are in excellent agreement. We feel that the space motions quoted here are generally trustworthy.

gram (Fig. 42), and $|W|$ (Fig. 43), for those of the Survey stars for which the kinematic data are available. Note the total or almost total lack of correlation in these diagrams; only in the last one is there any sign of a trend, and the numbers involved are small enough so that this may merely be statistical. The diagram for $|W|$ is in reasonable accord with similar diagrams given by Eggen, Lynden-Bell, and Sandage (1962), Wallerstein (1962), and Pagel (1966), but the Haas-Bottlinger diagram suggests the possibility of disagreement with these authors, since it contains a few metal-rich stars with $e > 0.35$.

The abundance-kinematic data for the field program stars are given for the subgiants in Figures 44 (Q) and 46 (Haas-Bottlinger diagram) and for the giants in Figures 45 (Q), 46, and 47 ($|W|$). In common with the Survey data, as may be seen, they exhibit no correlations. The Haas-Bottlinger diagram for these stars exhibits noticeable disagreement with those given in the three investigations cited above, since it contains a number of stars for which $\Delta(U - B) > 0$ and $0.35 < e < 0.5$. The diagram for $|W|$ is again

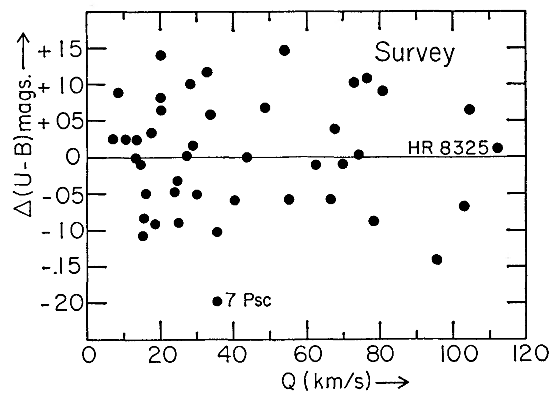

FIG. 41.—Metal abundance, as measured by $\Delta(U - B)$, versus total space velocity (Eggen 1962 and 1966) for Survey giants. Note lack of correlation out to $Q = 110$ km sec^{-1}. Both metal-rich and metal-poor stars fall into the high-velocity regime; most metal-poor stars actually have rather low velocities ($Q \leq 40$ km sec^{-1}).

largely in accord with the results of those investigations, but note an outstanding exception—HD 29038, an SMR star with $|W| = 63$ km sec^{-1}.

Violations of the accepted correlations may also exist among the clusters investigated. The M67 stars have potential energy such that $|W|$ would equal 36 km sec^{-1} at $z = 0$ kpc (Murray, Corben, and Allchorn 1965), and we estimate that the corresponding parameter for NGC 188 would be slightly higher.

Indirect evidence for supermetallicity at relatively large distances above the plane is to be found in Upgren's (1962) spectroscopic investigation of high-latitude K giants (for which generally 1 kpc $\leq z \leq$ 1.6 kpc).[3] Upgren notes strong CN in about 2.5 percent of his stars. Since HD 104998 (CN + 3; Keenan 1963) is thus described, but γ Com (Fig. 11; Table 12) is not, we conclude that only extreme SMR stars were noticeable as unusual at his dispersion, and that the actual percentage of SMR stars in his sample is undoubtedly noticeably higher. (One could, of course, suppose as an alternative explanation that these stars are supergiants, but then they would be intolerably young for their galactic positions.)

We conclude that the correlations found by Eggen *et al.*, Wallerstein, and Pagel are not completely valid for K giants. Since we find a considerable range in angular momentum and potential energy with respect to the plane for our SMR stars, we further conclude that they have originated throughout the disk and well into the halo. We have no

[3] We are indebted to Dr. A. Klemola for pointing out the existence of this investigation to us.

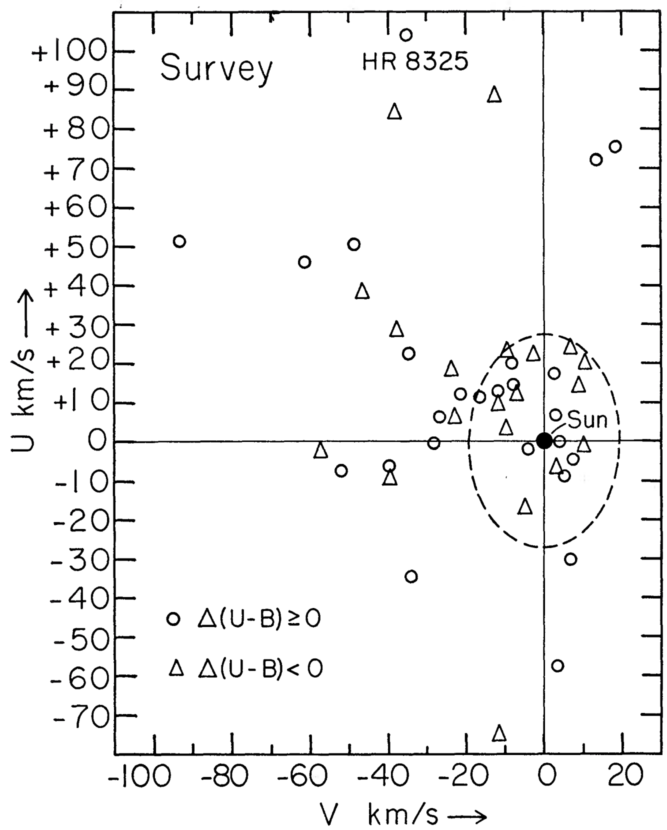

FIG. 42.—A Haas-Bottlinger diagram for the Survey stars. *Open circles*, metal-rich stars; *triangles*, metal-poor stars. The ellipse around the solar vicinity is the approximate locus for galactic orbital eccentricity of 0 1; HR 8325 at $U = +100$ km sec^{-1}, $V = -36$ km sec^{-1} has an eccentricity near 0 4. The Survey stars are a low-velocity sample—typical of stars in a modest volume near the Sun.

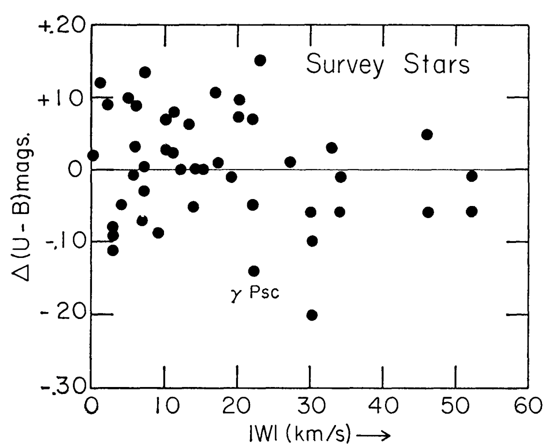

FIG 43

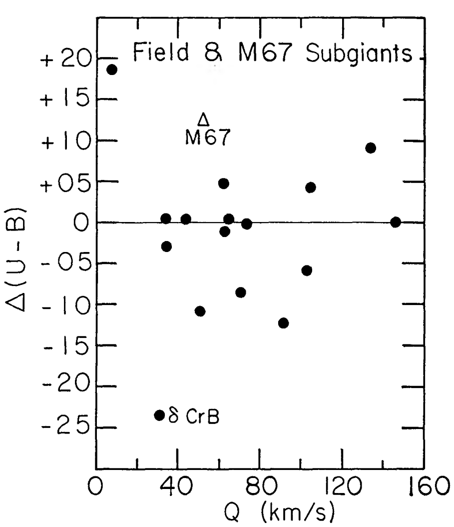

FIG 44

FIG. 43.—Plot of $\Delta(U - B)$ versus $|W| = (|dz/dt|)$ for Survey stars Here there may be a very weak correlation between abundance and kinematic property, in the sense that stars of low metal abundances are more frequent than metal-rich stars at larger $|W|$ values However, the number of stars sampled with $|W| \geq 30$ km sec^{-1} is very small, so this trend may or may not be statistically meaningful.

FIG. 44 —Plot of $\Delta(U - B)$ versus Q for field and M67 subgiants, There is no obvious correlation between abundance and the total space motion of class IV stars sampled here, despite the fact that our stars include some rather high-velocity objects.

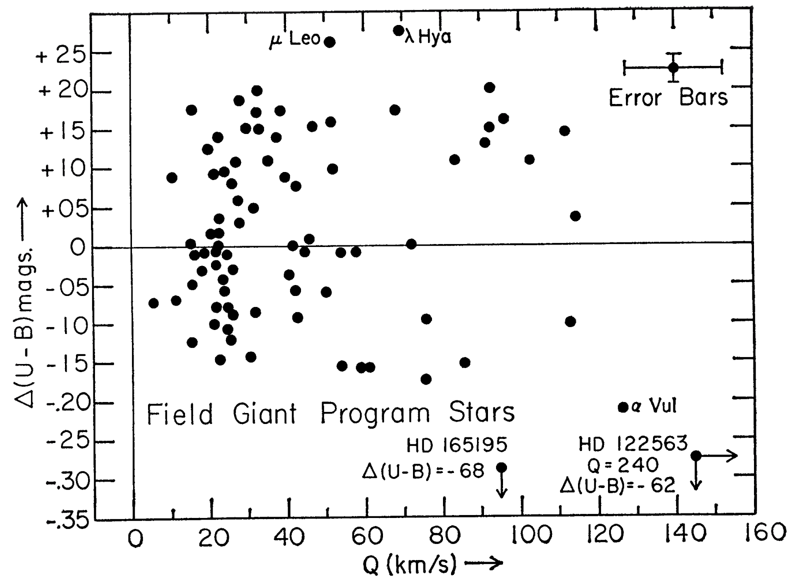

FIG. 45.—Plot of $\Delta(U - B)$ versus Q for program field giants. Again note the large scatter and the lack of any systematic trends. The galactic clusters of interest can be mentally superposed onto the diagram at the following approximate locations: Hyades at +0.15 mag and 45 km sec^{-1}, NGC 752 at +0.01 mag and 15 km sec^{-1}, M67 at +0.20 mag and 50 km sec^{-1}, and NGC 188 at +0.18 mag and 60 km sec^{-1}.

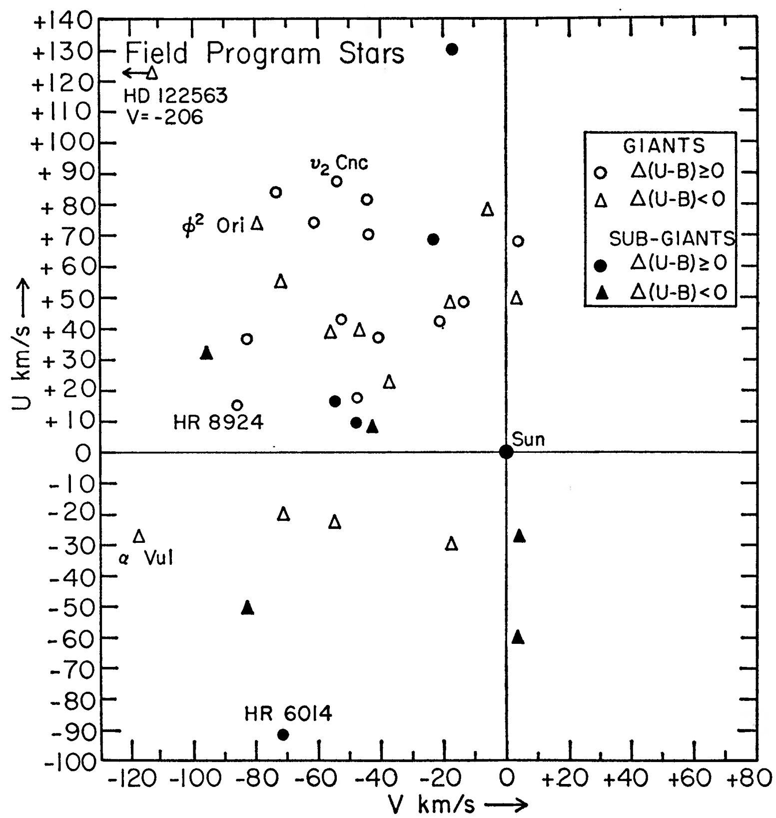

FIG. 46.—The Haas-Bottlinger diagram for field giants and subgiants. *Open circles*, metal-rich giants; *filled circles*, metal-rich subgiants; *triangles*, metal-poor stars. The limit of eccentricity at the left edge of the figure is about $e = 0.5$. Note the lack of correlation between abundance and U, V velocity vectors.

ready explanation for the lack of G-dwarf counterparts to our more kinematically extreme K giants in the three investigations mentioned; what data are available indicate that such stars do exist (Eggen 1964). Taylor is currently investigating this matter as part of a thesis project consisting of scanning nearby late-G and K dwarfs.

XVIII. AGE-ABUNDANCE CONSIDERATIONS

In this section we discuss the ages of the SMR stars and attempt to reassess the age-abundance scheme of the Galaxy in light of their existence. We illustrate in Figure 48 a conventional color-magnitude diagram showing schematic loci for M67 (Eggen and Sandage 1964) and NGC 188 (Eggen and Sandage 1968), together with those of our field stars which have trigonometric parallaxes (Jenkins 1952) or K reversal widths (Wilson and Bappu 1957; Wilson 1967) and which are either SMR or below the M67 locus. The diagram indicates that the SMR stars plotted include some which are extremely old—perhaps as old as the disk itself—and none younger than M67. Admittedly the sample

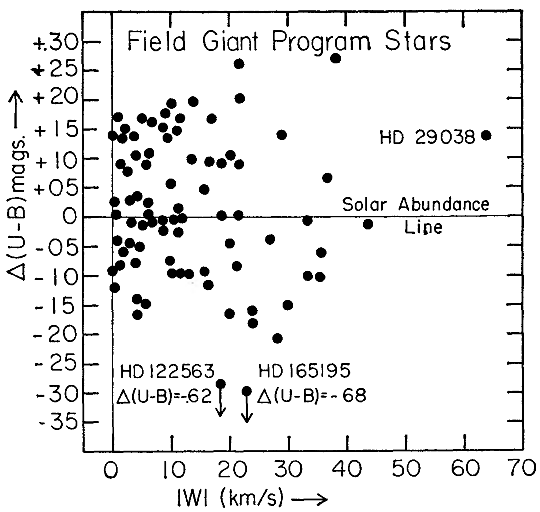

FIG. 47.—$\Delta(U - B)$ versus $|W|$ for program giants. Again we find little or no correlation. Compare with the trend noted by Pagel (1966) for K-dwarf velocities and abundances. See text.

is small and the luminosities are rather imprecise, but the possibility that a lower age limit exists for SMR stars is nonetheless striking enough to merit further attention.

In order to check on this matter, we need an unbiased statistically significant sample of stars which will include SMR stars younger than M67, if such exist. In order to obtain such a sample, we turn to the catalog of Strömgren and Perry (1962).[4]

Figure 49 contains a plot of m_1 versus $(b - y)$ of all main-sequence stars listed in the catalog which have $(b - y)$'s in the range 0.240–0.420 (which corresponds approximately to the spectral-type range F0–G2), have right ascensions in the range 0^h–16^h, and are not noticeably evolved (as judged from their c_1 indices). The Hyades and M67 iso-abundance trajectories are also depicted; the former is from Crawford and Perry (1966), and the latter is derived from our results and the relations of Strömgren (1964) between abundance and m_1. On inspecting this plot, we see that SMR F stars do in fact exist, but we also note that for spectral types earlier than about G0—which is roughly the M67 turnoff position—the region around and above the M67 trajectory is devoid of stars. We note further that the percentage of SMR stars is noticeably greater in the F8–G2 region than in either the F2–F5 or F5–F8 regions (Table 17). The prima facie conclusion to be drawn by combining this plot and our data is that, for stars with M67-like and higher

[4] We are indebted to Dr. R. P. Kraft for referring us to this catalog.

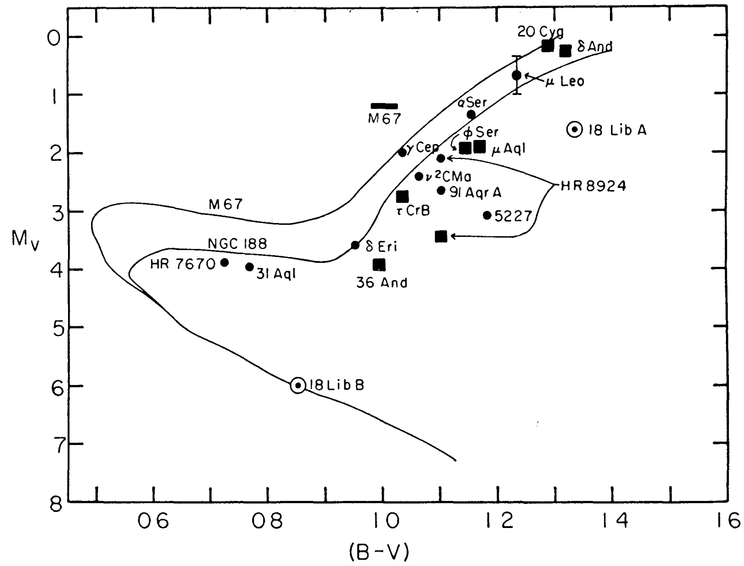

FIG. 48.—Conventional C-M diagram for the old galactic clusters M67 and NGC 188 (corrected for reddening and absorption) and old field giants and subgiants scanned at Lick. All field stars plotted are SMR except δ Eri (solar abundances) and 91 Aqr A and τ CrB (slightly metal rich). Absolute magnitudes are from trigonometric parallaxes (circles), Olin Wilson's unpublished K-line widths and the calibration given by Wilson and Bappu (1957) (filled squares), Spinrad's K-line width for μ Leo and the same calibration (with estimated error flags), and, in the case of the brighter component of the visual binary 18 Lib, from the assumption that the secondary lies on the Hyades main sequence An idea of the uncertainty of individual M_v determinations may be obtained by examination of the two plotted positions of HR 8924. The thrust of this figure is to point out that most SMR stars are underluminous; also, their rough positions on the C-M diagram indicate that they may be very old. There is certainly little indication that many, if any, SMR K giants are young.

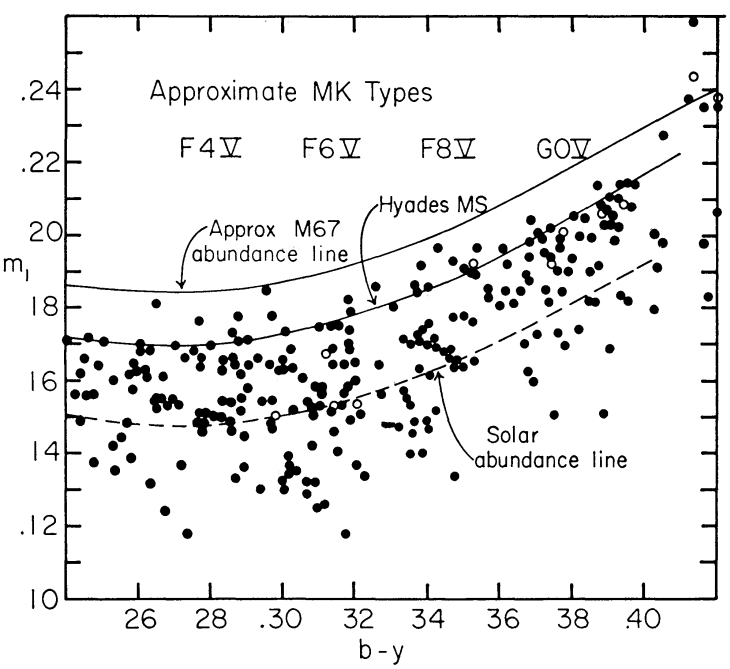

FIG 49.—Strömgren's m_1 metal index versus his intermediate band color $(b - y)$, for main-sequence F and G dwarfs. Data were taken from the Strömgren-Perry (1962) catalog; these stars are represented by filled circles. Only the first two-thirds of the catalogue has been plotted The few open circles are high-velocity "disk" stars noted by Strömgren (1964). The Hyades main-sequence line and computed M67 and solar abundance trajectories, parallel to the Hyades, are indicated. Note absence of stars hotter than G0 V in the neighborhood of or above the M67 line. See discussion in text.

abundances, there is indeed a lower age limit, and that the maximum metallicity of newly formed disk stars dropped fairly abruptly by at least three tenths in the log shortly after the formation of M67.

If the above conclusion is correct, we would expect to see the higher percentage of SMR dwarfs below the M67 turnoff persist into later spectral types. The investigations of van den Bergh (1963), Schmidt (1963), and Spité (1966) all indicate SMR fractions of about 10 per cent for G dwarfs, a marginal difference at best from the fraction found for the stars earlier than F8. However, the photometry of Argue (1963, 1966) and that of Johnson *et al.* (1968) yield, respectively, SMR fractions of 24 percent for the range G4–K4 and 20 percent for the range G3–K3; these are decisively different from the F-star fraction. These numbers are all necessarily imprecise, due to the sizes and natures of the samples involved, but they provide a fair indication that the expected effect is present. We are certain that the strongly blanketed stars found in the latter two investigations are indeed SMR, since Taylor has scanned and described SMR dwarfs previously (Taylor 1967).

On the basis of the available data, we conclude that the cutoff described above did take place. Since this appears to be incompatible with the "uniform enrichment" hypothesis described by Burbidge *et al.*, it would seem necessary to reexamine the case for this

TABLE 17

FRACTIONS OF SMR STARS IN FIGURE 49

$b-y$ Interval	Spectral-Type Interval	Percent SMR	Total Number
0 24–0 30 .	F2–F5	8	78
0 30–0 35 .	F5–F8	9	81
0 35–0 42.. .	F8–G2	17	66

postulate.[5] If uniform enrichment occurred during the formation of the halo, we would expect to find a certain minimum primordial metallicity for all stars formed subsequently in the disk; this conclusion is reached by Dixon (1965), and is supported by the data of Strömgren and Perry and by our Survey data. If, on the other hand, uniform enrichment has occurred in the disk itself, we would expect the metallicity of newly formed disk stars to have steadily increased with time; judging from our data on the cutoff, this has not happened. We therefore suggest that uniform enrichment was operative only during the formation of the halo, and has played no important role in the history of the disk. We refrain from proposing an alternative enrichment mechanism at this time, since we know of none which will account for the existence of the cutoff; the mechanism of dust depletion by radiation pressure suggested by Schmidt and van den Bergh (1969), which is the only hypothesis on this subject extant, probably fails because the depletion envisioned by these authors is gradual, while the cutoff appears to be relatively abrupt.

Because of the widespread belief that of the uniform-enrichment hypothesis is probably approximately correct, we should note at this point that no reasonably decisive observational proof has ever been given to show that uniform temporal and/or spatial enrichment has taken or is taking place in the galactic disk. Previous investigations have shown only that, if enrichment has been taking place in the disk, the enrichment rate has been small. Arp (1961), Sandage (1962), and Eggen and Sandage (1964) have suggested enrichment rates of near zero over the past $5–10 \times 10^9$ years, primarily on the basis of *UBV* observations of NGC 188 and M67. The physical situation is complicated, however, by the probable presence of large-scale chemical inhomogeneities in the inter-

[5] The uniformity referred to here may be either spatial or temporal or both.

stellar medium; the existence of these inhomogeneities may be demonstrated by comparisons between star clusters, examples being a comparison of the Hyades and Coma (Johnson and Knuckles 1955; Strömgren 1958; Mendoza V. 1963; Price 1966*b*) and a comparison of the Hyades and the Pleiades (Fig. 50; see also Arp 1961), and also by examination of the extensive data on luminosities and ultraviolet excesses of stars as cool as or cooler than the Sun (cf. Eggen 1964; Eggen and Sandage 1964; Pagel 1963), although interpretation of the latter data is somewhat confused by the dependence of a star's rate

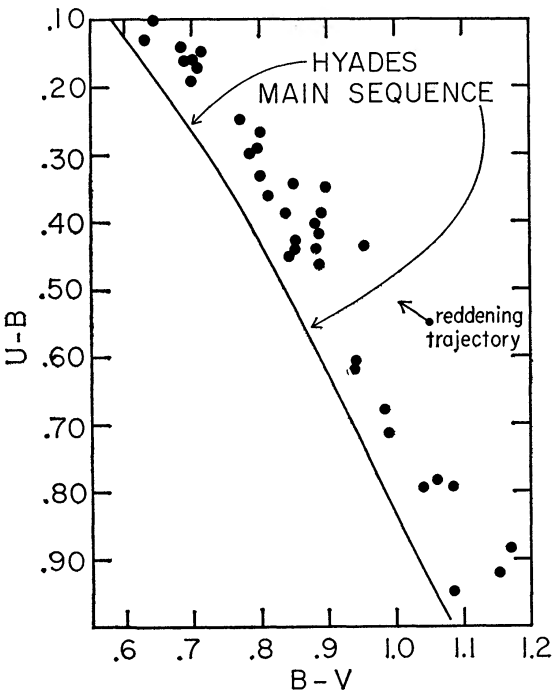

FIG. 50.—Pleiades main-sequence stars, approximately over the range G5 V–K3 V, plotted in the $(U - B, B - V)$ plane, compared with the Hyades main sequence (Morgan and Hiltner 1965). Pleiades data from Iriarte (1967) and Johnson and Mitchell (1958). Points should be moved upward and to the left in the figure by the lengths of the small arrow, a mean reddening value derived from the hot stars in the Pleiades cluster. The Pleiades appear to have a definite ultraviolet excess compared with the Hyades stars.

of evolution on its metallicity (cf. Demarque 1968). These inhomogeneities have prevented ruling out the possibility that metal enrichment has been taking place in the disk—averaged over the inhomogeneities—at a low but nonzero rate.

We end this discussion with a note of caution. The conclusions drawn in this section from our data depend either wholly or in part on the nonexistence of stars with M67-like or higher abundances which are younger than M67 itself. The available observations make this appear very likely, but it is by no means certain, and further work is needed on young stellar groups and young field stars for the sake of confirmation.

XIX. SUPERMETALLICITY IN THE NUCLEI OF GALAXIES

Recent evidence from synthesis of integrated photoelectric spectra of galaxies indicates that supermetallicity is found in the cores of giant ellipticals and also in the nuclei of spirals (Spinrad 1966, 1967; McClure and van den Bergh 1968). We cite this result here in view of the possibility that there may be some connection with the results presented in this paper. The data of § XVII, which indicate that the SMR stars studied have originated in a variety of places in the Galaxy, make it appear unlikely that there is a physical connection between disk and halo supermetallicity, on the one hand, and supermetallicity in the nucleus, on the other (assuming that the nucleus of the Galaxy is indeed SMR, as seems likely). However, the existence of supermetallicity under the conditions found in giant ellipticals and the nuclei of spirals may provide a clue to the nature of the enrichment mechanism generally responsible for primordial stellar metal abundances; we feel that this is a possibility which might be profitably explored.

XX. SUMMARY

In summary, we have described a technique for deriving abundances from observations with a photoelectric spectrum scanner, and we have presented data on cool stars obtained by using this technique. From these data, we have arrived at the following conclusions:

1. Evolved K stars with metal abundances greater than that of the Hyades exist. The available evidence leaves little doubt that these abundances are primordial and are not the product of the star's own nuclear evolution. The abundances found range as high as a factor of 4 times solar values for Ca, Mg, and Na. The K-giant and subgiant members of the old galactic clusters M67 and NGC 188 have abundances higher than those of the Hyades; independent data on the hotter stars in M67 indicate that this is likely to be true of them also.
2. The range of abundances in K giants tends to cause systematic errors in MK spectral classification of these stars, and makes supplementary red photometry necessary.
3. At least one significant source of error exists in standard differential curve-of-growth and model-atmosphere techniques for giants cooler than about K0.
4. A tight correlation exists between N, Na, and Fe abundances for the stars studied, and is presumably of general validity. This correlation does not, however, extend in full strength to Ca and Mg.
5. K giants and subgiants exist which have solar or higher abundances and orbital eccentricities up to 0.5 or maximum heights above the galactic plane of 1.5 kpc. The velocity-abundance correlations found previously for G dwarfs are probably not valid for evolved K stars and may not be valid generally.
6. A relatively abrupt cutoff in the production of stars with M67-like and higher element abundances took place shortly after the epoch of formation of M67 itself. From this result and the results of other investigations, it is concluded that uniform enrichment was probably important during the formation of the halo but has played no significant role in the history of the disk.

We wish to acknowledge conversations with and suggestions from many astronomers during the course of this research. In particular, we thank Drs. J. L. Greenstein, A. R. Sandage, I. R. King, R. F. Wing, L. V. Kuhi, P. S. Conti, A. Klemola, R. P. Kraft, and M. and S. Peimbert. We are gratefully indebted to Dr. S. Strom for the model-atmosphere data on damping lines. Dr. E. J. Wampler introduced us to the Lick Observatory scanner which made this project possible. Mr. S. Shawl computed the results necessary for the assessment of side-band blanketing.

Financial support for this project came from ONR contract N 00014-67-C-0215, project NR 046-811, and also (in the case of B. J. T.) from the Davidson Fund of the University of California. Financial support for the Lick Observatory scanner is derived from NSF grant GP 63-10.

APPENDIX

For the convenience of other observers, we give in Table 1A a list of possible SMR stars which we have either not observed or observed incompletely, together with the references from which the stars have been selected. This list is by no means exhaustive.

TABLE 1A

POSSIBLE K-GIANT SMR STARS

Star	Spectral Type	Reference
HD 104998	K0 III	Keenan (1963)
HD 112127.	K2 III	Keenan (1963)
HR (1779A)	K1 III–IVp	Bidelman (1958)
HD 29122.	gK, λ4150	Bidelman (private comm.)
HD 154277	gK, λ4150	Bidelman (private comm.)
HD 171767	gK, λ4150	Bidelman (private comm.)
HD 174350	gK, λ4150	Bidelman (private comm.)
HR 645	K0 III	Roman (1952)
38 Aur .	K0 III	Roman (1955)
HD 43624	K1 III	Roman (1955)
HR 315.	K2 III	Roman (1955)
HR 3110	K0 III	Roman (1955)
HD 9166	K3 III	Roman (1955)
132 Tau.	G8 III	Gyldenkerne (1964)
73 Leo .	K3 III	Gyldenkerne (1964)
τ Dra..	K3 III	Gyldenkerne (1964)
HR 8485	K3 III	Gyldenkerne (1964)
HR 8779	K3 III	Gyldenkerne (1964)
HR 285	K2 III	Gyldenkerne (1958)
65 And.	K4 III	Gyldenkerne (1958)
HR 999.	K4 III	Gyldenkerne (1958)
HR 4997	K4 III	Gyldenkerne (1958)
HR 6476	gK1	Yoss (1961)
HR 5924	K4 III	Deeming (1960)
ρ Ser	K5 III	Price (1966*a*)
17 Mon	K4 III	Price (1966*a*)
ψ^7 Aur.	K3 III	Peat (1964)
31 Leo	K4 III	Peat (1964)
3 Dra...	K3 III	Peat (1964)
HR 4521	K3 III	Peat (1964)

REFERENCES

Alexander, J. B. 1967, *M.N.R.A.S.*, **137**, 41.
Argue, A. N. 1963, *M N.R.A.S.*, **125**, 557.
———. 1966, *ibid.*, **133**, 475.
———. 1967, *ibid.*, **135**, 23.
Arp, H. C. 1961, in *Problems of Extra-Galactic Research,* ed. G. C. McVittie (New York: Macmillan Co), p. 42.
———. 1962, *Ap J.*, **136**, 66.
Arp, H. C , and Johnson, H. L. 1955, *Ap J.*, **122**, 171.
Barry, D. C 1967, *Ap. J.* (*Letters*), **148**, L87.
Bidelman, W. P 1958, *Pub. A S P.*, **70**, 168.
Burbidge, E. M., and Burbidge, G. R. 1959, *Ap. J.*, **129**, 513.
Burbidge, E. M., Burbidge, G. R., Fowler, W. A., and Hoyle, F. 1957, *Rev. Mod Phys.*, **29**, 547.
Burbidge, E. M., and Sandage, A. R. 1958, *Ap. J.*, **126**, 322.
Cayrel, G. 1966, *Ann. d'ap.*, **29**, 413.
———. 1967, paper presented at the first meeting of the International Association of Geochemistry and Cosmochemistry (Paris).
Cayrel, G., and Cayrel, R. 1963, *Ap. J.*, **137**, 431.

Cayrel, R. 1968, *Ap. J.*, **151**, 997.
Crawford, D. L., and Perry, C. L. 1966, *A J* , **71**, 206
Davis, S. P., and Phillips, J. G. 1963, *The Red System of the CN Molecule* (Berkeley and Los Angeles: University of California Press).
Demarque, P. 1968, *A.J.*, **73**, 669.
Deeming, T. J. 1960, *M.N.R.A S.*, **121**, 52.
Deutsch, A. J. 1966, in *Abundance Determinations in Stellar Spectra IAU Symposium No. 26*, ed. H. Hubenet (London: Academic Press), p 112.
Dixon, M. E 1965, *M N.R.A.S.*, **129**, 51.
Eggen, O. J. 1962, *R.O B.*, No. 51.
———. 1963, *Ap. J.*, **138**, 356.
———. 1964, *A J.*, **69**, 570
———. 1966, *R.O.B.*, No. 125.
Eggen, O. J , Lynden-Bell, D., and Sandage, A. R. 1962, *Ap. J.*, **136**, 748.
Eggen, O. J., and Sandage, A. R. 1964, *Ap. J.*, **140**, 130.
———. 1969, *Ap. J.* (in press).
Greene, T. F. 1968, *A J.*, **73**, S515.
Greenstein, J. L. 1968, *Ap J.*, **152**, 431.
Greenstein, J. L., and Keenan, P. C. 1964, *Ap. J.*, **140**, 673.
Greenstein, J. L., and Oinas, V. 1968, *Ap J.*, **153** (*Letters*), L91.
Griffin, R. F. 1961, *M.N.R.A S.*, **122**, 181.
Griffin, R. F., and Redman, R. O. 1960, *M N.R.A S.*, **120**, 287.
Gyldenkerne, K. 1958, *Pub. Copenhagen Obs* , No. 175.
———. 1964, *ibid.*, No. 178.
Hall, D. S. 1967, *A.J.*, **72**, 301.
Hayes, D. 1967, unpublished dissertation, University of California, Los Angeles.
Hazelhurst, J. 1963, *Observatory*, **83**, 128.
Helfer, H. L., and Wallerstein, G. 1964, *Ap. J. Suppl.*, **9**, 81.
———. 1968, *ibid.*, **16**, 1.
Helfer, H. L., Wallerstein, G., and Greenstein, J. L. 1959, *Ap. J* , **129**, 700.
Hoffleit, D. 1964, *Catalogue of Bright Stars* (3d ed.; New Haven: Yale University Observatory).
Hoyle, F., and Fowler, W. A. 1960, *Ap. J* , **132**, 565.
Iriarte, B. 1967, *Bol. Obs. Tonantzintla y Tacubaya*, **4**, 79.
Jenkins, L. F. 1952, *General Catalogue of Trigonometric Stellar Parallaxes* (New Haven: Yale University Observatory).
Johnson, H. L. 1953, *Ap. J.*, **117**, 357.
———. 1966, *Ann Rev. Astron and Ap.*, **4** (Palo Alto, Calif.; Annual Reviews, Inc).
Johnson, H. L , and Knuckles, C. F. 1955, *Ap. J.*, **122**, 209.
Johnson, H. L., MacArthur, J. W., and Mitchell, R. I. 1968, *Ap J* , **152**, 465.
Johnson, H. L., and Mitchell, R. I. 1958, *Ap. J.*, **126**, 134.
Johnson, H. L., Mitchell, R. I., Iriarte, B , and Wisniewski, W. Z. 1966, *Comm. Lunar and Planetary Lab.*, **4**, 99.
Johnson, H. L., and Morgan, W. W. 1953, *Ap. J.*, **177**, 313.
Johnson, H. L., and Sandage, A. R. 1955, *Ap. J.*, **121**, 616.
Keenan, P. C. 1963, in *Stars and Stellar Systems*, Vol. **3**, ed. K. Aa. Strand (Chicago: University of Chicago Press), p. 530.
Kraft, R. P., Kuhi, L. V., and Kuhi, P. S. 1968, *A.J.*, **73**, 221.
Kron, G. E. 1968 (private communication).
McClure, R. D., and van den Bergh, S. 1968, *A.J.*, **73**, 313.
McNamara, D. H. 1967, *Pub. A.S.P.*, **79**, 434.
Mannery, E., Wallerstein, G., and Welch, G. A. 1968, *A J.*, **73**, 548.
Mendoza V., E. E. 1963, *Bol. Obs. Tonantzintla y Tacubaya*, **3**, 137.
———. 1967, *ibid.*, **4**, 149.
Miner, E. D. 1966, *Ap. J.*, **144**, 1101.
Minnaert, M., Mulders, G. F. W., and Houtgast, J. 1940, *Photometric Atlas of the Solar Spectrum 3332* Å *to 8771* Å (Amsterdam: Schnabel).
Moore, C. E , Minnaert, M., and Houtgast, J. 1966, *N B.S. Monog.*, No. 61 (Washington: U.S. Government Printing Office).
Morgan, W W. 1956, *Pub. A.S.P.*, **68**, 509.
Morgan, W. W., and Hiltner, W. A. 1965, *Ap. J.*, **141**, 177.
Murray, C. A. 1967 (private communication).
Murray, C. A., Corben, P. M., and Allchorn, M. R. 1965, *R.O B.*, No. 91.
Oke, J. B. 1964, *Ap. J.*, **140**, 689.
Pagel, B. E. J. 1962, *R.O B* , No. 55.
———. 1963, *Observatory*, **83**, 133.
———. 1965, *R.O.B.*, No. 104.

Pagel, B. E. J. 1966, in *Abundance Determinations in Stellar Spectra IAU Symposium No. 26*, ed. H. Hubenet (London: Academic Press), p. 359.
Peat, D. W. 1964, *M.N.R.A.S.*, **128**, 475.
Peat, D. W., and Pemberton, A. C. 1968, *M.N.R.A.S.*, **140**, 21.
Pesch, P. 1967, *Ap. J.*, **148**, 781.
Pettit, E., and Nicholson, S. B. 1928, *Ap. J.*, **68**, 279.
Price, M. J. 1966*a*, *M.N.R.A.S.*, **134**, 135.
———. 1966*b*, *ibid.*, p. 171.
Roman, N. G. 1952, *Ap. J.*, **116**, 122.
———. 1955, *Ap. J. Suppl.*, **2**, 195.
———. 1967, in *Stars and Stellar Systems*, Vol. **5**, ed. A. Blaauw and M. Schmidt (Chicago: University of Chicago Press), p. 345.
Sandage, A. R. 1962, *Ap. J.*, **135**, 333.
———. 1968 (private communication).
Sargent, W. L. W. 1968, *Ap. J.*, **152**, 885.
Scarfe, C. D. 1966, *M.N.R.A.S.*, **133**, 99.
Schmidt, K.-H., and van den Bergh, S. 1969, *Astr. Nach.*, **291**, 115.
Schmidt, M. 1963, *Ap. J.*, **137**, 758.
Schwarzschild, M., Schwarzschild, B., Searle, L., and Meltzer, A. 1957, *Ap. J.*, **125**, 123.
Searle, L., and Sargent, W. 1964, *Ap. J.*, **139**, 793.
Sharpless, S. 1956, *Ap. J.*, **124**, 342.
Spinrad, H. 1966, *Pub. A.S.P.*, **78**, 367.
———. 1967, oral communication to IAU Commissions 28 and 45, Prague.
Spinrad, H., and Taylor, B. J. 1967, *A.J.*, **72**, 320.
Spité, F. 1966, *Ann. d'ap.*, **29**, 601.
Strömgren, B. 1958, *Ric. astr. Spec. astr. Vatic.*, **5**, 257.
———. 1964, *Ap. Norvegica*, **9**, 333.
Strömgren, B., and Perry, C. 1962, *Photoelectric uvby Photometry for 1217 Stars Brighter than* $V = 6^{m}.5$, *Mostly of Spectral Classes A, F, and G* (Princeton, N.J.: Institute for Advanced Study).
Sturch, C. 1969, *A.J.*, **74**, 82.
Taylor, B. J. 1967, *Pub. A.S.P.*, **79**, 441.
———. 1968, oral communication at the Conference on Low Luminosity Stars, Charlottesville.
Upgren, A. R. 1962, *A.J.*, **67**, 37.
van den Bergh, S. 1963, *A.J.*, **68**, 413.
van den Bergh, S., and Sackmann, I. J. 1965, *A.J.*, **70**, 353.
Wallerstein, G. 1962, *Ap. J. Suppl.*, **6**, 407.
Wallerstein, G., and Conti, P. 1964, *Ap. J.*, **140**, 858.
Wallerstein, G., Greenstein, J. L., Parker, R., Helfer, H. L., and Aller, L. H. 1963, *Ap. J.*, **137**, 280.
Wampler, E. J. 1966, *Ap. J.*, **137**, 280.
Weller, W., Crull, H., and Hynek, J. A. 1968, *Ap. J.*, **153**, 349.
Whiteoak, J. B. 1967, *Ap. J.*, **150**, 521.
Whitford, A. E. 1958, *A J.*, **63**, 201.
Wildey, R. L., Burbidge, E. M., Sandage, A. R., and Burbidge, G. R. 1962, *Ap. J.*, **135**, 94.
Williams, E. G. 1936, *Ap. J.*, **83**, 279.
Wilson, O. C. 1967 (private communication).
Wilson, O. C., and Bappu, V. 1957, *Ap. J.*, **125**, 661.
Wing, R. 1967, unpublished doctoral dissertation, University of California, Berkeley.
Wolff, S. C. 1967, *Ap. J. Suppl.*, **15**, No. 134.
Yoss, K. M. 1961, *Ap. J.*, **134**, 809.